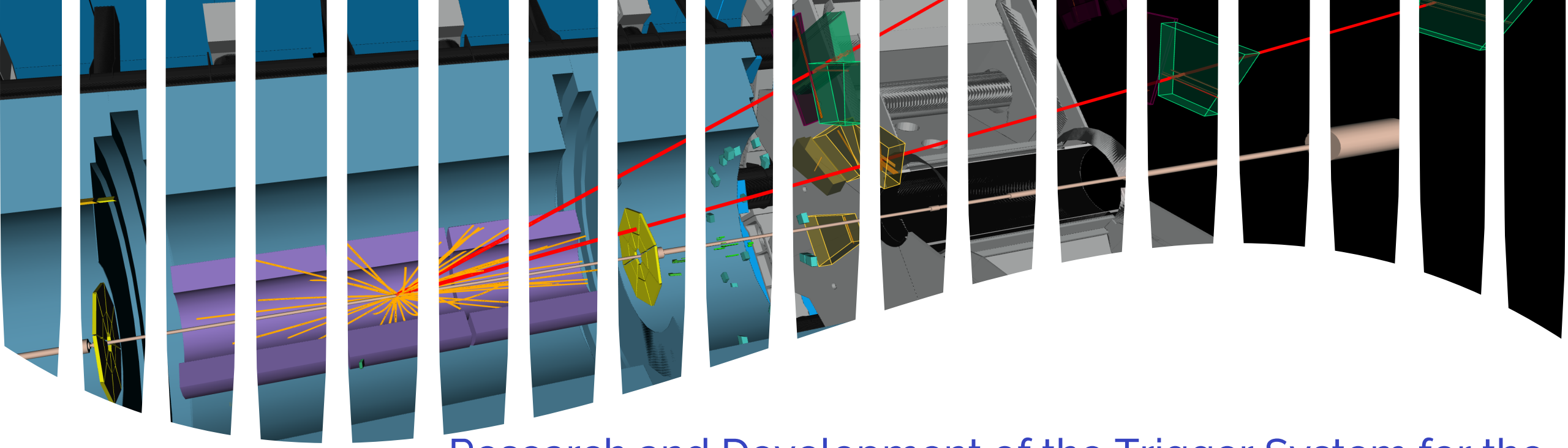

Research and Development of the Trigger System for the New Small Wheel Upgrade of the ATLAS experiment at CERN and Performance Evaluation of the sTGC detector. Study for the precise determination of the Z-boson mass.

PhD Defense

Olga Zormpa

Advisory Committee: T. Geralis, T. Alexopoulos, G. Stavropoulos, M. Kokkoris, I. Kopsalis, S. Maltezos, A. Psallidas

Athens, 08 July 2024

Outline

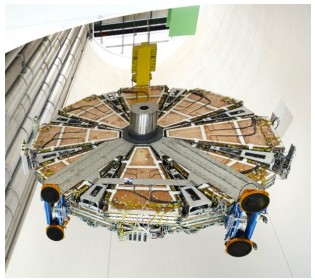

New Small Wheel

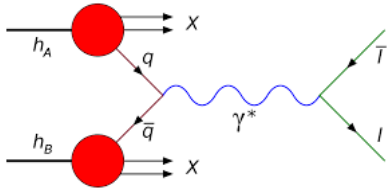

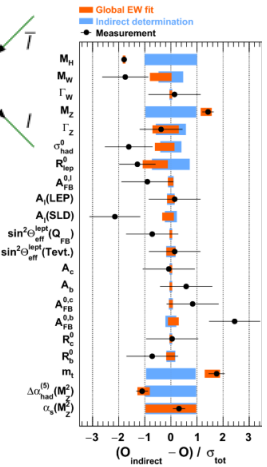

Z mass Precision measurement

Summary Publications Talks

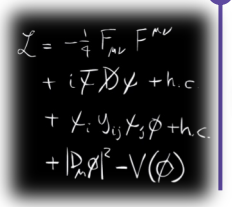

Introduction

Test Beam

ESSnuSB

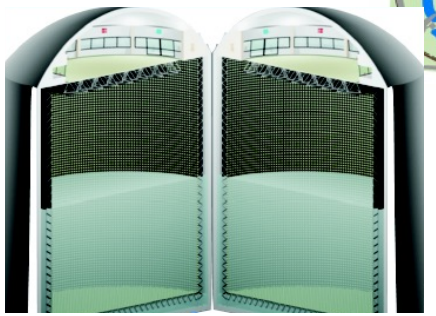

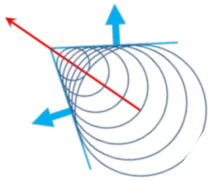

Outline

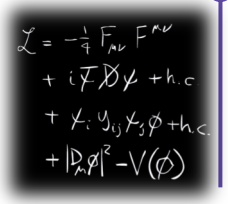

Introduction

The Standard Model

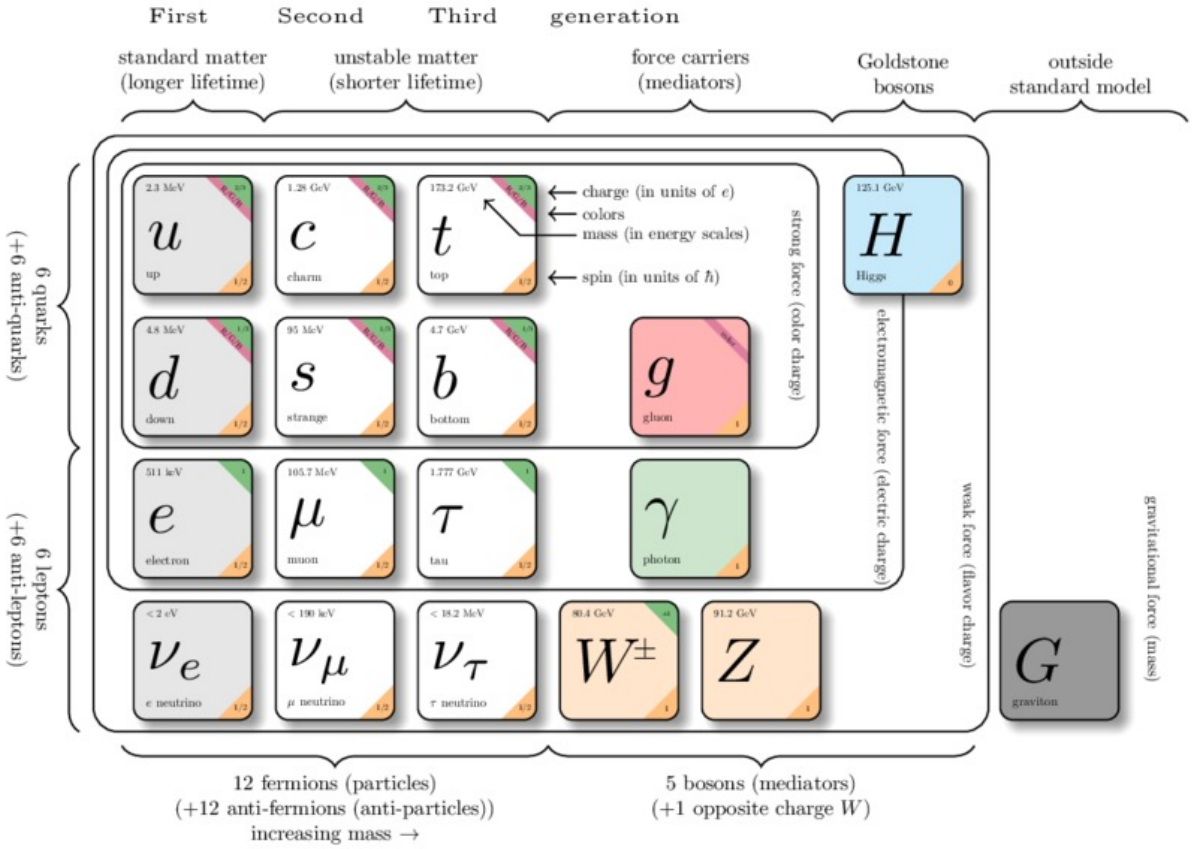

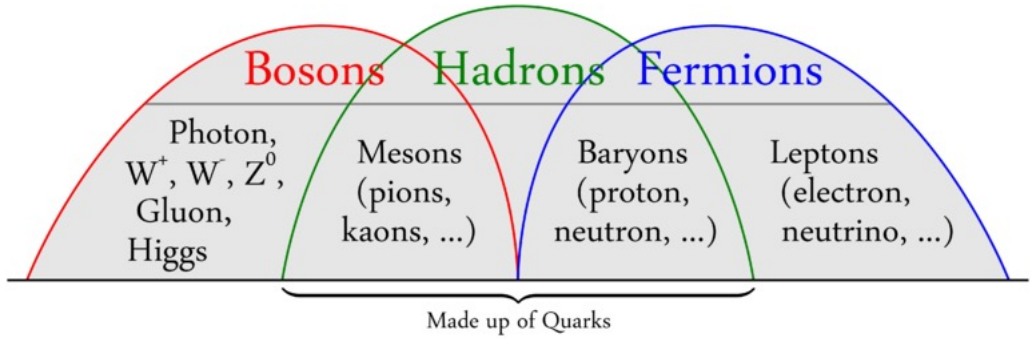

- Particle physics theory describing the fundamental particles and their interactions
- **Fermions** - Fermi-Dirac statistics
  - Building blocks of matter
  - Half-integer spin
  - Quarks and Leptons
- **Bosons** - Bose-Einstein statistics
  - Force carriers mediating interactions
  - Integer spin
  - Gauge bosons (gluon, photon, $W^{\pm}$, Z)
  - Scalar bosons (Higgs)
- **Mathematical Formalism**
  - $\mathcal{L} = \mathcal{L}_{EW} + \mathcal{L}_{QCD} + \mathcal{L}_{Higgs} + \mathcal{L}_{Yukawa}$
  - Based on QFT
  - Built on the Gauge group $SU(3)_C \times SU(2)_L \times U(1)_Y$

The Large Hadron Collider (LHC)

- World's largest and most powerful particle accelerator
- 27 km circumference
- Accelerates and collides hadrons (p-p and ion-ion collisions)
- LHC upgrades to HL-LHC
  - Operational by 2029
  - Peak Luminosity 7.5 x 10^{34} cm^{-2} s^{-1}
  - Experiments upgrades required

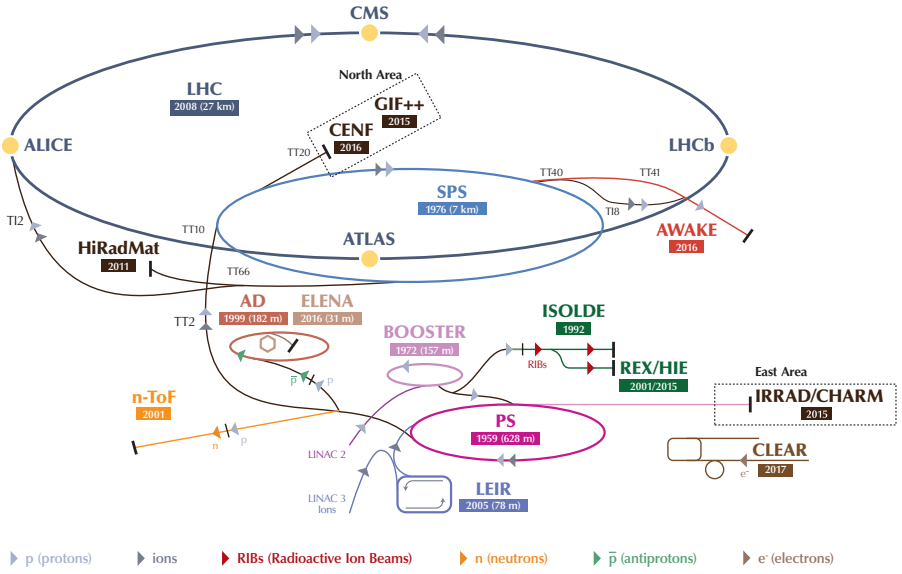

LHC - Large Hadron Collider // SPS - Super Proton Synchrotron // PS - Proton Synchrotron // AD - Antiproton Decelerator // CLEAR - CERN Linear Electron Accelerator for Research // AWAKE - Advanced WAKefield Experiment // ISOLDE - Isotope Separator OnLine // REX/HIE - Radioactive EXperiment/High Intensity and Energy ISOLDE // LEIR - Low Energy Ion Ring // LINAC - LINear ACcelerator // n-ToF - Neutrons Time Of Flight // HiRadMat - High-Radiation to Materials // CHARM - Cern High energy AcceleRator Mixed field facility // IRRAD - proton IRRADiation facility // GIF++ - Gamma Irradiation Facility // CENF - CErn Neutrino platForm

Multiple LHC experiments

ATLAS and CMS are general purpose experiments

ALICE heavy-ion physics and LHCb studies b quark

TOTEM, LHCf, MoEDAL-MAPP, FASER, SND@LHC

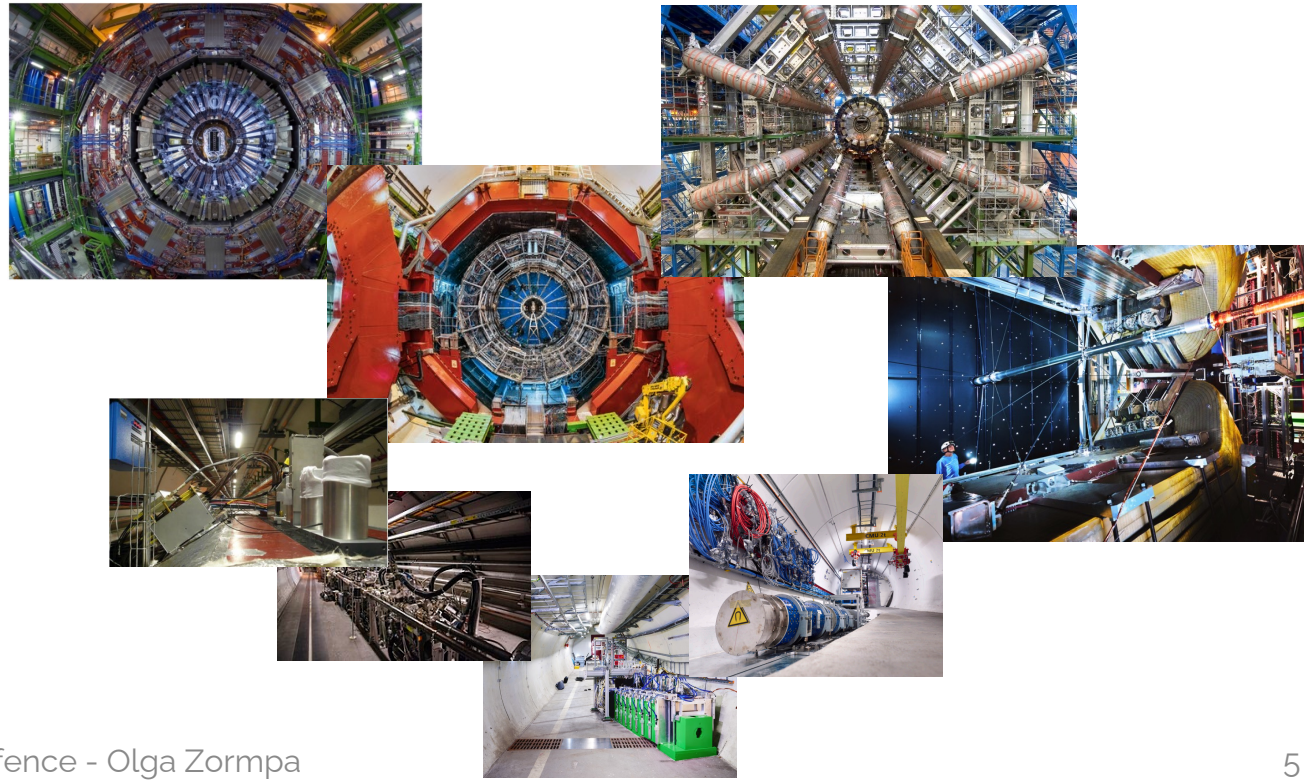

The ATLAS experiment

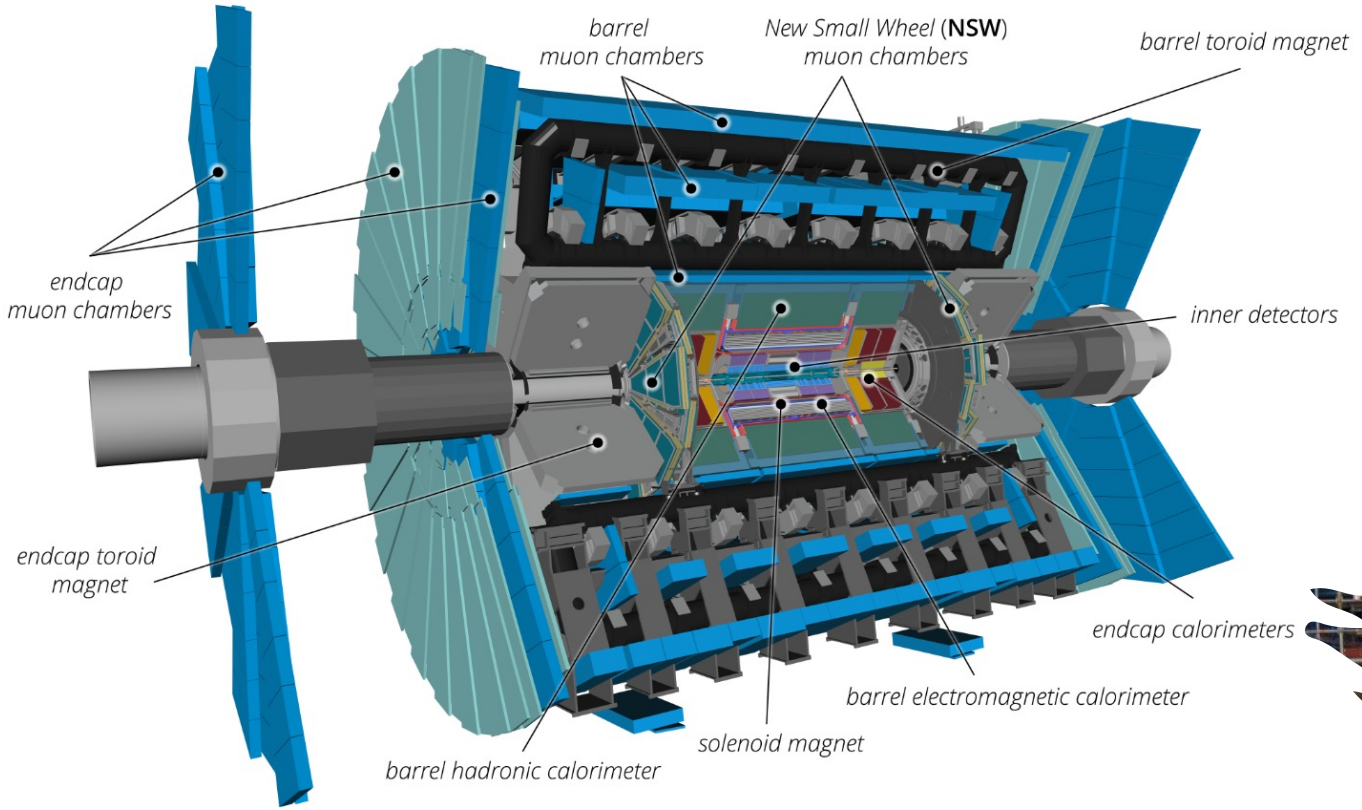

- General Purpose experiment in Meyrin site
- 100 m underground
- Cylinder, 46 m long, 25 m in diameter
- Weights 7,000 tonnes
- Multiple detector subsystems
- Very strong magnet system (solenoid and toroid magnets)

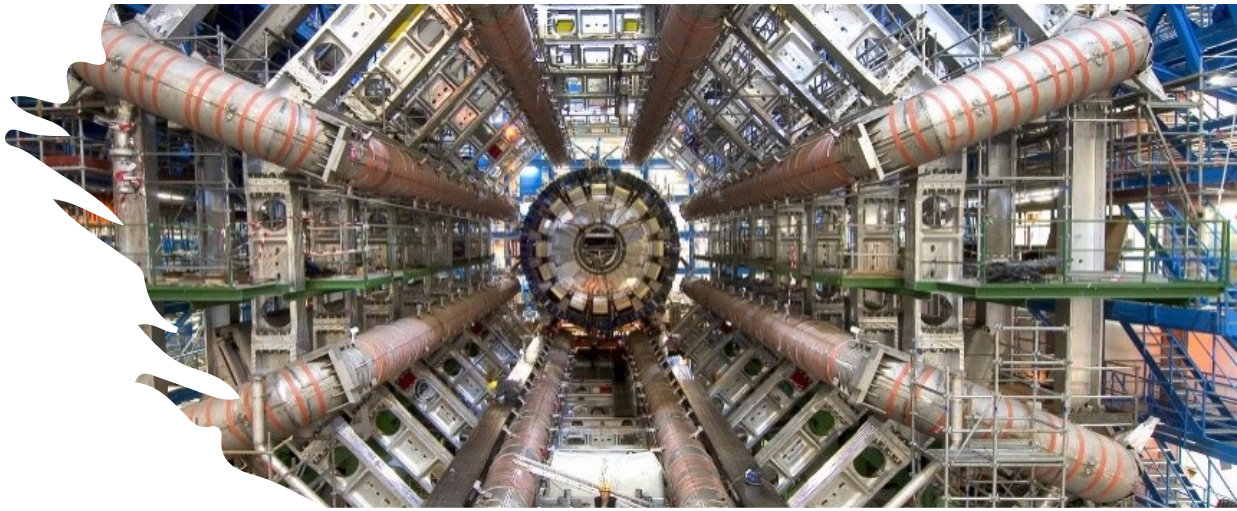

ATLAS Upgrades

Multiple ATLAS upgrades during LS2 (Phase I).

Biggest ATLAS Phase I upgrade:
New Small Wheel

Replacement of the inner station of the muon spectrometer

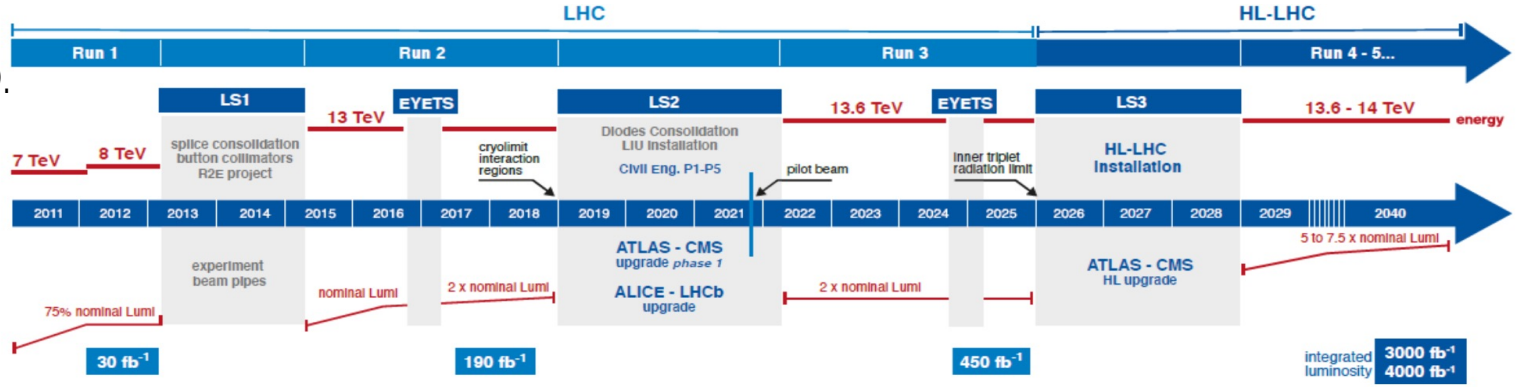

Motivation

- Increasing Luminosity:
  - targeting $L = 2 - 2.5 \times 10^{34}\ cm^{-2}s^{-1}$ during Run-3
  - up to $L = 7.5 \times 10^{34}\ cm^{-2}s^{-1}$ at HL-LHC era
- High pile-up during Run-3 and HL-LHC
  - expected average pile-up level during Run-3 $< \mu > = 60 - 65$

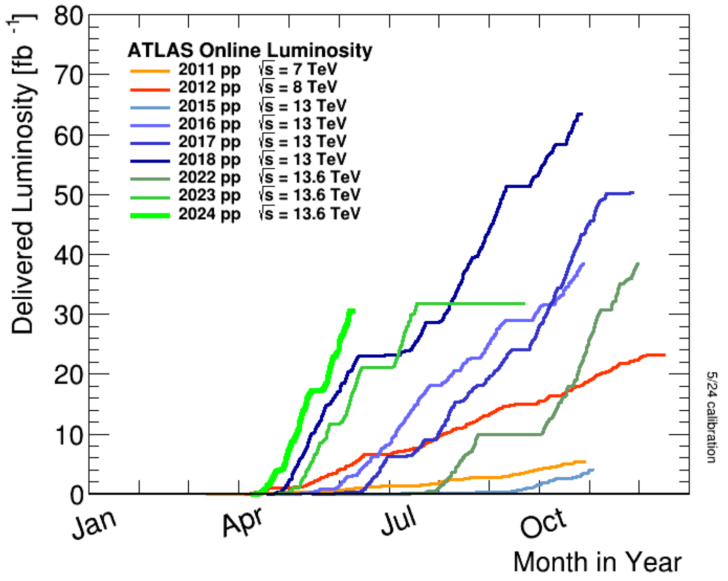

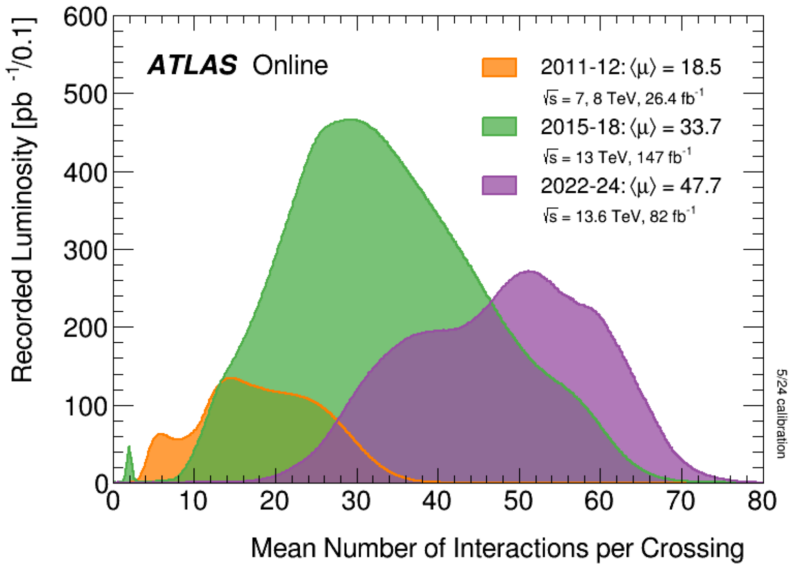

ATLAS Upgrades

- NSW: 2 new detector technologies
  - Micromegas (MM)
  - Small-strip Thin Gap Chambers (sTGC)
- Replace old SW
  - Not optimized for HL-LHC
  - Faced issues related to aging and radiation damage
- New Small Wheel can cope with rates up to $20\ kHz/cm^2$
- "Fake" muons triggers elimination in the endcap region
  - According to ATLAS TDR 90% of muon trigger rate at the endcap region are "fake" triggers!
- Improve accuracy in muon tracking → maintain ATLAS performance
- Improve triggering

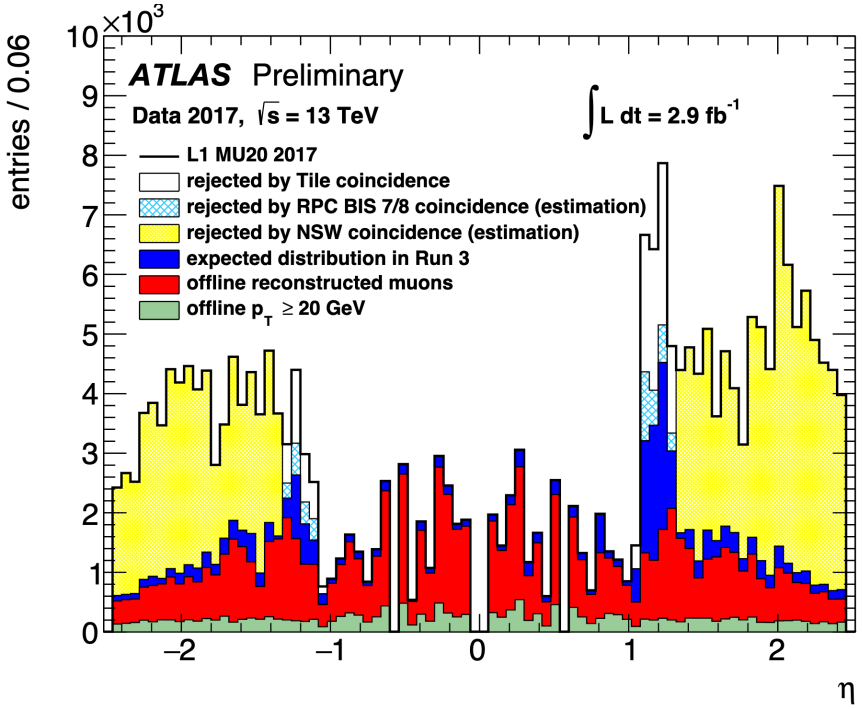

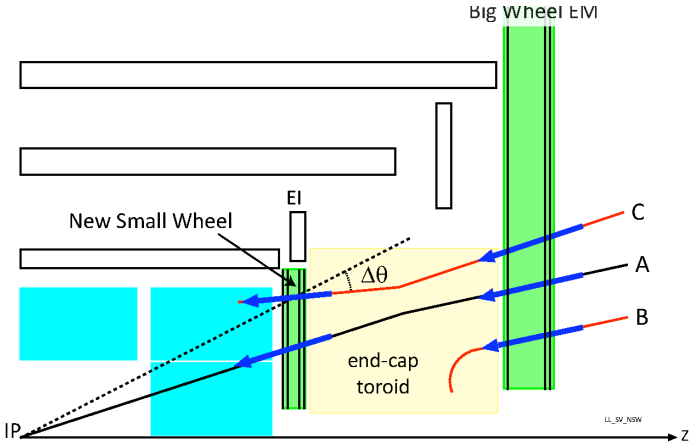

Outline

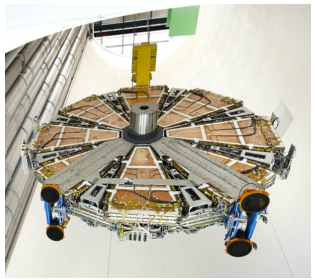

New
Small
Wheel

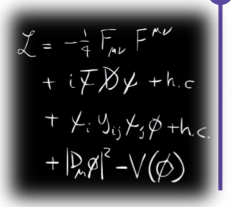

Introduction

New Small Wheel

- 2 new detector technologies
  - Micromegas (MM)
  - Small-strip Thin Gap Chambers (sTGC)
- 2 Wheels
  - Wheel A
  - Wheel C
- 16 Sectors/wheel
  - 8 Small Sectors
  - 8 Large Sectors
- 4 Wedges/Sector (sTGC-MM-MM-sTGC)
  - 2 sTGC wedges
  - 2 MM wedges
- 4 Layers/wedge

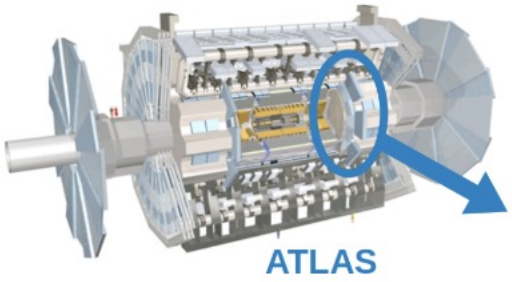

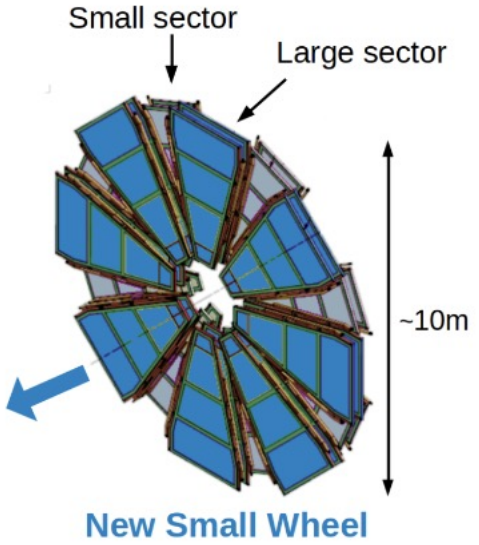

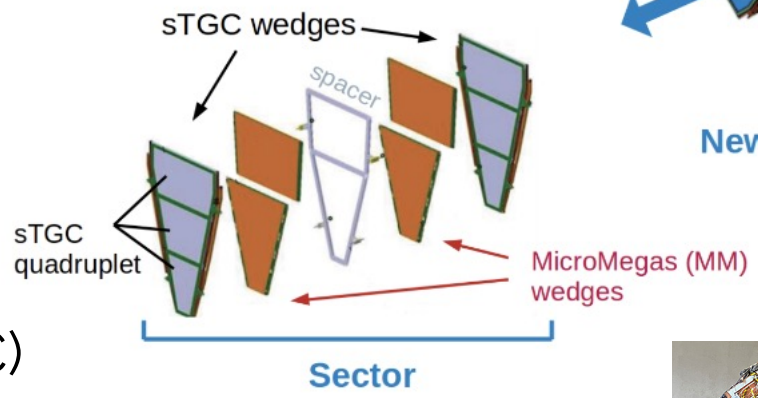

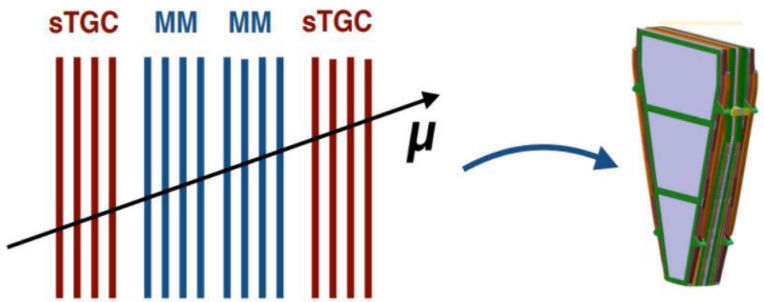

New Small Wheel

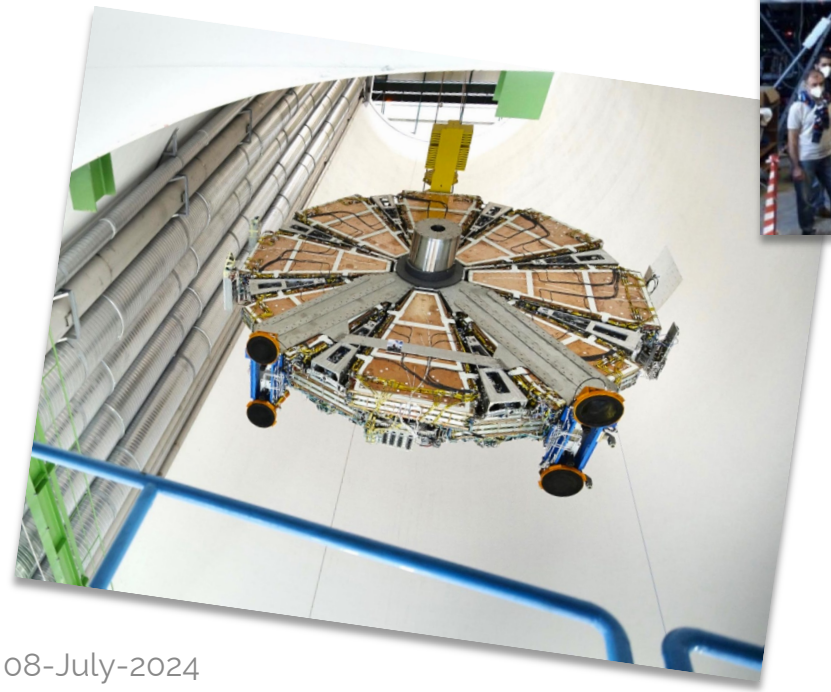

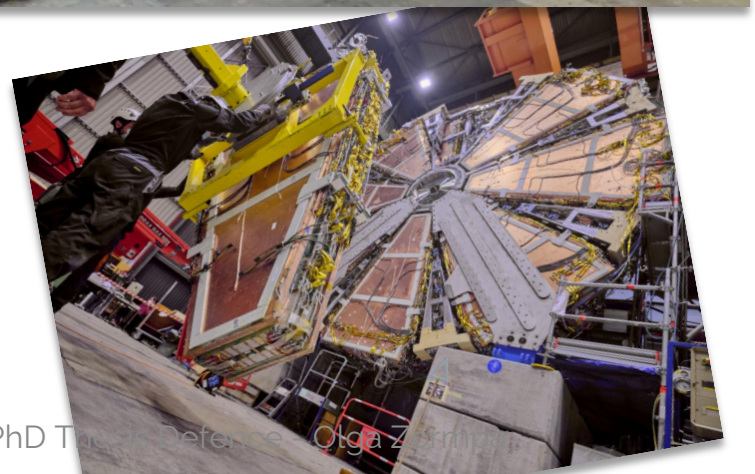

NSW Detectors

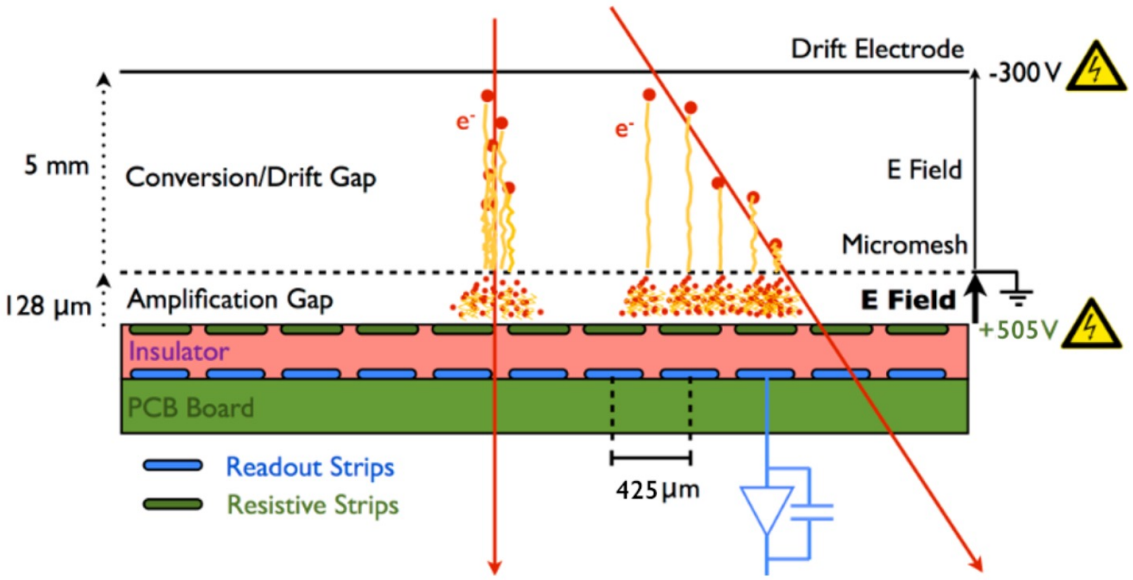

Micromegas Detectors (MM)

- Gaseous Detectors (Ar : CO_2 : iC_4H_{10} - 93 : 5 : 2)
- Mainly for precision tracking, also for trigger
- Good timing resolution
- Spatial resolution < 100 µm independent of track incidence angle
- Good tracking due to 0.4 mm readout strips
- Structure:
  - Planar drift electrode (-300 V)
  - Conversion/Drift Gap (5 mm)
  - Thin metallic mesh (grounded)
  - Amplification Gap (128 µm)
  - Readout electrode covered by insulator and a layer of resistive strips (*to reduce sparks*) (+505 V)

NSW Detectors

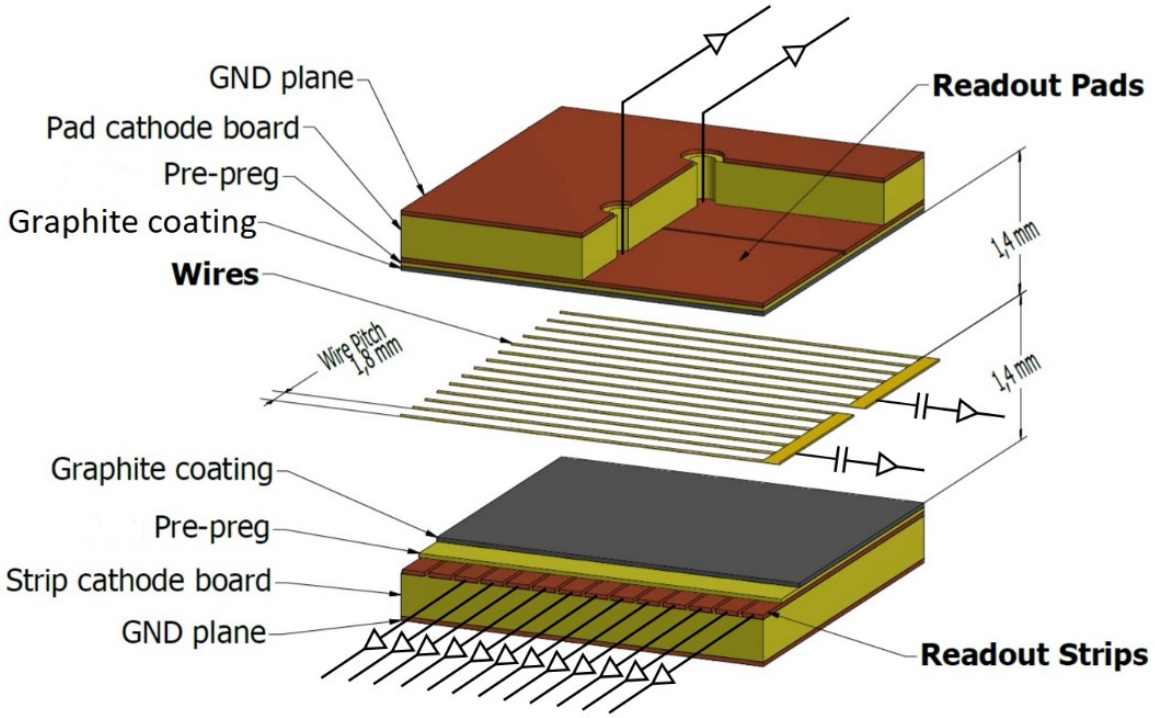

small-strips Thin Gap Chamber (sTGC)

- Gaseous Detectors (**n-pentane : CO_2 – 45 : 55**)
- Mainly for trigger, also for precision tracking
- Good timing resolution - BC identification
  - Drift time for most electrons < 25ns (1 BC)
- Very good position resolution (100 μm)
- Better than 1mrad angular resolution
- Structure:
  - Grid of 50 μm gold-plated tungsten wires - anode (1.8 mm pitch) (2800 V)
  - 2 cathode planes 1.4 mm from anode with surface resistivity 100 kΩ/□
    - Strips (3.2 mm pitch) perpendicular to wires
    - Pads (H=8 cm, W depends on the pad position)

NSW TDAQ electronics

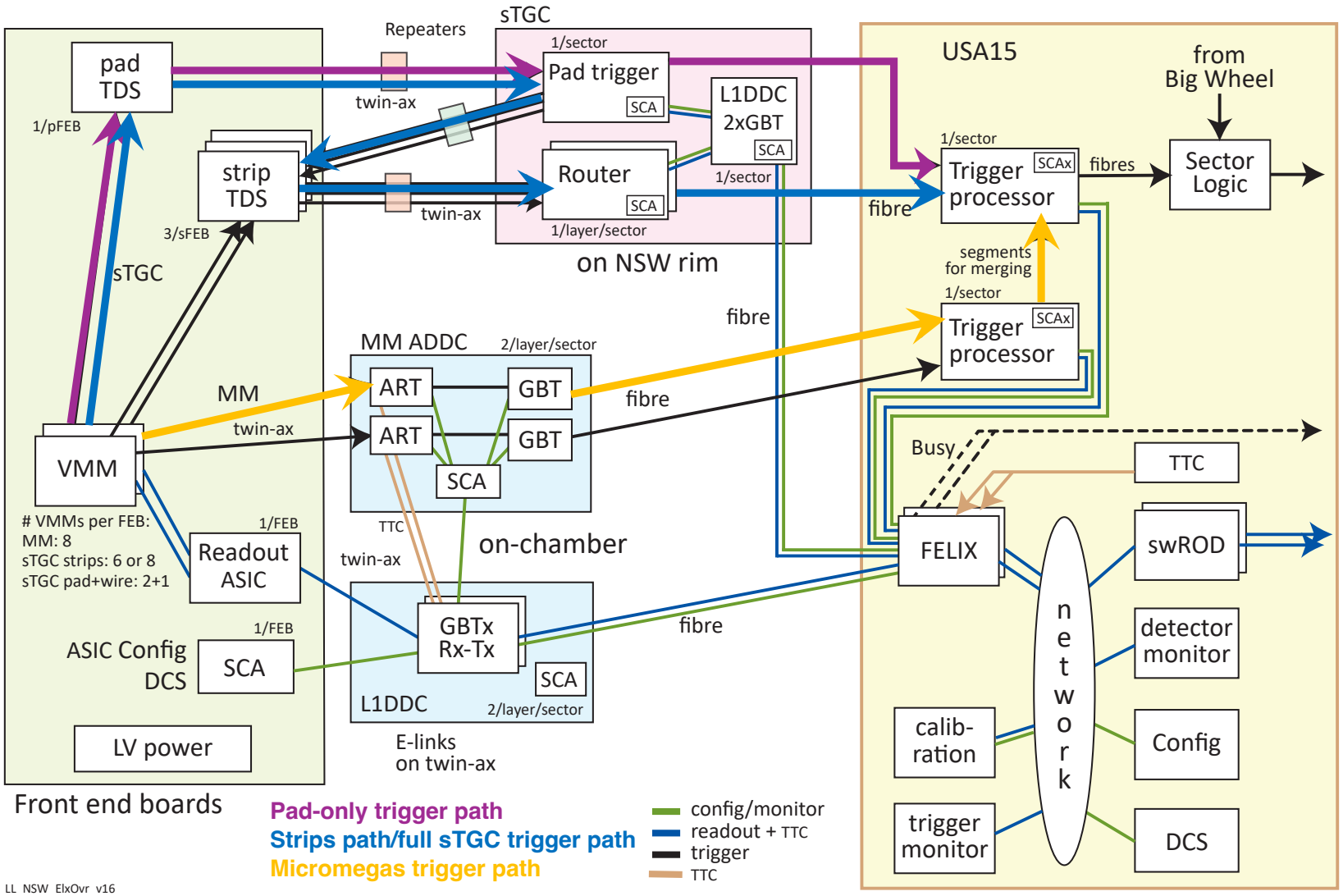

Custom ASIC chips + FPGA

FEBs:
pFEB, sFEB, MMFE8,
L1DDC
ADDC

Rim Electronics:
Pad Trigger, Router, RimL1DDC

Off-detector:
Trigger Processor
(MM+sTGC+Carrier FPGA/sector)

DAQ system:
FELIX, swROD, ALTI/SBC (TTC)

NSW Trigger Commissioning

Various tests
- Low Voltage checks
- Communication with FELIX
- OPC and SCA communication checks (Pri and Aux SCA)
- Optical power measurements
  - FELIX fibers in Rim-L1DDC board
  - Direct Clock fibers in Rim-L1DDC board
  - Pad Trigger and Router fibers in Trigger Processor

Connectivity Tests
- PFEB to Pad Trigger path (*next slide*)
- Pad Trigger to SFEB path (*next slide*)
- SFEB to Router path (*next slide*)
- Pad Trigger to Trigger Processor
- Router to Trigger Processor

Data transmission quality tests
- PFEB to Pad Trigger (24 electrical links)
- SFEB to Router (12 electrical links per Router, total of 96 links)
- Pad Trigger to Trigger Processor
  (2 optical links - 1 duplex TX/TX fiber)
- Router to Trigger Processor (*next slide*)
  (4 optical links - 2 duplex TX/TX fibers per Router, total of 32 optical links)

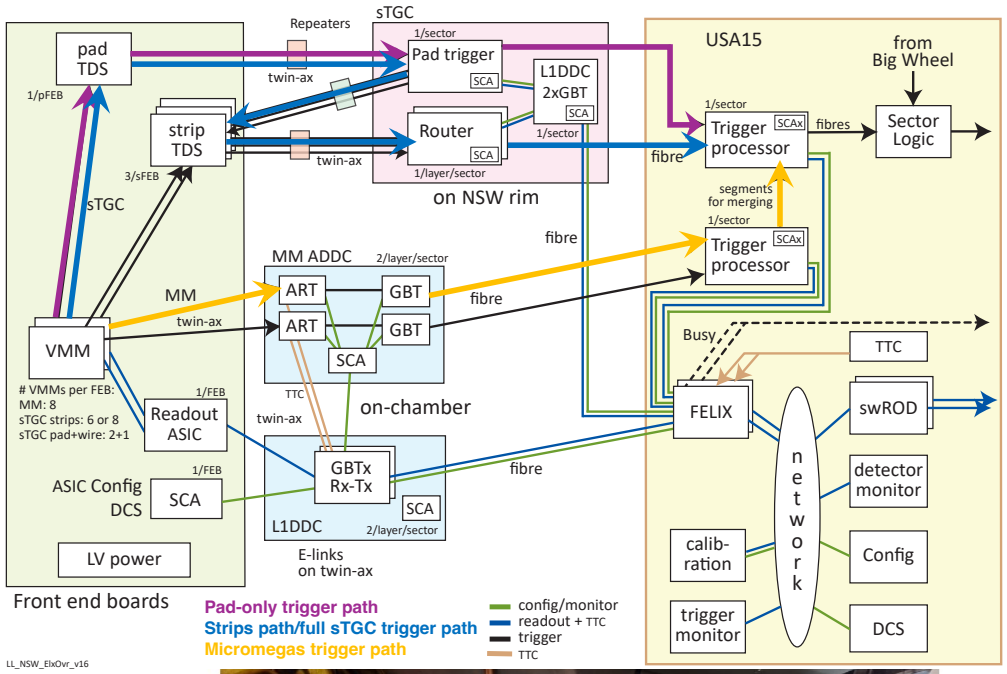

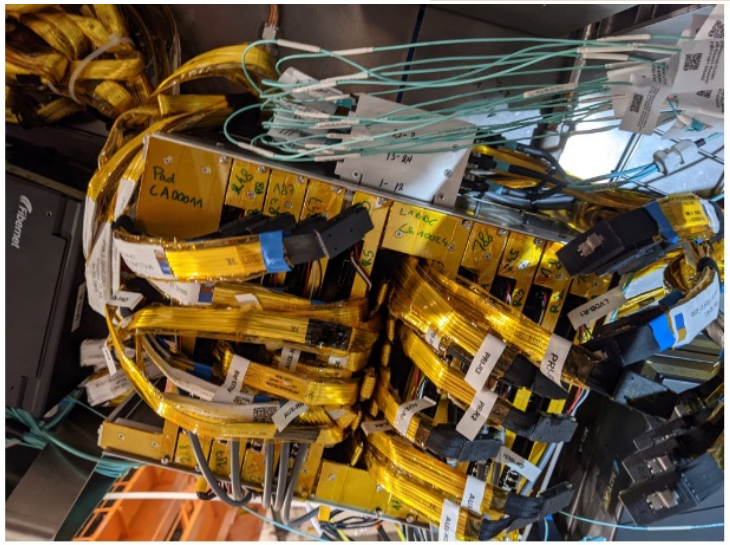

Selected Results – P1

Pad Connectivity

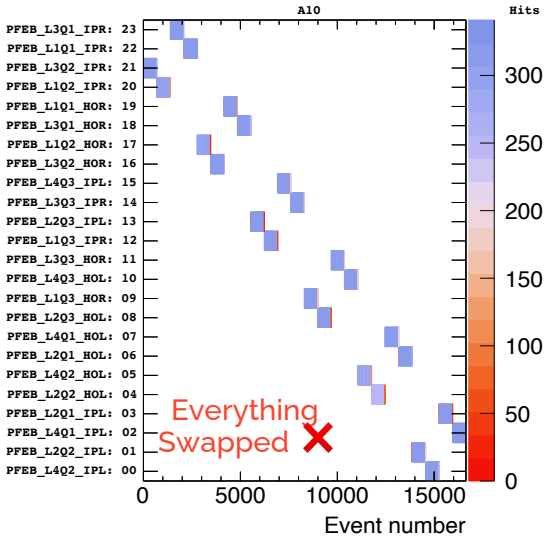

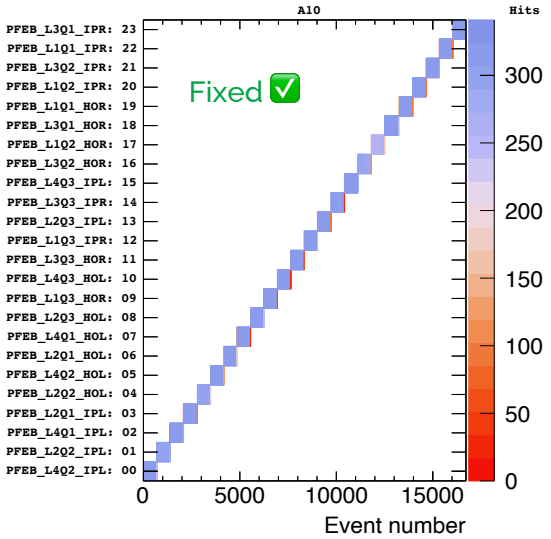

Strip Connectivity

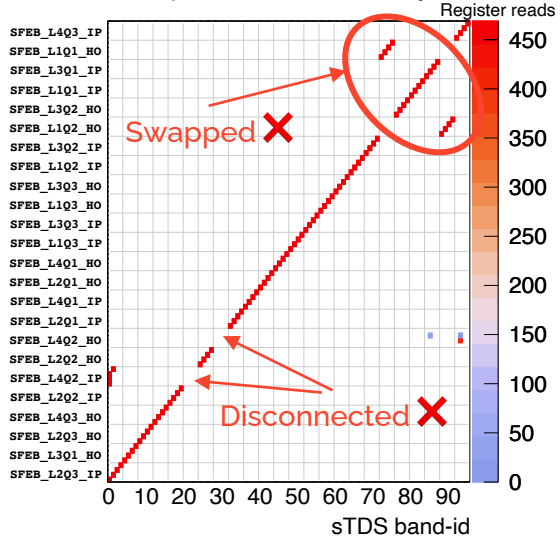

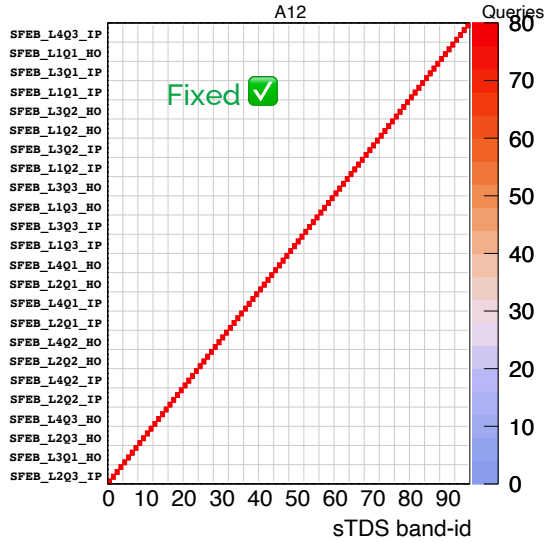

Router Connectivity

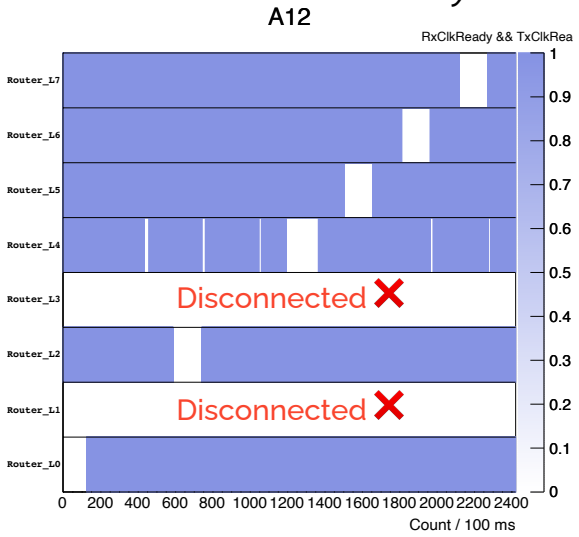

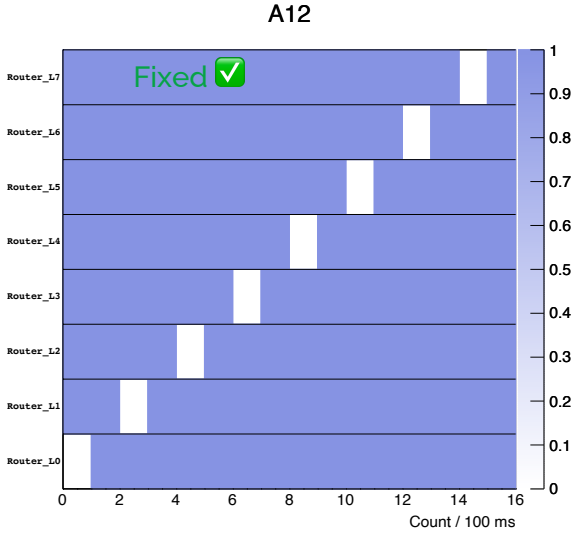

Router-TP Eye Diagrams

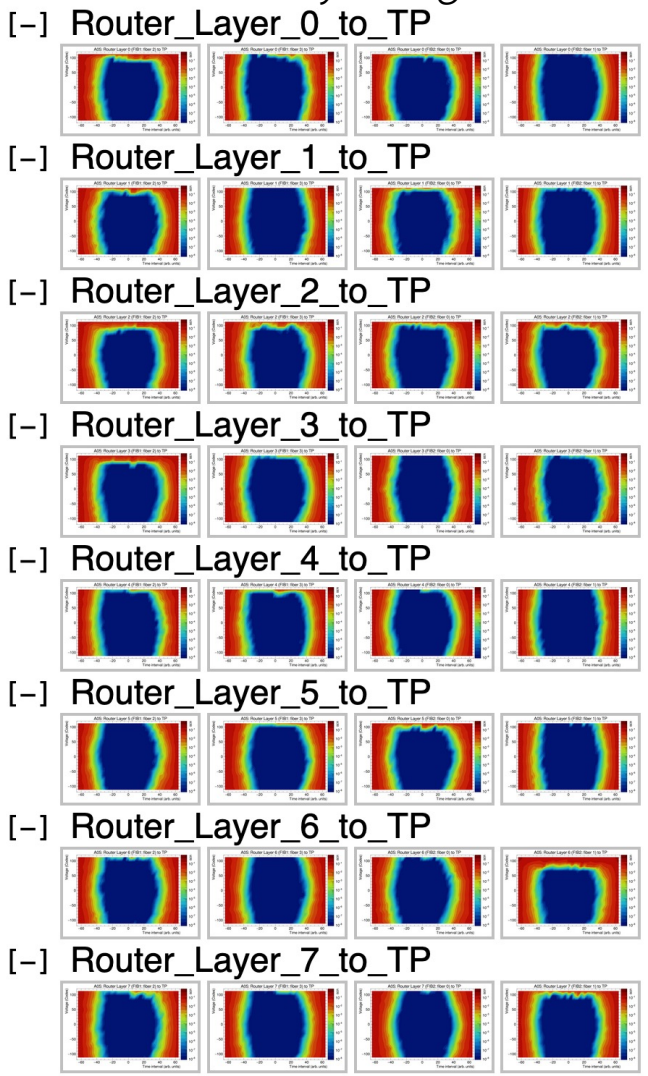

NSW Trigger @ Run-3

- NSW Trigger has participated in ATLAS Trigger decision with pad-only trigger path.
- Prioritize and integrate Pad Trigger while giving the chance to MM and sTGC strip paths to continue their commissioning and validation and be merged as soon as they are ready
- Main goal:
  - Extrapolating from 2022, Hybrid <μ>~60 would result in ~101 kHz at L1 with deadtime above 5%
  - Even pad-only trigger → Decrease L1A rate by ~8 kHz

Estimates for I_b=1.8x10^{11}ppb (target for 2023)

Brian Peterson		8b4e	Hybrid	36b	48b
	#coll bunches	1967	2440	2484	2740
μ=54	L_{peak} [x10^{34}cm^{-2}s^{-1}]	1.5	1.86	1.89	2.1
	$L_{int.,day}$ [fb^{-1}]	1.00 (-11%)	1.25 (+10%)	1.27 (+12%)	1.4 (+24%)
μ=60	L_{peak} [x10^{34}cm^{-2}s^{-1}]	1.65	2.05	2.08	2.3
	$L_{int.,day}$ [fb^{-1}]	1.07 (-5%)	1.32 (+17%)	1.35 (+20%)	1.49 (+32%)
μ=65	L_{peak} [x10^{34}cm^{-2}s^{-1}]	1.8	2.23	2.27	2.5
	$L_{int.,day}$ [fb^{-1}]	1.11 (-0%)	1.39 (+24%)	1.42 (+26%)	1.57 (+39%)

2023?

Only accounts for 4h turn-around, not availability

Leveling: ~12h
Optimal fill: 15.5h

Leveling: ~10h
Optimal fill: 14h

Leveling: ~9h
Optimal fill: 12.5h

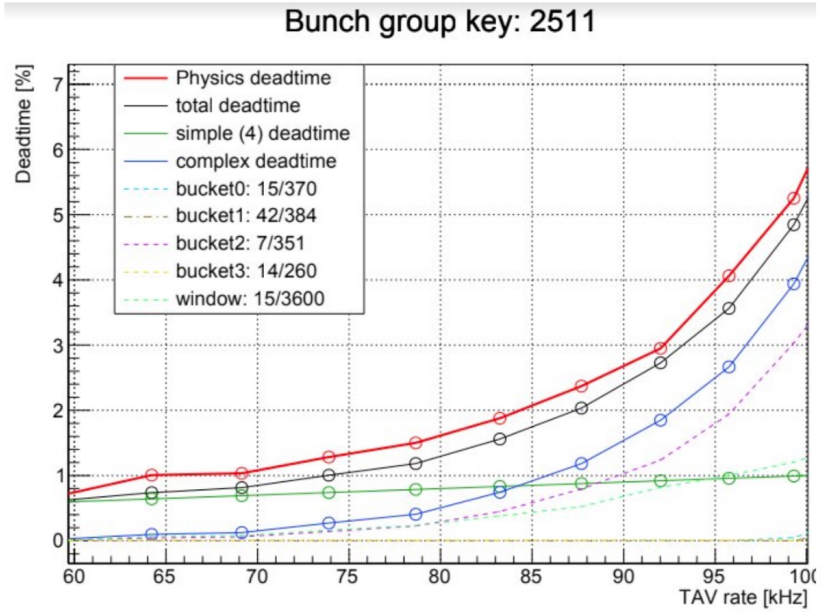

Pad-only Trigger – What changed?

The Stretching

Timing problems → Stretching logic introduced in Pad Trigger and Trigger Processor

- Configurable option in both boards
- PT **stretches the hits** by 2 BCs (duplicate incoming hits in the next 2 BCs)
- TP **stretches the trigger** by 1 BC (duplicate the trigger in the next BC)
  - Duplicate removal mechanism is applied

Caveat!

PT: Up to 4 trigger segments/BC

segments (bandID/phiID/BCID)

TP: Up to 8 trigger segments/BC

segments (R-index/phiID/BCID)

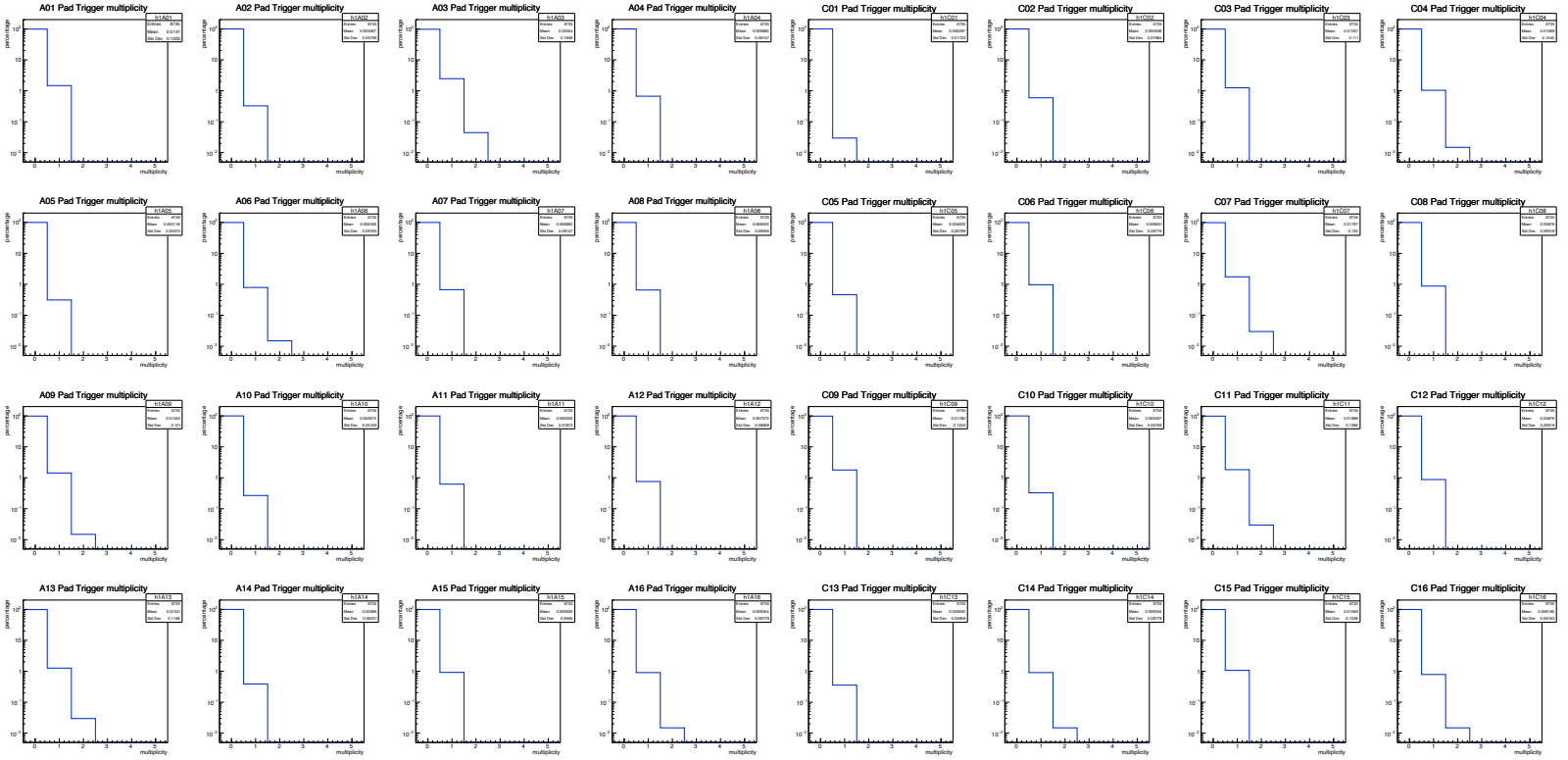

Pad-only Trigger – What changed?

The coincidence logic

- Our detectors are not perfect, HV issues, FEBs that fail to be configured, missing FEBs etc.
- 3/4 AND 3/4 coincidence logic was replaced by **2/4 AND 3/4 coincidence logic**.
  - Configurable choise.

New Pad Trigger Patterns

- New patterns were created to cover the transition regions between quads.

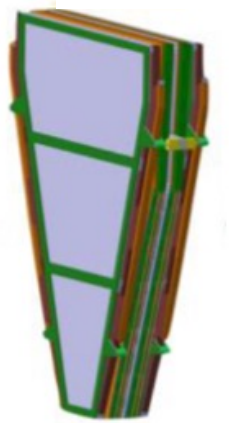

Run 454163
A10: No patterns in the transition regions

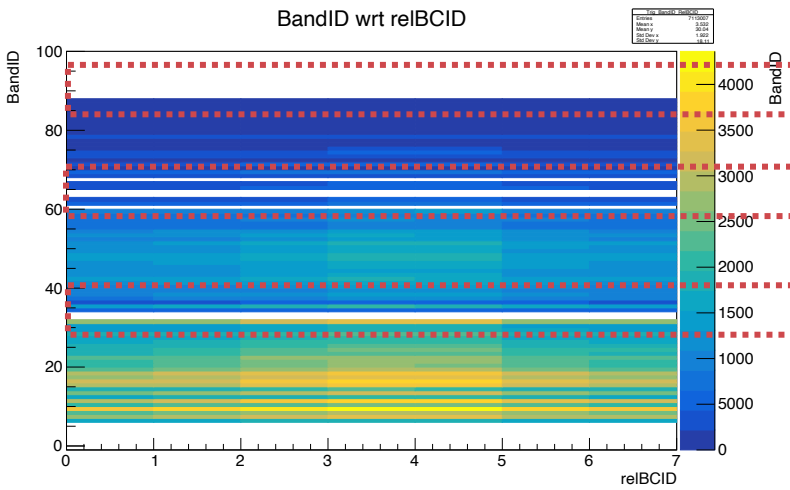

Run 454188
A10: Patterns in the transition regions

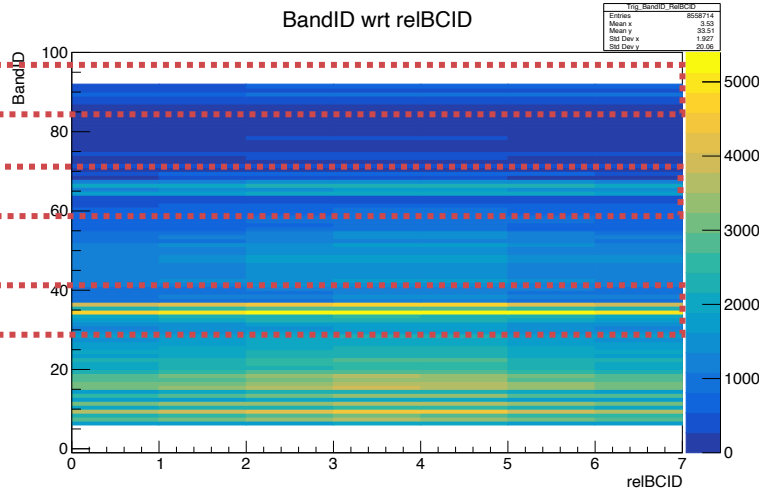

Pad-only Trigger – What changed?

Other Changes

- Option to mask to 1 or mask to 0 Pad Trigger channels
- Trigger Processor adjusted TTC phases to guarantee fixed latency to Sector Logic
- MM trigger was just included in trigger decision but its inclusion is a configurable option
- A safety check is included on the TP side. If the synchronization between PT and TP is lost the TP masks the output to the SL and sends only null segments.
- STG Pad Trigger and Trigger Processor L1A is in place, further optimization is ongoing

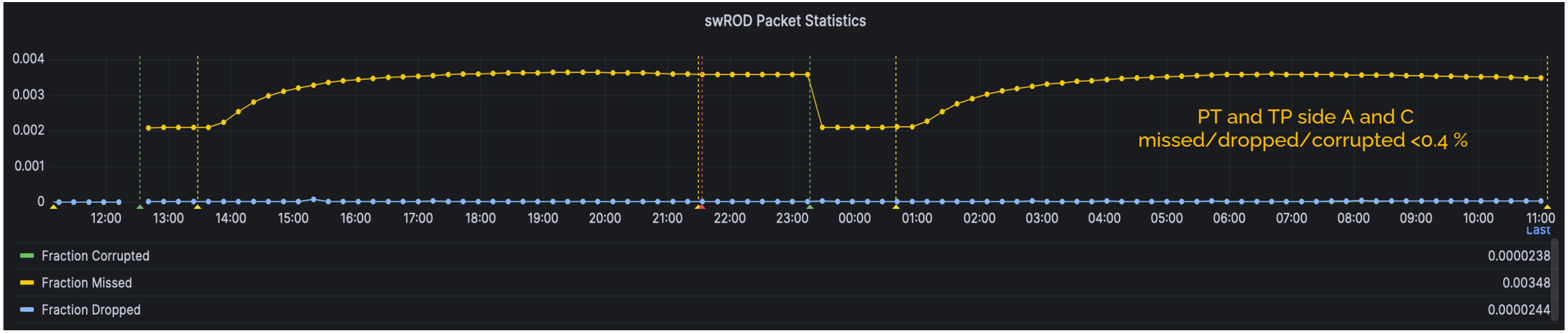

Online/Offline monitoring

- Grafana dashboards
  - NSW Trigger registers
    published in ATLAS partition IS
  - NSW Trigger FELIX/swROD status
  - NSW Trigger BCID select
    sync PT BCID with LHC Isolated Bunch BCID
- GNAM Online plots
  - Pad Trigger
  - Trigger Processor
- Shifter Assistant
  - Definition of conditions that trigger messages to the Muon Shifter
- Small contribution in debugging Muon Tester Ntuples and creating a pad-only trigger analysis framework

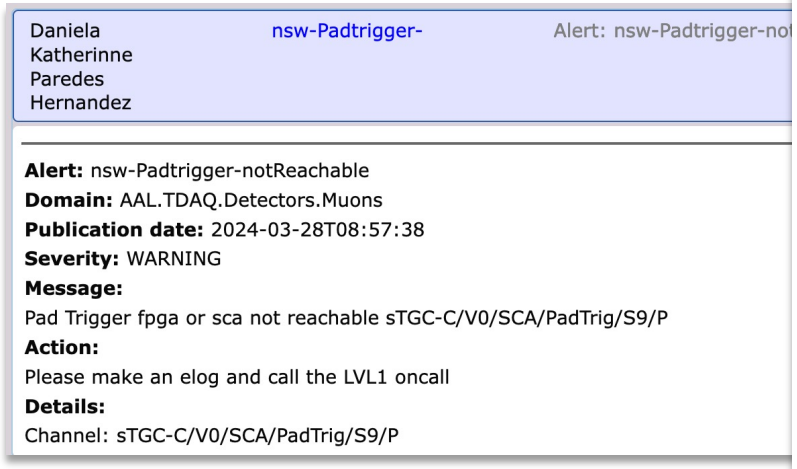

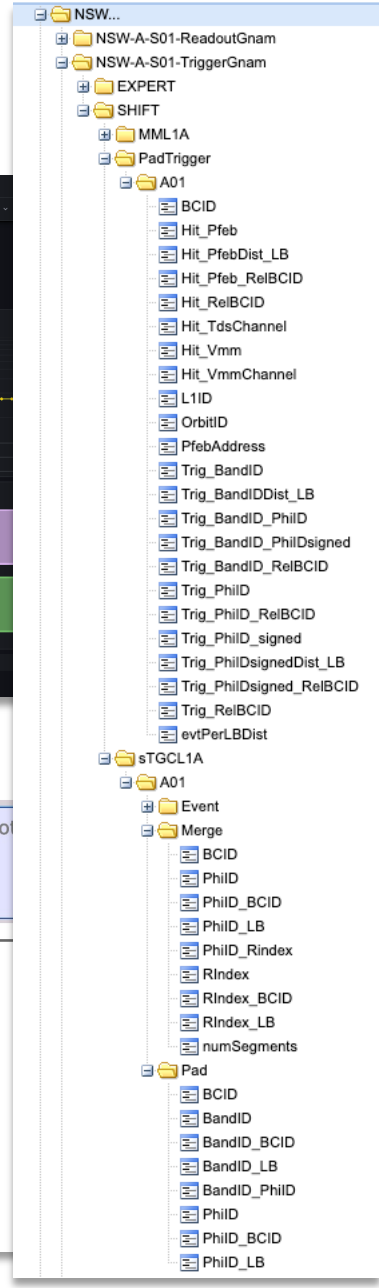

Some results – SL side

- *Public L1Muon Endcap trigger*
- *Data 2023*
- *Transverse momentum (p_T) threshold of 14 GeV (L1_MU14)*
- *sTGC pad-only trigger included*

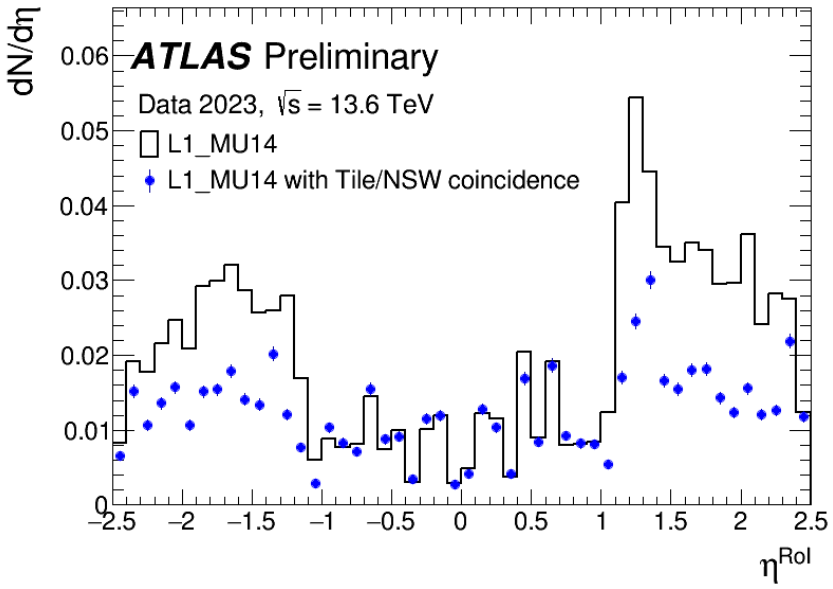

The pseudorapidity (η) distribution of the level-1 ROIs, which fulfil the primary level-1 muon trigger. The rate reduction at $L = 2{\times}1034\ cm^{-2}s^{-1}$ was 8 kHz.

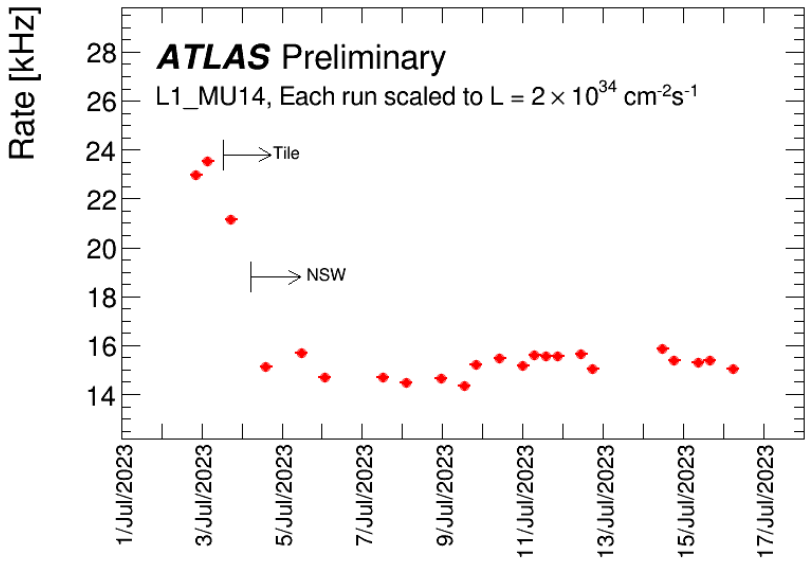

The trigger rate of the primary level-1 muon trigger. The rate reduction at $L = 2{\times}10^{34}\ cm^{-2}s^{-1}$ was measured as ~2 kHz by Tile and ~6 kHz by NSW. NB during 2023 ~70% of NSW was included in ATLAS trigger

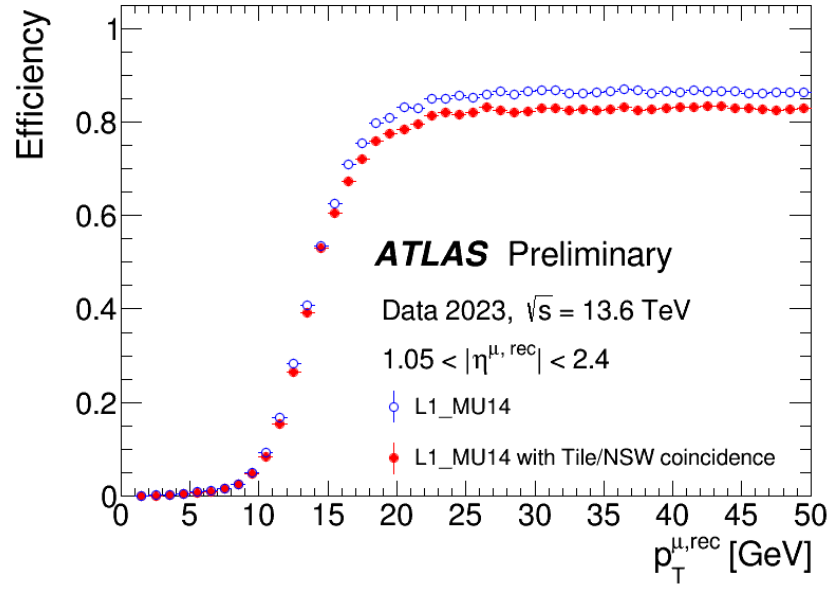

Efficiency of the primary level-1 muon trigger, during Run-3. The additional inefficiency attributed to the Tile/NSW coincidence is approximately 4%

Some results – SL side

- *Public L1Muon Endcap trigger*
- *Data 2024*
- *Transverse momentum (p_T) threshold of 14 GeV (L1_MU14FCH)*
- *sTGC pad-only trigger included*

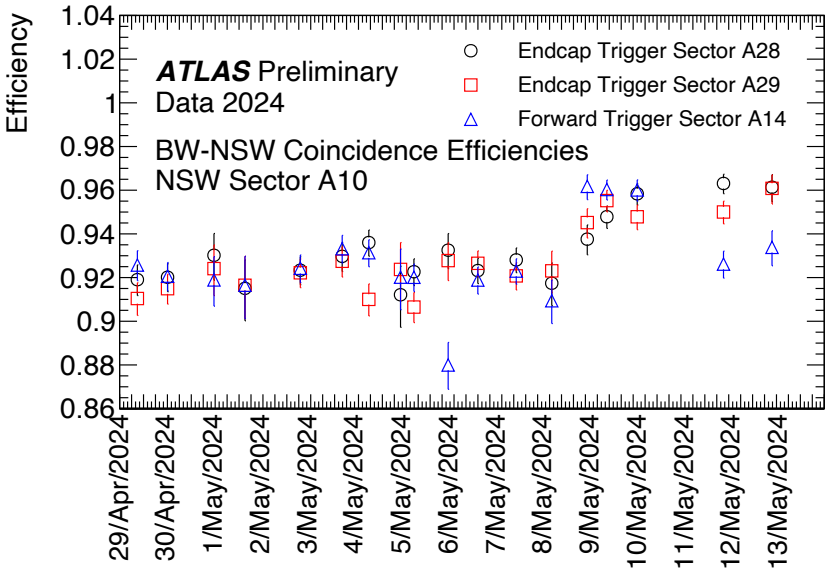

Relative efficiency of the coincidence between the TGC BW and NSW detectors compared to BW-only triggered events for A10 as a function of date. On 09/05, candidates from the MM have been merged to improve efficiency.

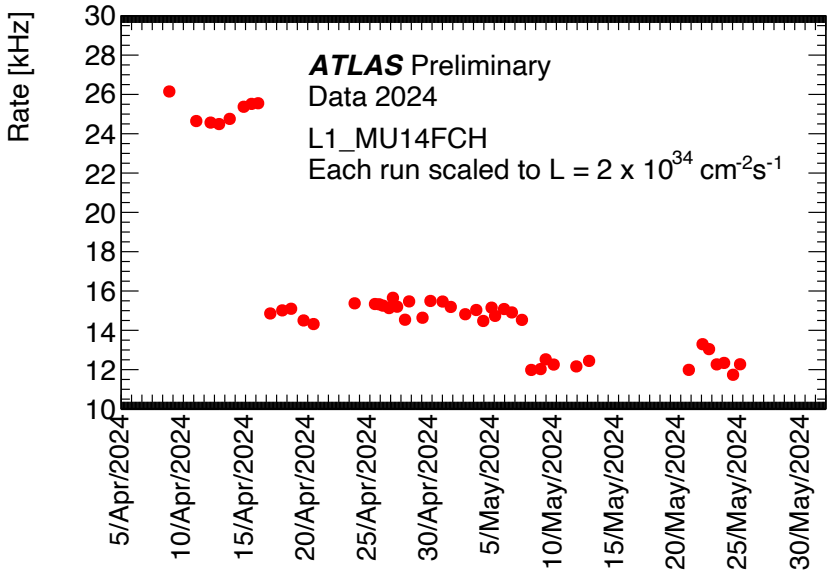

The trigger rate of the primary level-1 muon trigger. The rate reduction at $L = 2{\times}10^{34}\,cm^{-2}s^{-1}$ was measured as:

17/04: Tile + NSW (65%) **~10 kHz**

08/05: Tile + NSW (85%) **~13 kHz**

21/05: Tile + NSW with MM (65%) **~14 kHz**

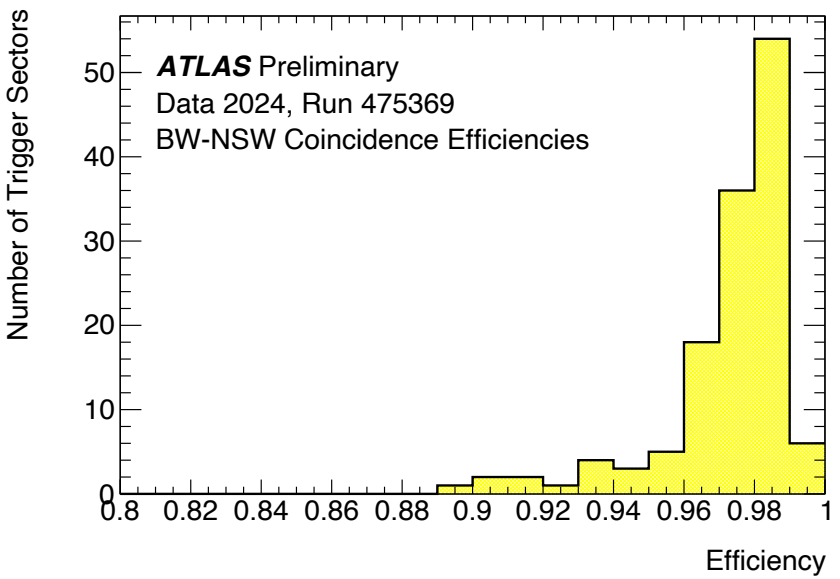

Efficiency of the primary level-1 muon trigger, during Run-3. The additional inefficiency attributed to the Tile/NSW coincidence is approximately 4%

Some results – NSW side

Pad Efficiencies Run 474991 @ 13.6 TeV

2/4 & 3/4 with Targeted masking implemented in all sectors

C05/C09 (known connectivity problems)

A10 (used by MMG)

125/144 (87%) of sectors included in ATLAS trigger decision

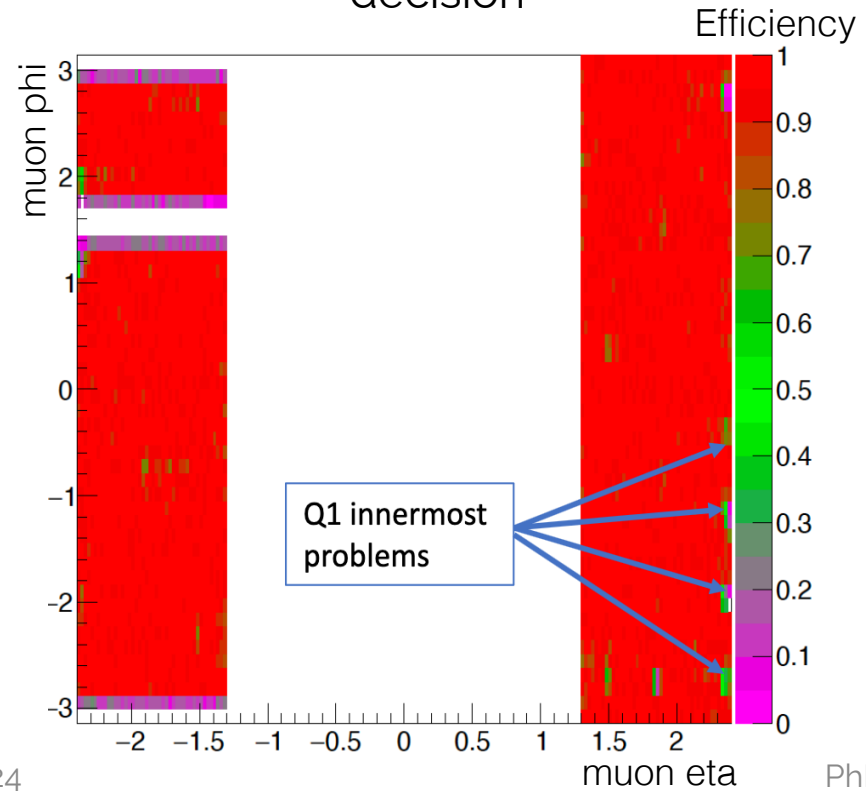

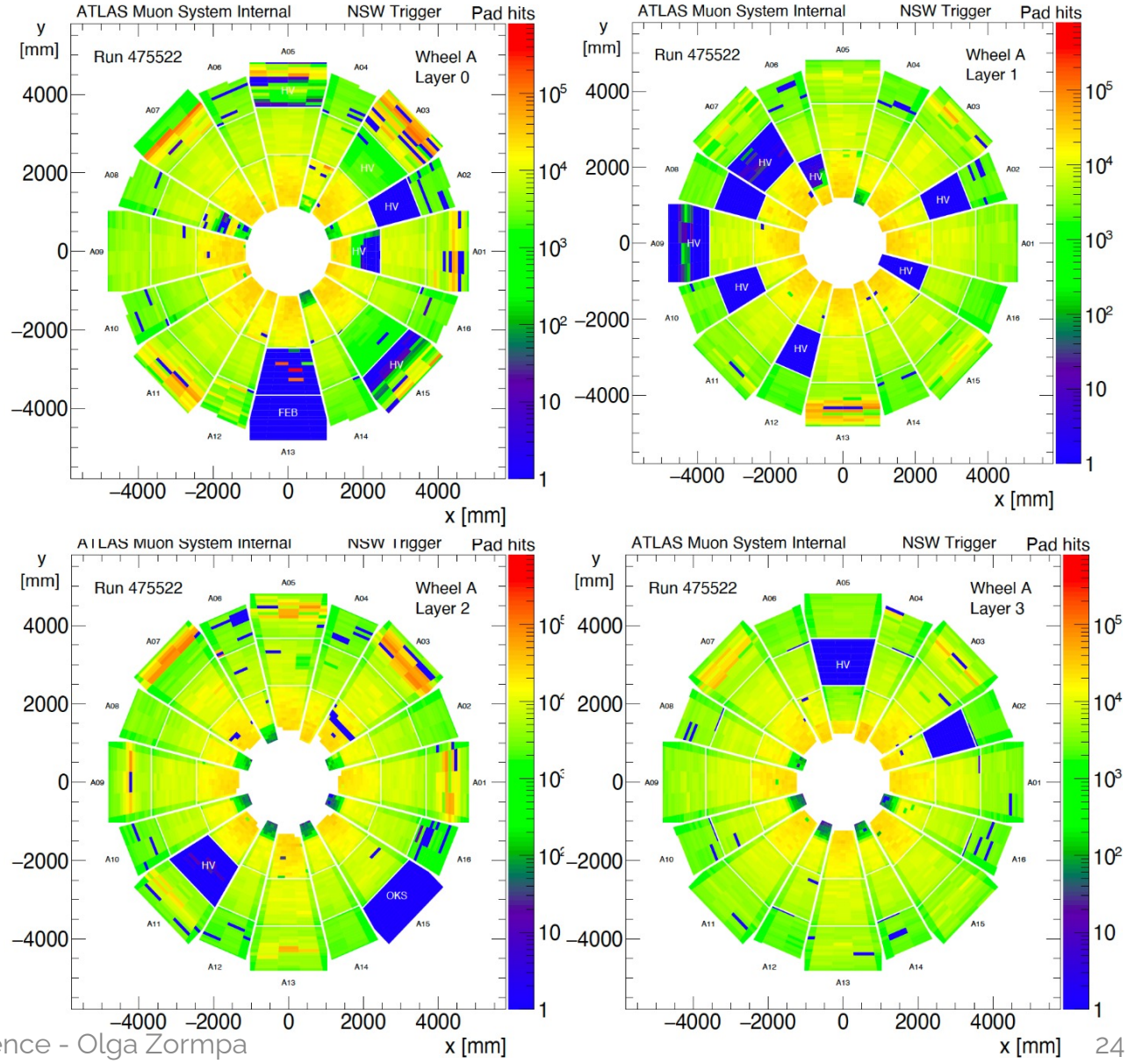

Some results – NSW side

Run 476718

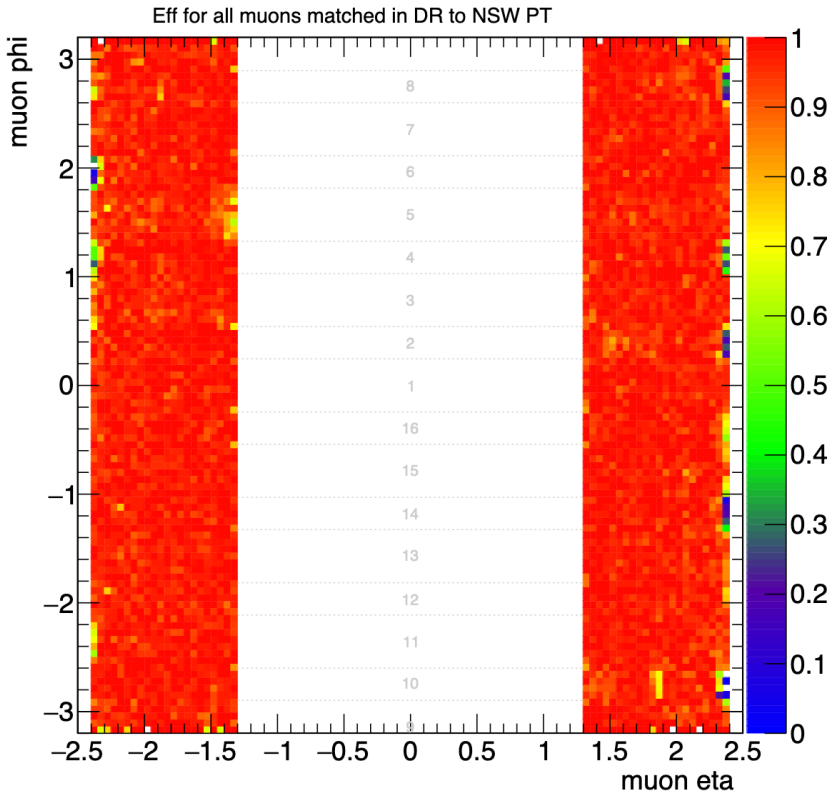

Pad Trigger

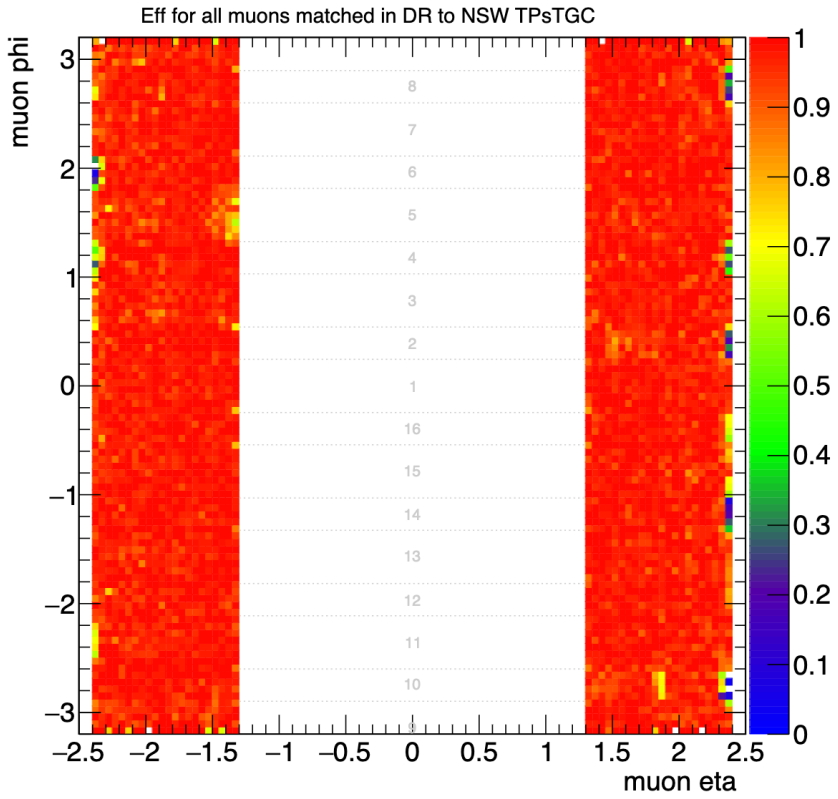

Trigger Processor (pad-only)

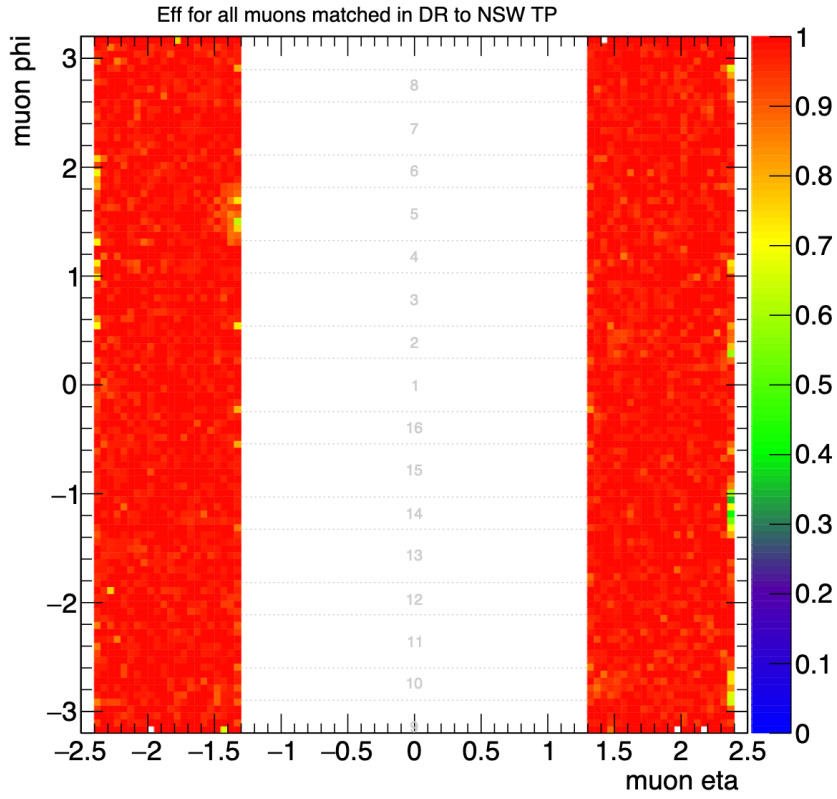

Trigger Processor (pad-only + MM)

Outline

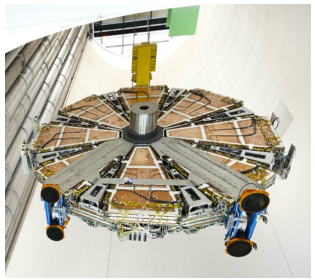

New
Small
Wheel

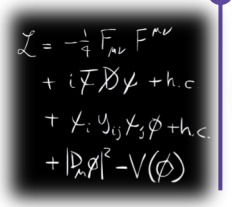

Introduction

Test
Beam

Test Beam setup

- October-November 2021 @ CERN GIF++.
- First extensive study with the final electronics, full readout chain and high-rate backgrounds
- No rim crate electronics were included
- QL1C quadruplet placed in the Micromegas frame
- Gas Mixture: CO2 + n-Pentane (45%)
- HV = 2.8 kV (also scanned 2.75kV-2.95kV)
- Beam size: 10 cm in radius
- Scintillator coincidences used:
  - GIF scintillators ~40x40cm² covering entire beam area
  - 4 scintillator coincidence (sTGC scintillators + GIF scintillators) ~2x5cm² (overlap) covering a 4-layer pad tower
- Source conditions:
  - ^{137}Cs source available for irradiation
  - Rate = 13.08 kHz/cm²
  - Attenuations factors: 1, 1.5, 2.2, 3.3, 4.6, 6.9, 10, 15, 22, 46, 100
- Angle with respect to the beam direction: 0°, 10°, 20°, with respect to the vertical level

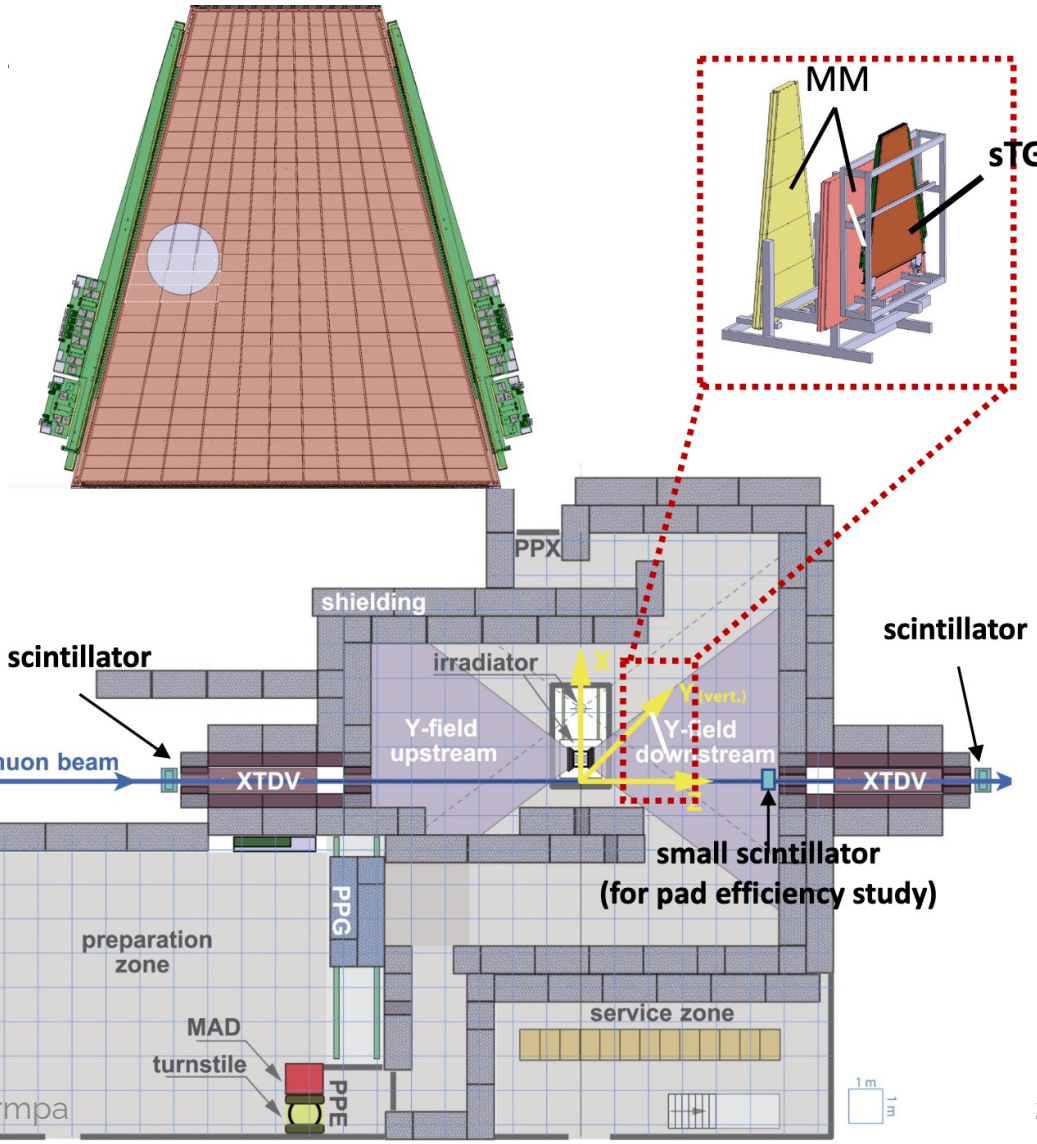

Test Beam setup

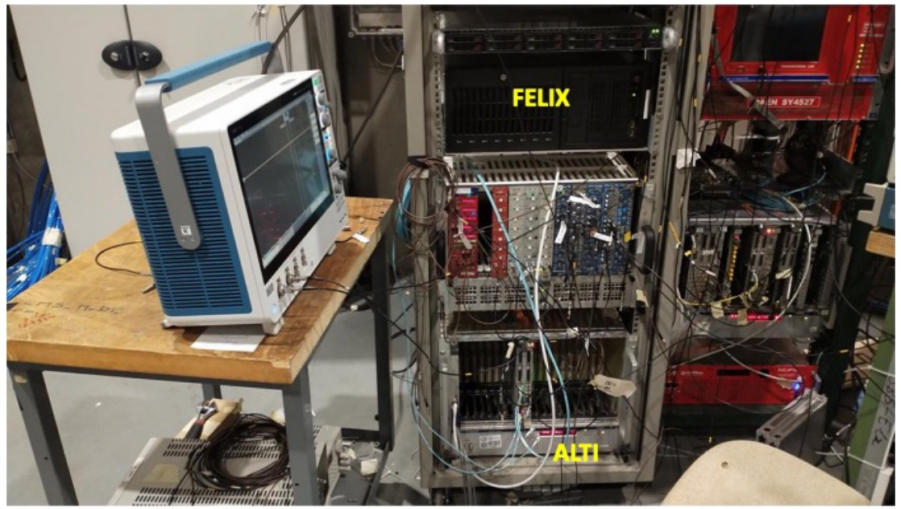

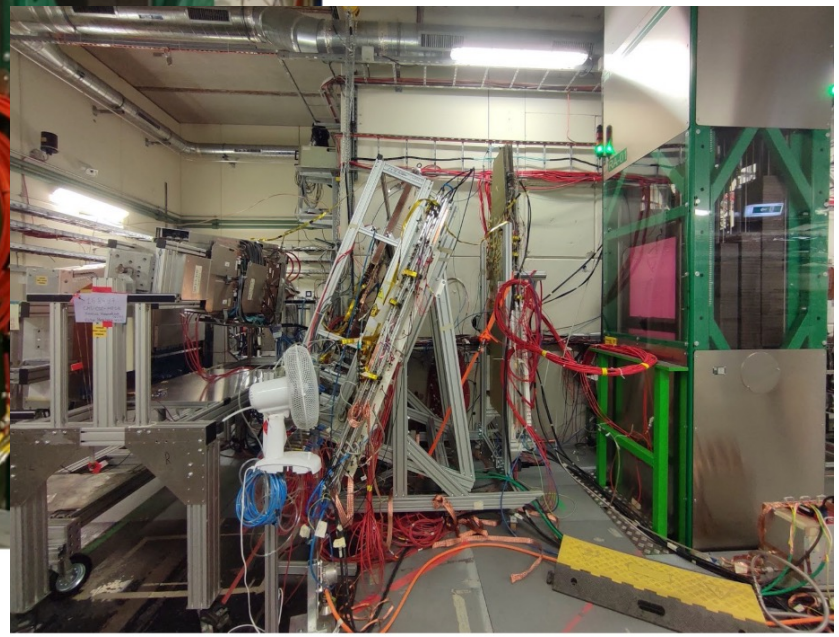

Details

- 4 scintillator coincidence
- Pulse Peaking Time = 50ns
- Events with PDO > 1022 are removed
  - At least 1 hit in every layer in the expected wire ROI
    - At least 1 hit in every layer in the expected strip ROI
      - Count the hits in the expected pad ROI
- Tried with:
  - 4 wires + 4 strips + pads
  - 4 wires + pads
  - ≥3 wires + pads

Efficiency per layer

$$L_{x,eff} = \frac{N_{4/4}}{N_{3/4} + N_{4/4}}$$

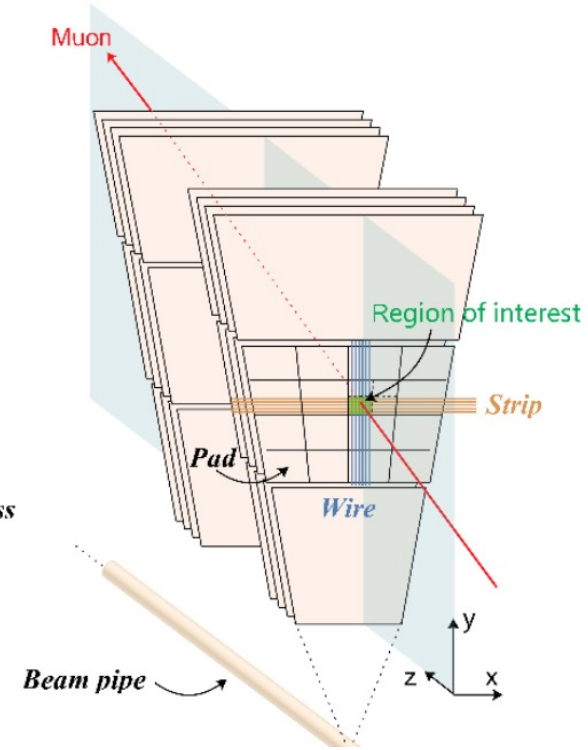

ROI

		Pads vmm channel	Strips cluster range	Wires wire group
Layer	L4	60	722-773	24-25
	L5	55	722-774	24-25
	L6	50	722-775	24-26
	L7	57	722-776	24-25

Comparison between selection cuts

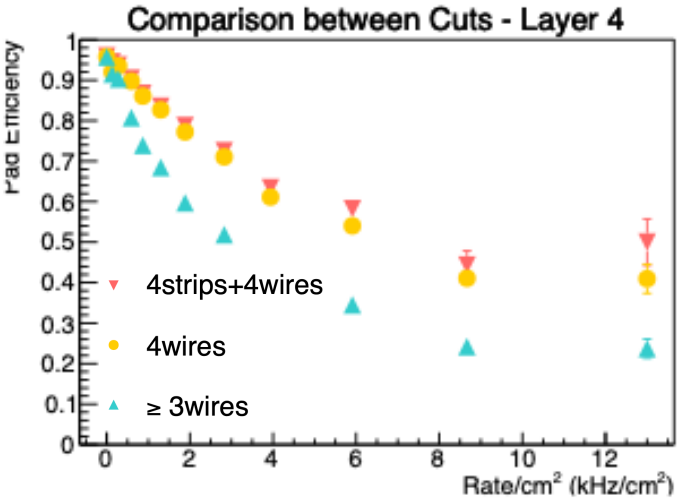

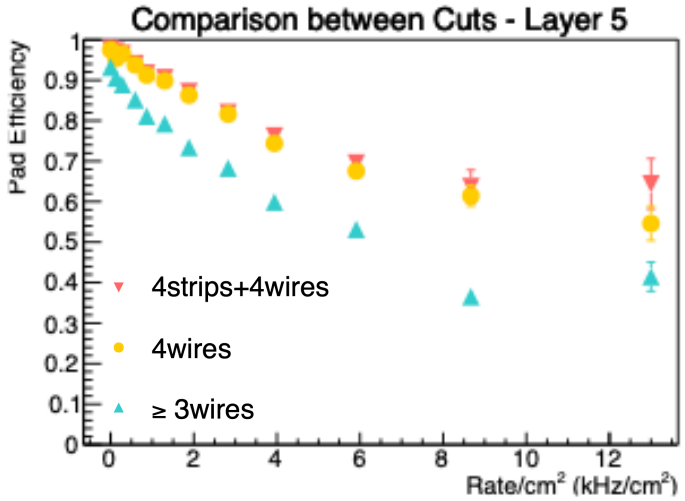

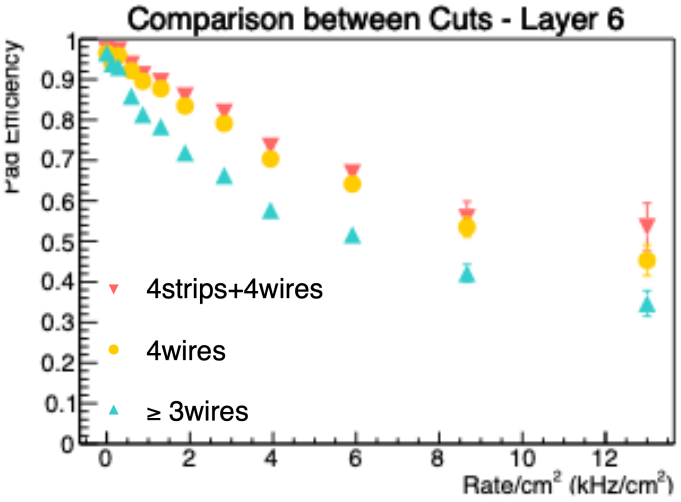

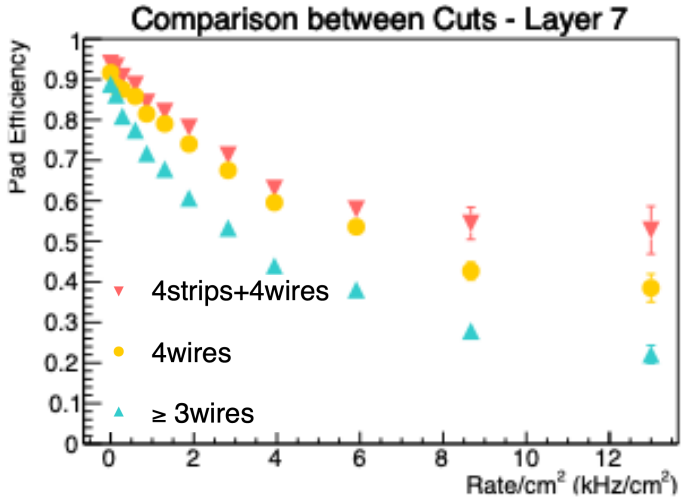

Efficiency per layer

$$L_{x,eff} = \frac{N_{4/4}}{N_{3/4} + N_{4/4}}$$

Selection of data:

- 4 Wires + 4 Strips + Pads
  - 1 hit in the wire group under the logical pad area of interest per layer
  - 1 strip cluster under the logical pad area of interest per layer
  - Pads of interest
- 4 Wires + Pads
- ≥3 Wires + Pads
- Requiring <4 wires includes more 3/4 coincidence events → lower efficiency
- Inclusion of strips in the event selection improves the pad efficiency for 4 scintillator coincidence

Pad Efficiency Calculation

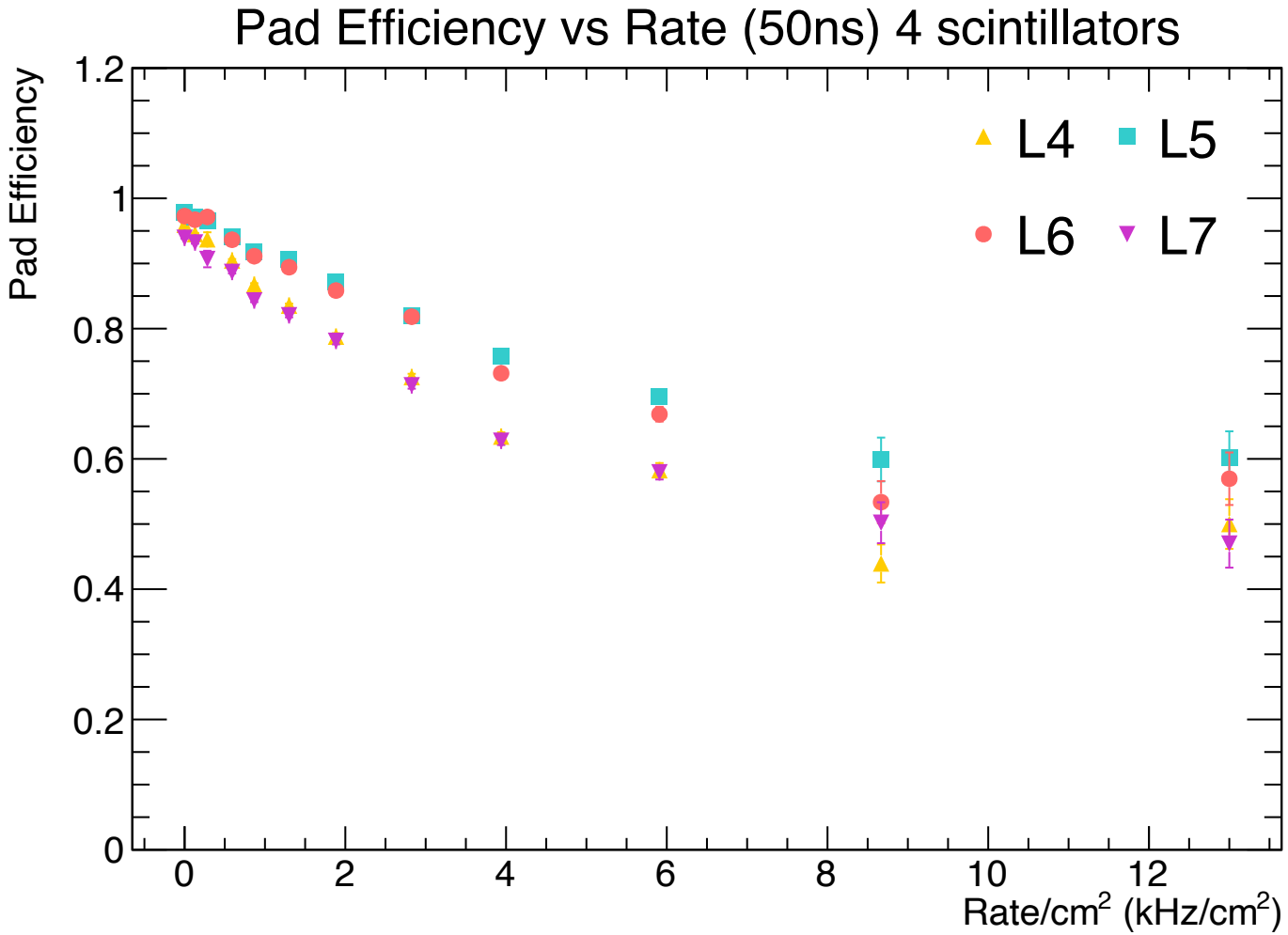

SourceOFF
Pad efficiency **94-98%**

High rate irradiation
Pad efficiency **>44%**

Layers 4 and 7 show lower efficiencies in all rates

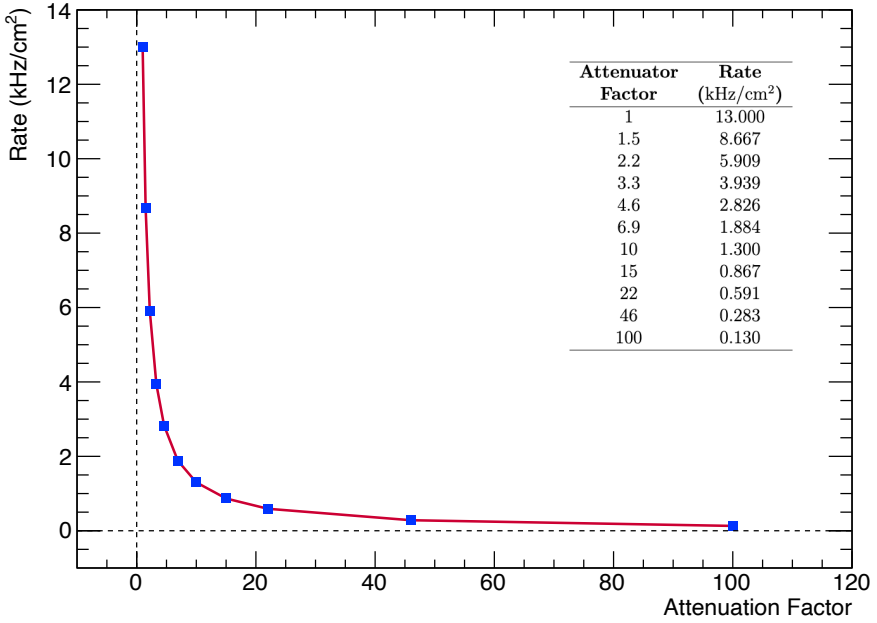

Attenuator Factor	Rate (kHz/cm²)
1	13.000
1.5	8.667
2.2	5.909
3.3	3.939
4.6	2.826
6.9	1.884
10	1.300
15	0.867
22	0.591
46	0.283
100	0.130

Outline

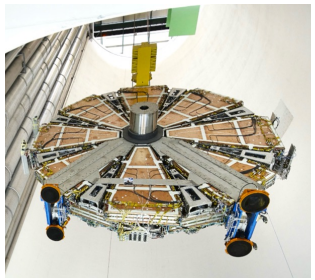

New Small Wheel

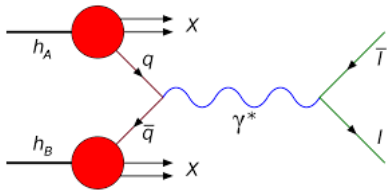

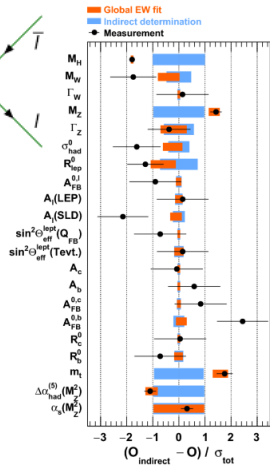

Z mass Precision measurement

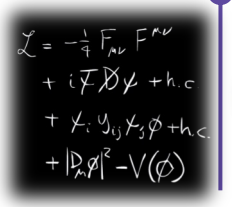

Introduction

Test Beam

Introduction - Motivation

- m_Z is a fundamental SM parameter precisely measured at LEP $m_Z = 91187.6 \pm 2.1\ MeV$.
- It would be interesting to cross check with LHC data.
  - The LEP measurement is dominated by the beam energy calibration, which is fully correlated among LEP experiments (common systematic).
- Even though there is no strong motivation about m_Z improvement and further improvements won't change significantly the overall sensitivity of the EW fit to new physics.
  - Can affect the precise measurement of m_W (EW sensitivity is dominated by m_W)
  - Can contribute to the precise measurement of the Higgs mass and width and reduce/increase the tension in EW fit.

  - TODAY: $m_Z = 91.1876 \pm 0.0021\ GeV$ (LEP)

    $\rightarrow\ m_H = 92^{+19}_{-17}\ GeV$ (indirect)

    $m_H = 125.14 \pm 0.15\ GeV$ (direct)
  - ASSUMING: $m_Z = 91.1897 \pm 0.001\ GeV$ (LHC)

    $\rightarrow \Delta m_H = 3.3\ GeV$ (indirect)

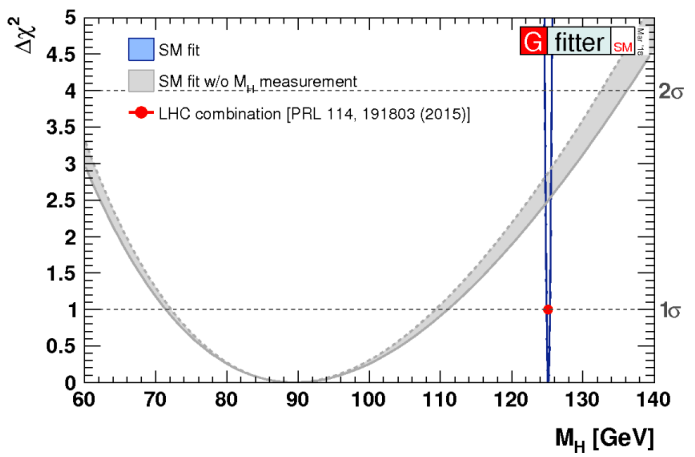

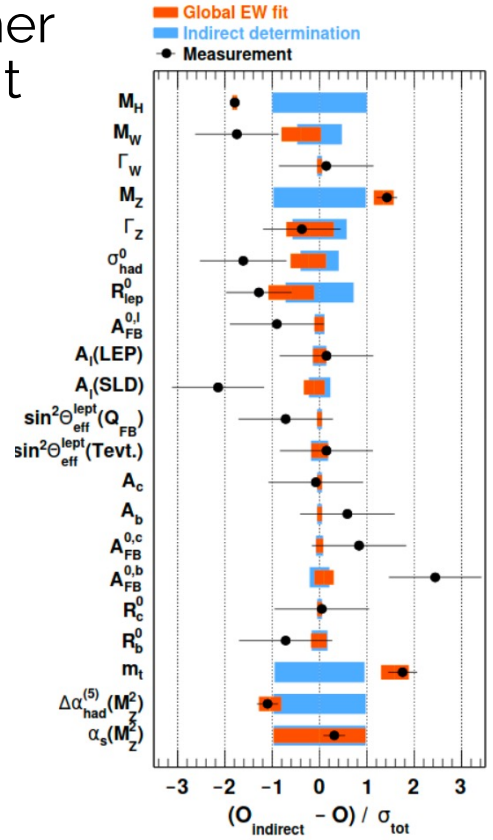

Introduction - Motivation

- Momentum calibration

  (emphasizes the importance of high-quality reconstruction of particle clusters and associated tracks for achieving accurate momentum calibration, which in turn is essential for precision measurements in particle physics experiments.)

  - Until now relying solely on LEP m_Z as reference point for momentum calibrations
  - J/psi resonance → can be an additional calibration point
    - Well known meson
    - Precisely measured properties
    - High statistics in LHC
  - The momentum scale should be calibrated using J/psi resonance and then propagate to Z boson momentum scale → cross check point and reduce systematic uncertainties

Summary of tasks – Momentum Calibration Improvement

- Participated in the precise measurement of the Z boson mass analysis group. Main responsibilities: in the muon momentum calibration part
- Study for the selections on eta regions.
  - J/psi → $\mu^+ \mu^-$ In eta regions η_1 and η_2
  - Calculation on J/psi invariant mass and comparison whether there is a significant difference when μ^+ in eta regions η_1 and μ^- in η_2 or the opposite.
- Perform a fit in the J/psi invariant mass distribution, using Roofit and an analytic model of the signal and background for background estimation
  - Signal:
    - 1 Crystal Ball function + 3 Gaussian functions
  - Background:
    - 1 Chebyshev polynomial (2nd degree)
- Radial Bias Analysis study
  - Quantification of the radial bias coefficient → Inclusion in the alignment systematics
    - Using analytic model – Model fit
    - Using MC data – Template fit

Selections on eta – Asymmetry Studies

- $J/psi \rightarrow \mu^+ \mu^-$
- Each muon in different eta region η_1, η_2.
- The number of events should be the same in both cases
- Sagitta bias correction was injected
- 2015-2018 data files
- Add P_T cut (P_T >6.5 GeV)
- Focusing on barrel pairs
- Studied 5 different cases with different binnings:
  - caseA = {-1.05, -0.80, -0.40, -0.10, 0.10, 0.40, 0.80, 1.05}
  - caseB = {-0.90, -0.45, -0.10, 0.10, 0.45, 0.90}
  - caseC = {-1.15, -0.60, -0.10, 0.10, 0.60, 1.15}
  - Case D: {-0.90, -0.70, -0.45, -0.25, -0.10, 0.10, 0.25, 0.45, 0.70, 0.90}
  - Case E: {-1.15, -1.00, -0.80, -0.60, -0.40, -0.10, 0.10, 0.40, 0.60, 0.80, 1.00, 1.15}

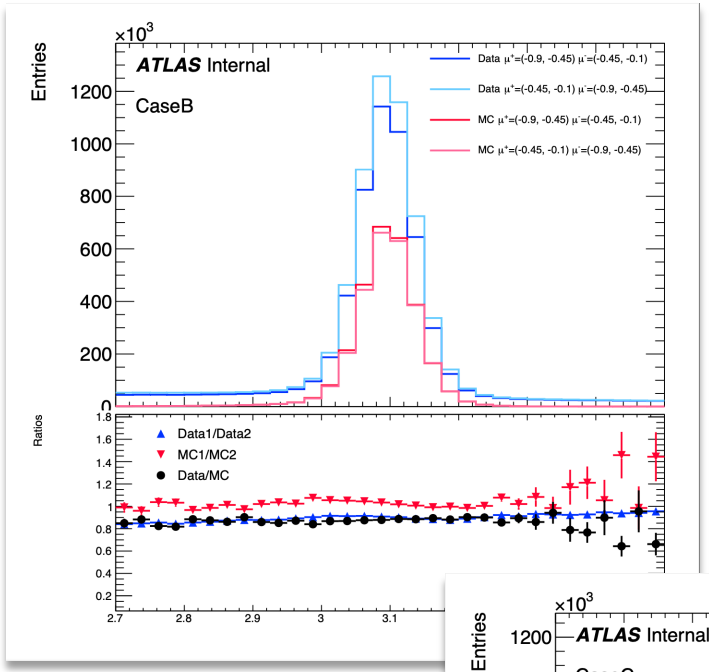

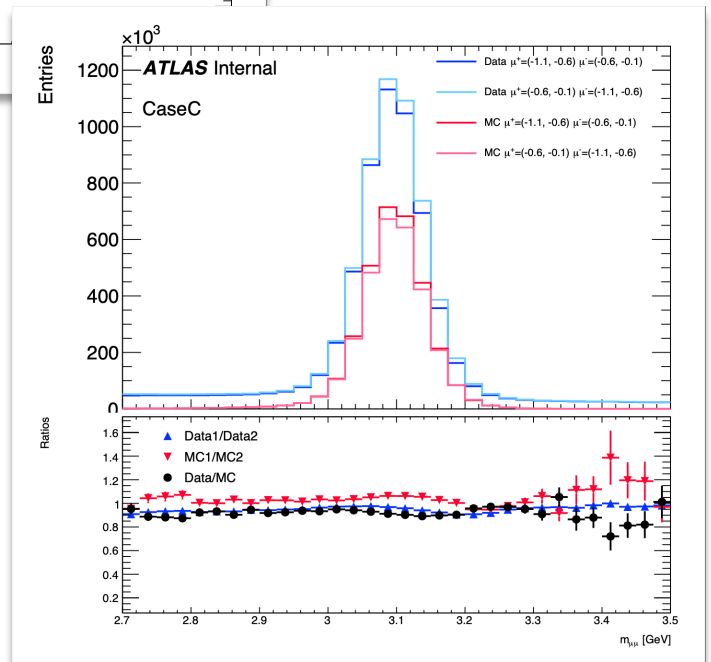

J/psi mass - Model fit

- J/psi is used for momentum calibration
- Estimation of the background
- ROOT's ROOFIT toolkit used for the model fit
- Signal
  - 1 Crystal Ball PDF + 3 Gauss PDF
- Background
  - 1 Chebyshev polynomial (2nd degree)

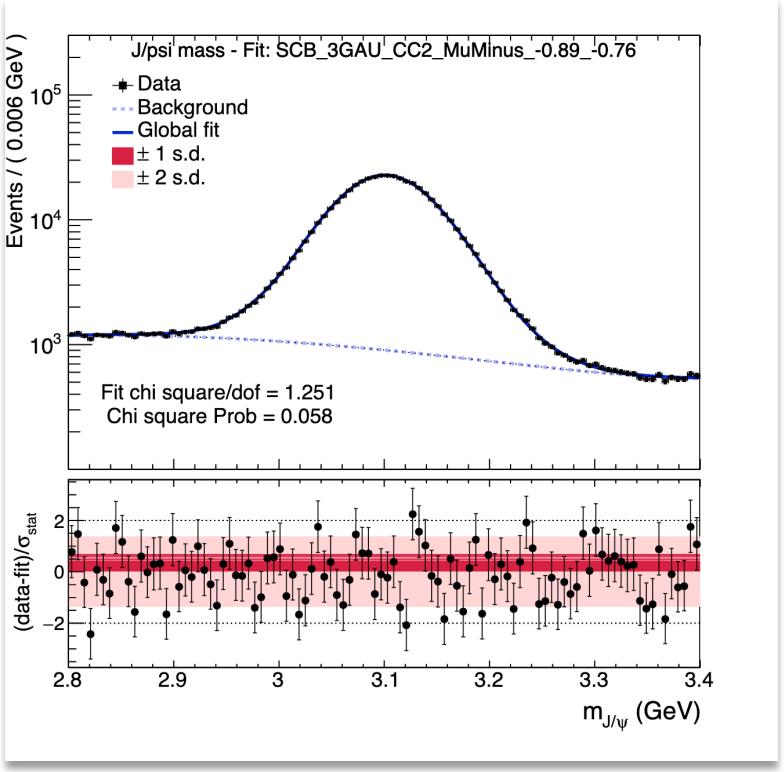

Data 2015

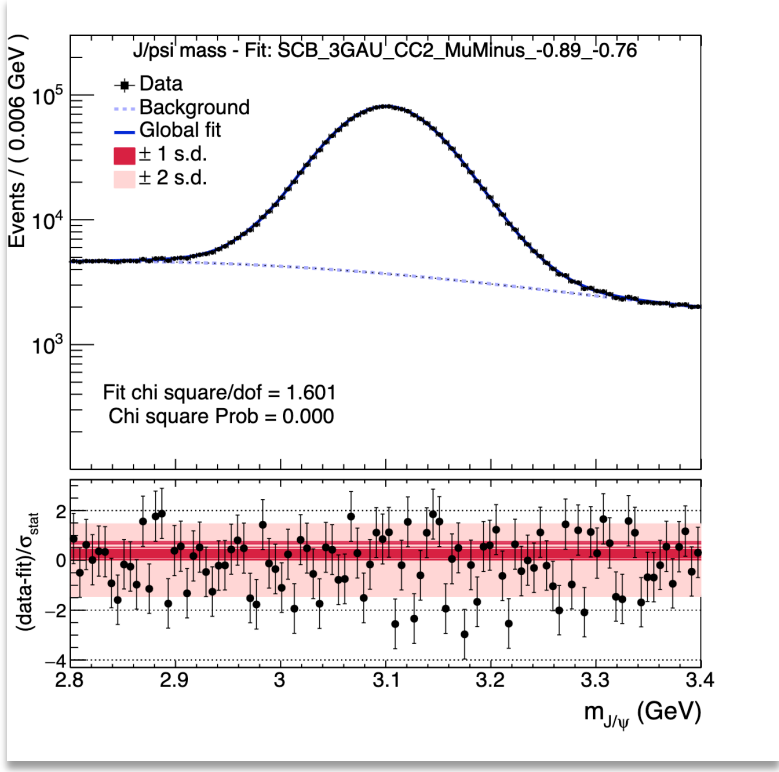

Data 2016

Radial Distortion - Introduction

- *Radial Bias Distortion*:
  - Geometrical distortion that affects the measurement of positions and angles
  - Caused by imperfections in the detector components and the way particle trajectories are measured
  - Charge independent

- *Aim of the study*:
  - investigate and quantify geometric distortions and misalignments in the Inner Detector with a focus on radial distortion.
  - Assess their impact on the momentum calibration of J/psi particles.
  - Determine an alignment systematic that affects the muon calibration → improved m_z precision.

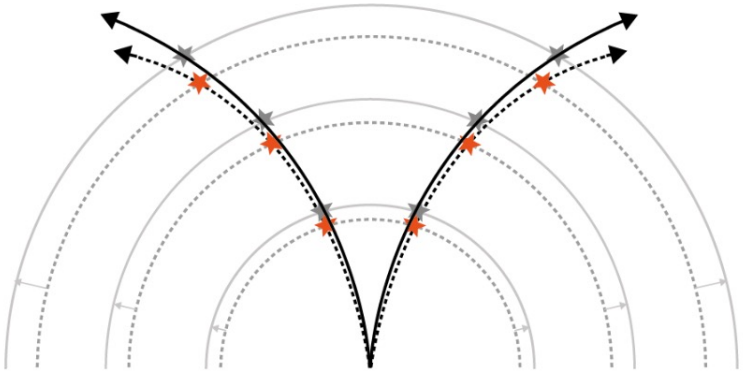

····· → real particle trajectories from the real hit positions (★)

——— → fitted particle trajectories from the biased reconstructed hit positions (★)

Radial Distortion Formula

Consider circular layers of detector radius R_0 expanded/contracted by $\Delta R \propto R_0$ ($\Delta R \ll R_0$).
Then we have:

$$R = R_0 + \Delta R = R_0(1+\epsilon)$$

** ϵ → radial distortion coefficient

The effect on the momentum $\vec{\boldsymbol{p}} = (\vec{\boldsymbol{p}}_{\boldsymbol{T}}, p_z)$ is:

$$p_T = p_{T0}(1+\epsilon)$$
$$p_z = p_{z0}$$
$$cot\theta = cot\theta_0(1+\epsilon)^{-1}$$

** θ → angle between the traverse (radial) and longitudinal (z) components

The effect on the invariant mass of the muon pair $m_{\mu\mu}$ is:

$$m^2_{\mu\mu 0} = (p_0^+ + p_0^-)^2 = 2m_\mu^2 + 2p_0^+p_0^- = 2m_\mu^2 + 2(\mathrm{E}_0^+\,\mathrm{E}_0^- - \boldsymbol{p}_0^+\boldsymbol{p}_0^-)$$

$$m^2_{\mu\mu 0} = m^2_{\mu\mu} - 2\left[\frac{E^-}{E^+}(p_T^+)^2 + \frac{E^+}{E^-}(p_T^-)^2 - 2\boldsymbol{p}_T^+\boldsymbol{p}_T^-\right]\epsilon$$

$$m^2_{\mu\mu} = m^2_{\mu\mu 0}\left(1+\epsilon\, sin^2\theta_\rho\right)$$

$$m_{\mu\mu} \approx m_{\mu\mu 0}\left(1+\epsilon\, sin^2\theta_\rho\right)$$

** *where,* $sin^2\theta_\rho = \frac{1}{m_{\mu\mu 0}{}^2}\left[\frac{E^-}{E^+}(p_T^+)^2 + \frac{E^+}{E^-}(p_T^-)^2 - 2\boldsymbol{p}_T^+\boldsymbol{p}_T^-\right]$

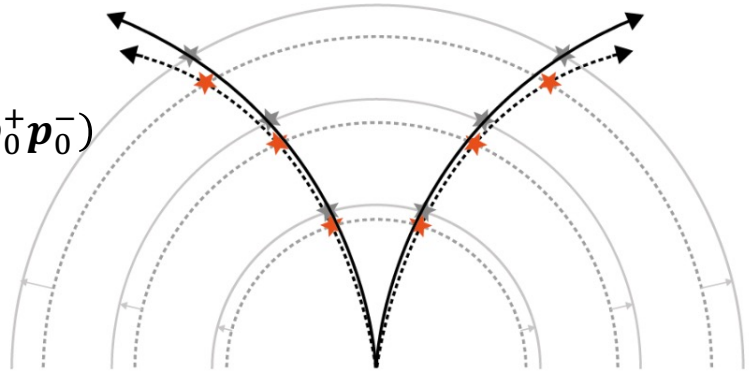

⋯⋯ → real particle trajectories from the real hit positions (★)

——— → fitted particle trajectories from the biased reconstructed hit positions (★)

Radial Distortion Analysis - Results

Model Fit

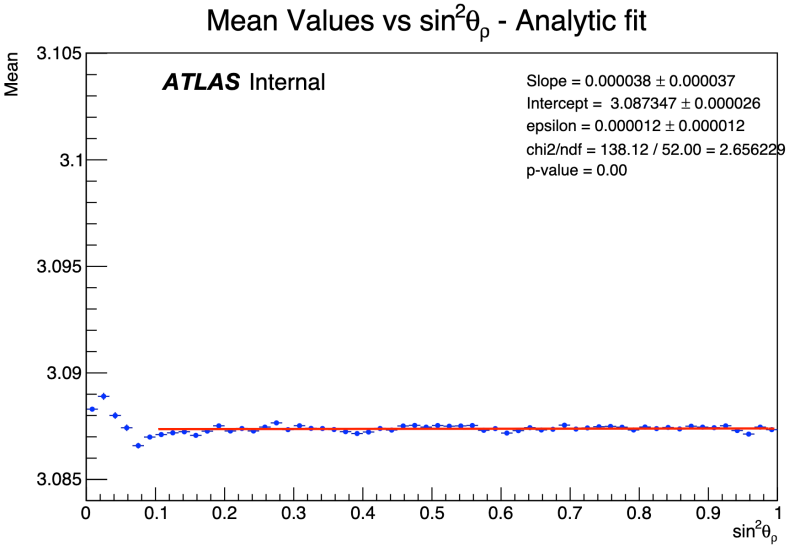

$\varepsilon = 0.000012 \pm 0.000012$

Analytic fit can be improved, low $\sin^2\theta_\rho$ have lower stats.

Template Fit

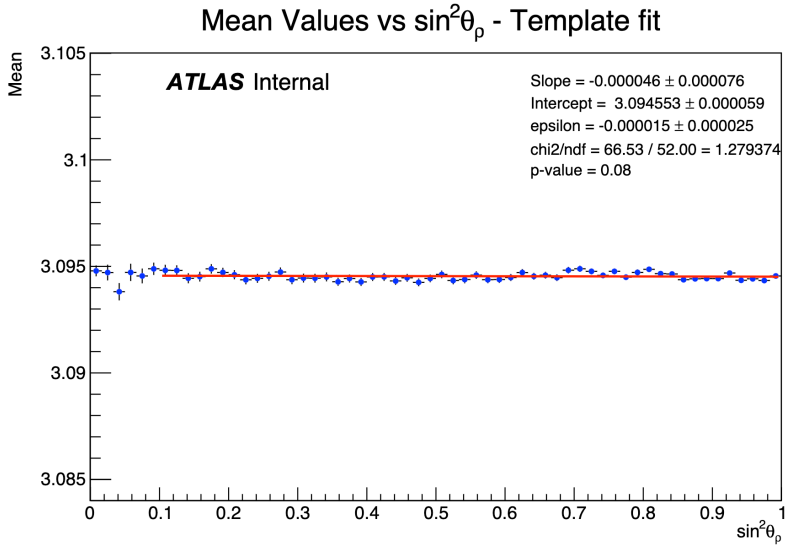

$\varepsilon = -0.000015 \pm 0.000025$

Template fit more successful, low MC dataset sample give higher uncertainty

Closure Test

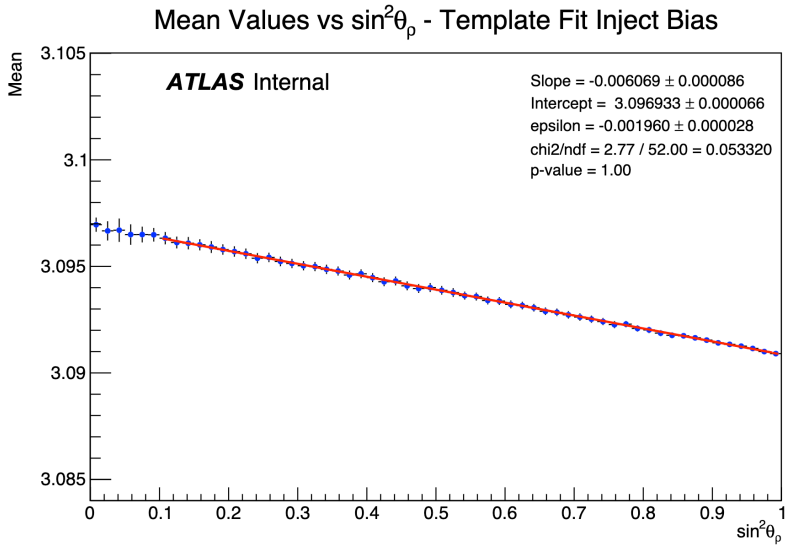

$\varepsilon = -0.001960 \pm 0.000028$

Inject radial bias -0.002. The method is successful since the injected and measured values are very close with a relative error of 2%.

Outline

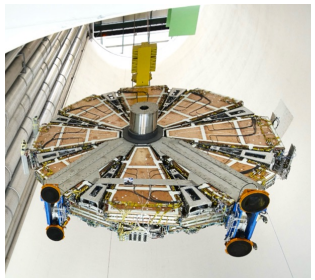

New Small Wheel

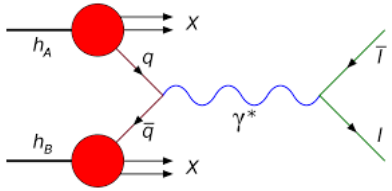

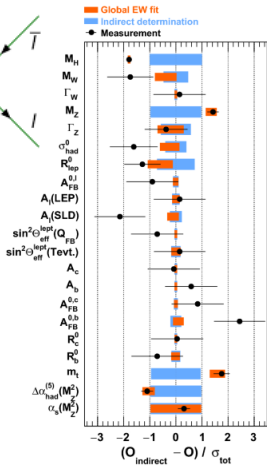

Z mass Precision measurement

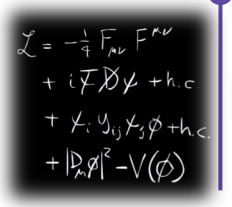

Introduction

Test Beam

ESSnuSB

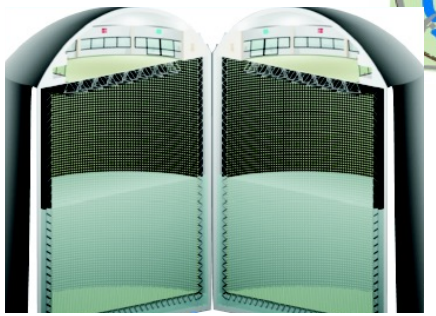

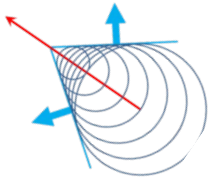

ESSnuSB – A Design Study

- ESS is a powerful proton accelerator
- ESSnuSB plans to measure CP violation by study neutrino oscillations $\nu_\mu \rightarrow \nu_e$, $\bar{\nu}_\mu \rightarrow \bar{\nu}_e$
- Second oscillation maximum selected because CP violation has bigger effect there
- Colliding protons on a target → pions are created → pions decay in flight → $\pi^+ \rightarrow \mu^+ + \nu_\mu$, $\pi^- \rightarrow \mu^- + \bar{\nu}_\mu$ → neutrino beam travelling to FD

$$\mathcal{A}_{CP}^{\mu\rightarrow e} = P_{\nu_\mu\rightarrow\nu_e} - P_{\bar{\nu}_\mu\rightarrow\bar{\nu}_e} = -16J\sin\frac{\Delta m_{31}^2 L}{4E}\sin\frac{\Delta m_{32}^2 L}{4E}\sin\frac{\Delta m_{21}^2 L}{4E}$$

$$J = c_{12}\,c_{23}\,c_{13}^2\,s_{12}\,s_{23}\,s_{13}\,\sin\delta_{CP}$$

$$U_{PMNS} = \begin{pmatrix} c_{12}c_{13} & s_{12}c_{13} & s_{13}e^{-i\delta_{\mathrm{CP}}} \\ -s_{12}c_{23} - c_{12}s_{23}s_{13}e^{-i\delta_{\mathrm{CP}}} & c_{12}c_{23} - s_{12}s_{23}s_{13}e^{-i\delta_{\mathrm{CP}}} & s_{23}c_{13} \\ s_{12}s_{23} - c_{12}c_{23}s_{13}e^{-i\delta_{\mathrm{CP}}} & -c_{12}s_{23} - s_{12}c_{23}s_{13}e^{-i\delta_{\mathrm{CP}}} & c_{23}c_{13} \end{pmatrix}$$

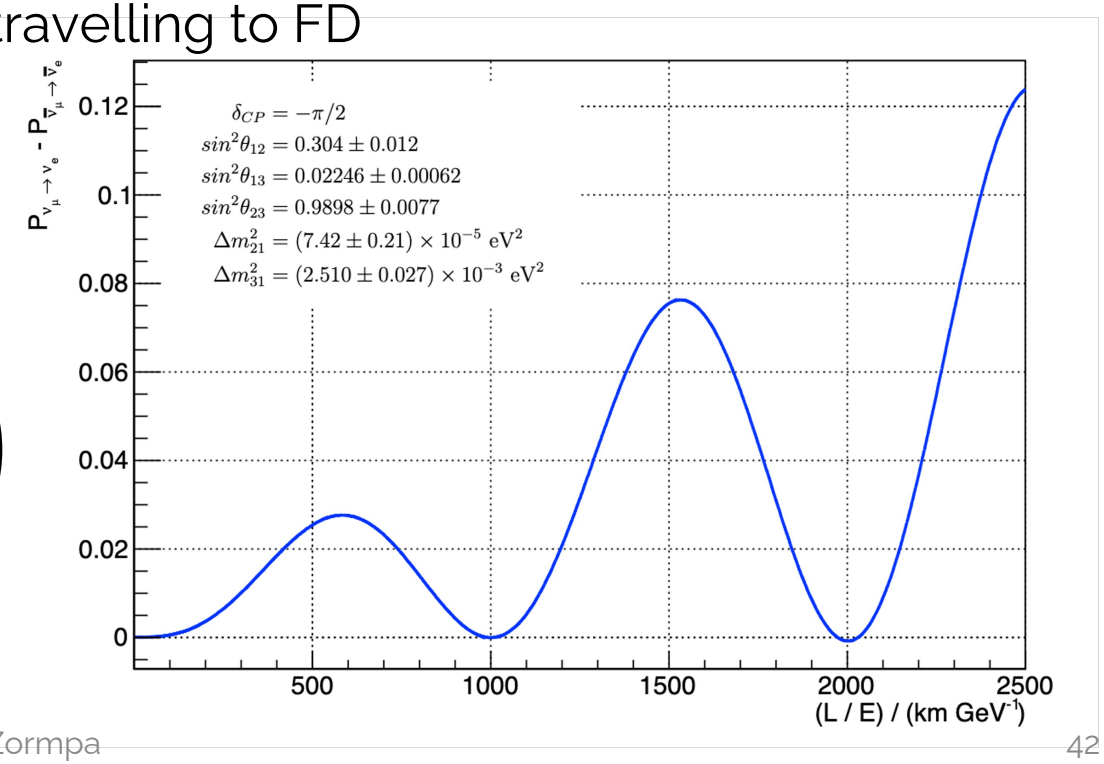

Far Detector

- 2 mine locations:
  - Zingruvan mine (360 km)
  - Garpenberg mine (540 km)
- 2 Water Cherenkov tanks
  - Cavern Dimensions cylinder: d = h = 78 m
  - Inner Dimensions cylinder: d = h = 74 m
- 20 inch PMTs (30% or 40% coverage)

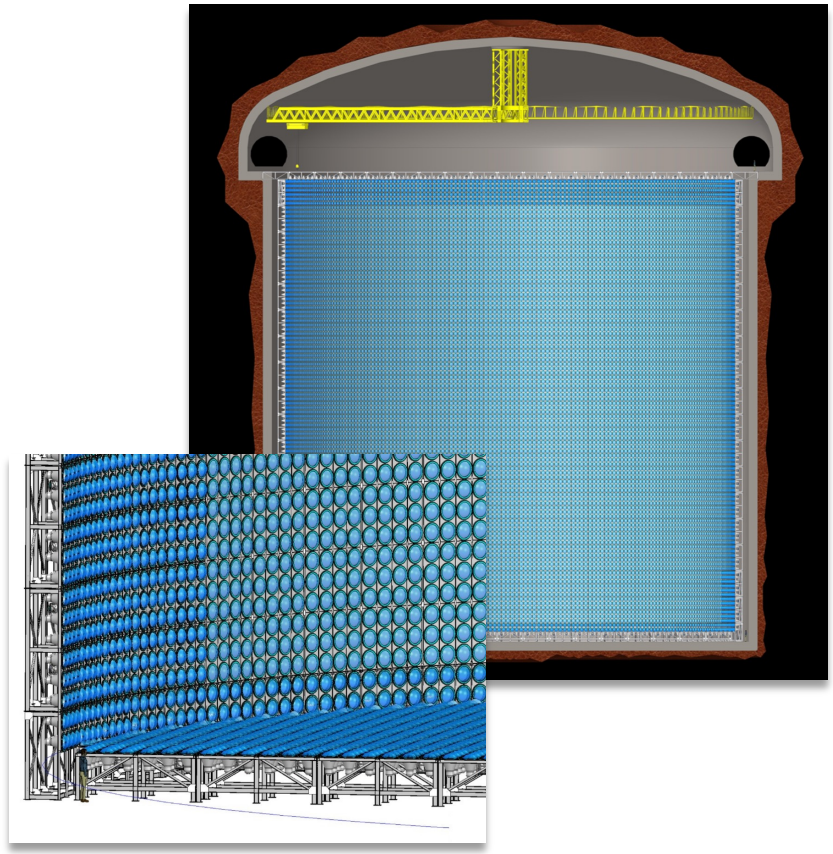

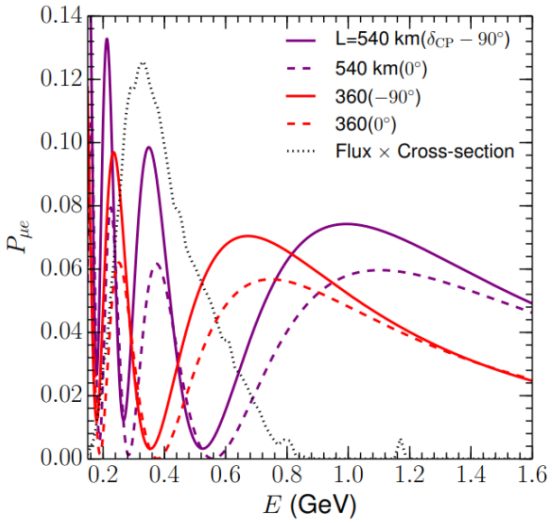

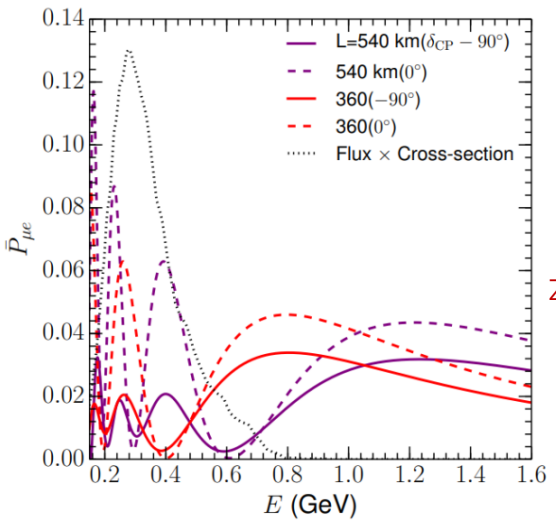

Garpenberg (540 km) sees mainly the second oscillation peak

Zinkgruvan (360 km) sees 1st at high E and second at low E ✅

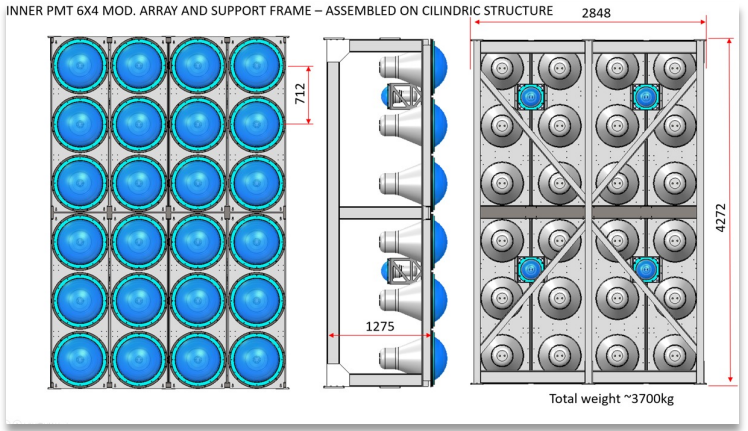

Production Details

- CC channel
  - 100k $\bar{\nu}_\mu$ events, 100k $\bar{\nu}_e$ events, 100k ν_e events, 99k ν_μ events
- ESSnuSB FD geometry (H = D = 74m)
- beam y direction
- ν vertices distributed randomly in the water volume of FD
- flat interacting neutrino energy up to 1.5 GeV
- 30% and 40% optical coverage is used
- T2K formula was used to calculate neutrino energy
- Event Selection Algorithm
  - Fiducial Volume Cut 2 m from the walls of the tank included

The simulation involved several components, starting with the simulation of neutrino interactions using the GENIE interaction generator. The propagation of particles through the WatCh detector and the PMT response was handled by the WCSim software. Finally, the detector response was reconstructed using the fiTQun reconstruction software.

$$E_\nu^{rec} = \frac{m_f^2 - (m_i')^2 - m_l^2 + 2m_i' E_l}{2(m_i' - E_l + p_l \cos\theta_l)} \quad (4)$$

where E_ν^{rec} is the reconstructed neutrino energy, m_i and m_f are the initial and final nucleon masses respectively, and $m_i' = m_i - E_b$, where $E_b = 27\,\text{MeV}$ is the binding energy of a nucleon inside ^{16}O nuclei. E_l, p_l and θ_l are the reconstructed lepton energy, momentum, and angle with respect to the beam, respectively. The selec-

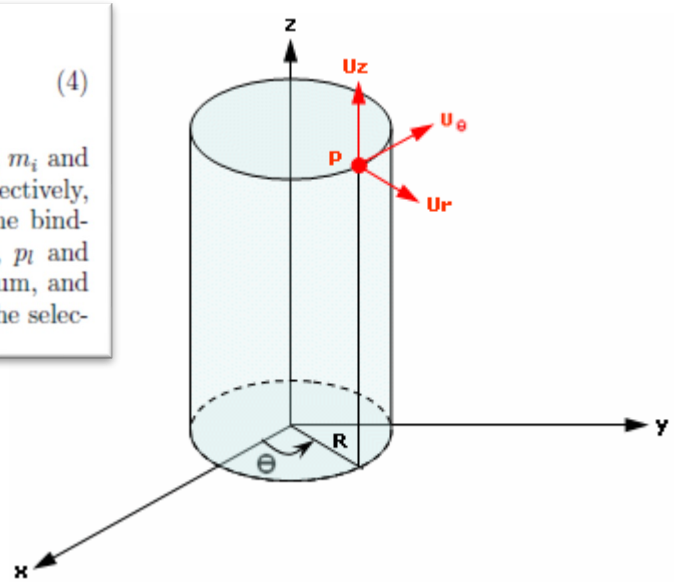

Quasi-elastic scattering

$\nu_e + n \rightarrow e^- + p$
$\nu_\mu + n \rightarrow \mu^- + p$
$\bar{\nu}_e + p \rightarrow e^+ + n$
$\bar{\nu}_\mu + p \rightarrow \mu^+ + n$

Selected Results

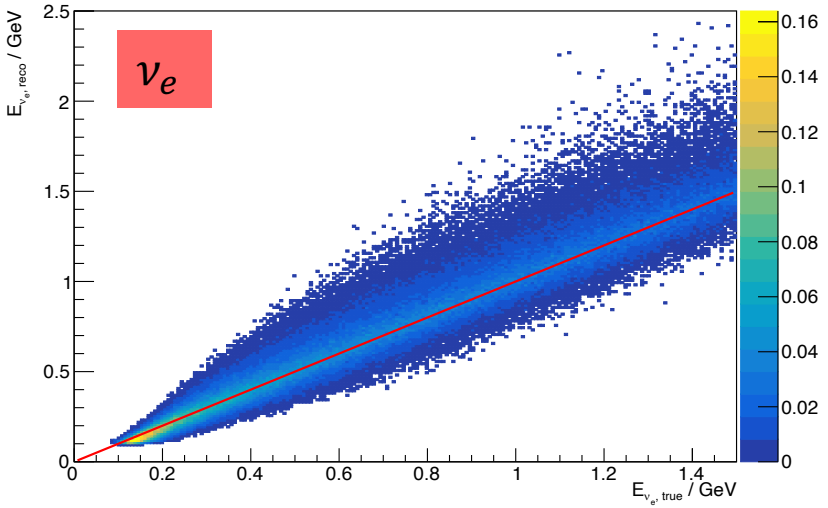

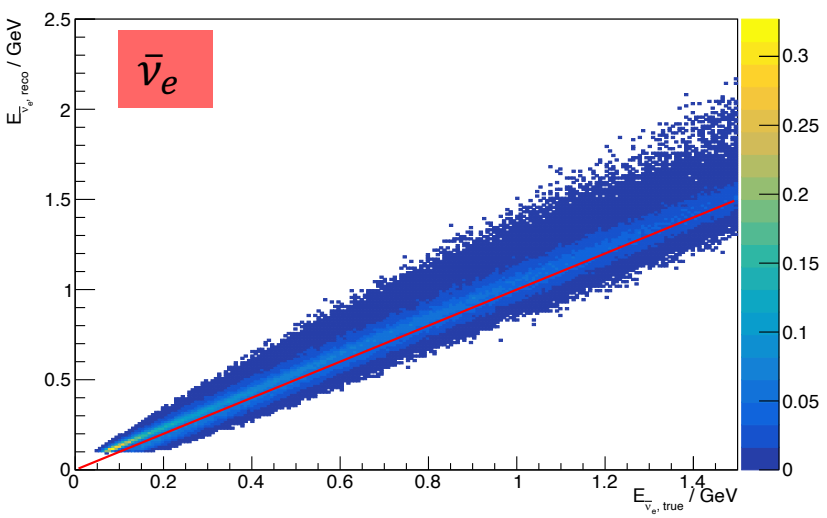

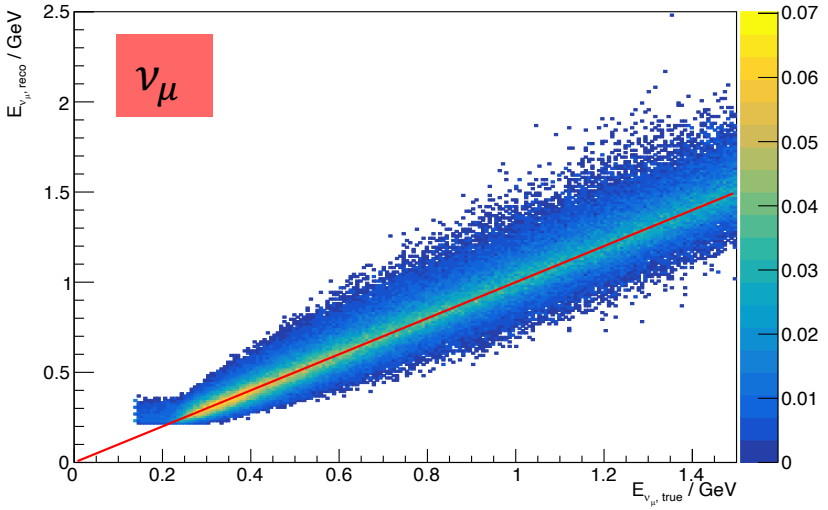

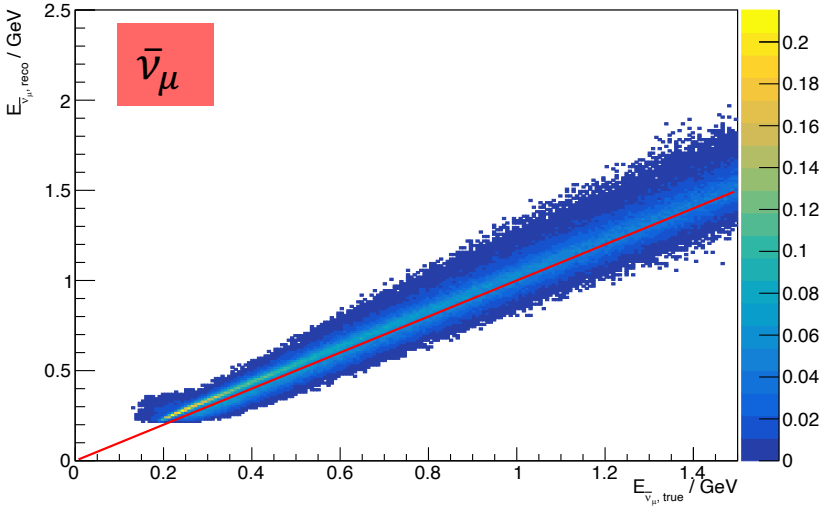

Migration Matrices

Distribution of reconstructed energy as a function of true energy for different flavours of charged leptons for QES sample.

The relative energy resolution for this sample is:

- 12–22% - electron neutrinos
- 15–28% - muon neutrinos
- 11–23% - electron antineutrinos
- 8–30% - muon antineutrinos

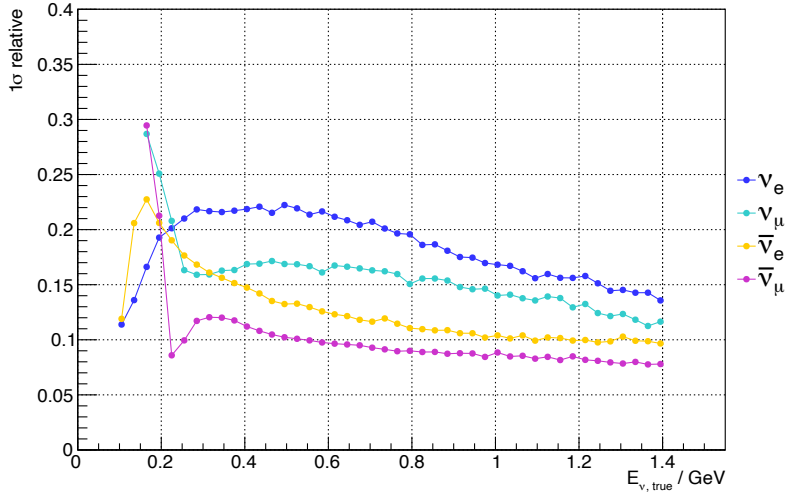

Outline

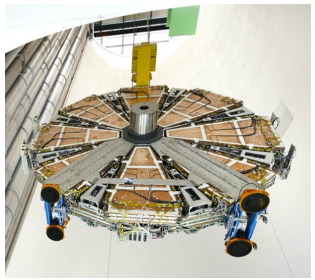

New Small Wheel

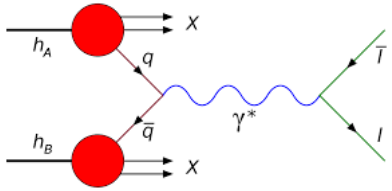

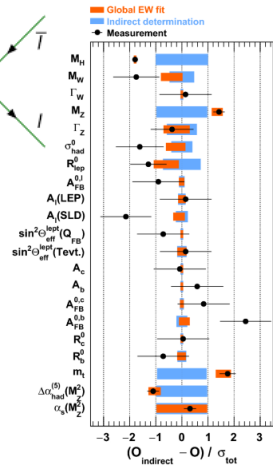

Z mass Precision measurement

Summary Publications Talks

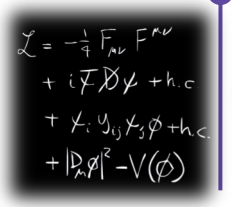

Introduction

Test Beam

ESSnuSB

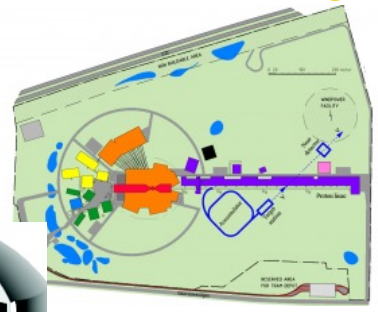

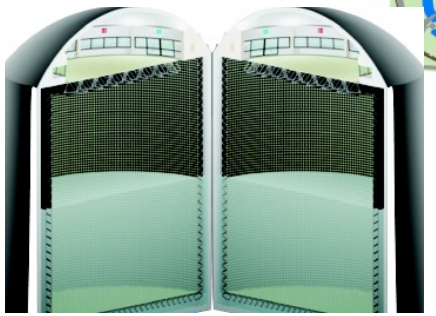

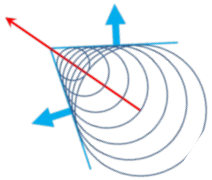

Summary

- New Small Wheel
  - Biggest persentage of my PhD time spent in NSW trigger
  - Commissioning of sTGC trigger chain at B191 and P1
  - Integration of sTGC trigger in ATLAS
  - Worked on Trigger operations – tests, debugging, communication with engineers
  - Pad-only trigger is now included in ATLAS level-1 muon trigger 🎉
    - Reducing fakes
    - Reducing trigger rate
- Test Beam Studies
  - Small task: Calculate the efficiency per layer for a ROI under a 4-scintillator coincidence
- Z mass precision measurement
  - Took over some important tasks on momentum calibration.
    - J/psi analytical fit – background estimation
    - Radial Bias Calculation – systematics
    - Asymmetry Study
  - Note to be published
- ESSnuSB
  - Work done on the Far Detector
  - Studies to calculate detector efficiency and energy resolution → Definition of detector geometry/location → Conceptual Design Report → ESSnuSB+

Summary

Other Tasks

- Study on the direct clock board
- Study on the sTGC Router MTx measurements
- Trigger Slice Test Bench – *Qualification task*
  - Designed/Built a test bench at VS lab at CERN with T. Geralis and I. Kiskiras
  - Fully operational with ½ sector trigger elx, DAQ system, cooling system accessible through network
  - Widely used during COVID until today
- Testing and assembly of SRL1 Repeaters and LVD6 Repeaters at VS lab
- Testing of ADDC boards at DAMA lab

Conferences/Publications/Notes

- O. Zormpa, *on behalf of ATLAS Collaboration*
  The New Small Wheel Trigger for the ATLAS experiment - Pisa Meeting 2024
  under review
- O. Zormpa, *on behalf of ESSnuSB Collaboration*
  ESSnuSB detector performance - NuFact 2021
  PoS, vol. NuFact2021, p. 206, 2022 DOI: 10.22323/1.402.0206
- **ATLAS Outstanding Achievement Award 2022**
  for outstanding contributions to the completion of the NSW integration and surface commissioning within the LS2 schedule.
- Olga Zormpa
  ATLAS NSW Upgrade - sTGC Trigger and Commissioning
  HEP 2021 - 38th Conference on Recent Developments in High Energy Physics and Cosmology, 16/06/2021
- NSW Trigger group
  The New Small Wheel electronics
  JINST 18 (2023) 05, P05012 DOI: 10.1088/1748-0221/18/05/P05012

Conferences/Publications/Notes

- T. Geralis, Y. Benhammou, A. Coimbra, K. Damanakis, P. Gkountoumis, L. Guan, I. Kiskiras, A. Koulouris, U. Landgraf, L. Levinson, I. Mesolongitis, J. Narevicius, O. Zormpa, M. Prapa, A. Roich, G. Stavropoulos, S. Sun, X. Wang
  The Serial and LVDS repeaters for the ATLAS New Small Wheel sTGC trigger
  ATL-MUON-PUB-2022-003, url = https://cds.cern.ch/record/2841848

- T. Alexopoulos, T. Geralis, P. Gkountoumis, L. Levinson, I. Mesolongitis, O. Zormpa
  Ultra-low jitter clock distribution for the trigger electronics of the New Small Wheel for the ATLAS experiment
  JINST 17 (2022) 05, C05012 DOI: 10.1088/1748-0221/17/05/C05012

- ESSnuSB Collaboration
  Particle Physics at the European Spallation Source
  Phys.Rept. 1023 (2023) 1-84 DOI: 10.1016/j.physrep.2023.06.001

- ESSnuSB Collaboration
  The ESSnuSB Design Study: Overview and Future Prospects
  Universe 9 (2023) 8, 347 DOI: 10.3390/universe9080347

- ESSnuSB Collaboration
  Study of non-standard interaction mediated by a scalar field at ESSnuSB experiment
  Phys.Rev.D 109 (2024) 11, 115010 DOI: 10.1103/PhysRevD.109.115010

Conferences/Publications/Notes

- ESSnuSB Collaboration
  The European Spallation Source neutrino super-beam conceptual design report
  Eur.Phys.J.ST 231 (2022) 21, 3779-3955, *Eur.Phys.J.ST* 232 (2023) 15-16 (erratum)
  DOI: 10.1140/epjs/s11734-022-00664-w (publication), 10.1140/epjs/s11734-022-00729-w (erratum)

- ESSnuSB Collaboration
  Updated physics performance of the ESSnuSB experiment: ESSnuSB collaboration
  Eur.Phys.J.C 81 (2021) 12, 1130 DOI: 10.1140/epjc/s10052-021-09845-8

- ESSnuSB Collaboration
  The European Spallation Source Neutrino Super Beam
  Snowmass 2021

- Joakim Cederkall, Peter Christiansen, Joochun Park, Colin Carlile, Tord Ekelöf, Maja Olvegård, Ye Zou, Eric Baussan, Elian Bouquerel, Marcos Dracos, Mariyan Bogomilov, Georgi Petkov, Roumen Tsenov, Budimir Klicek, Mario Stipčević, Mamad Eshraqi, BjöRn GåLnander, Mats Lindroos, Elena Wildner, George Fanourakis, Olga Zormpa
  The ESSνSB project
  PoS EPS-HEP2019 (2020) 392 DOI: 10.22323/1.364.0392

Conferences/Publications/Notes

- Joochun Park, Joakim Cederkall, Peter Christiansen, Guy Barrand, Mariyan Bogomilov, Georgi Petkov, Roumen Tsenov, Tord Ekelof, George Fanourakis, Olga Zormpa, Gül Gökbulut, Aysel Kayis Topaksu, Mehmet Oglakci, Budimir Klicek, Kaja Krhac, Mario Stipčević
  Status of the detector design studies for ESSνSB
  PoS NuFact2019 (2020) 041 DOI: 10.22323/1.369.0041
- **Qualified ATLAS author** (24/01/2020). Qualification Task: Work in the frame of the NSW, on the Trigger Slice Test Bench (at B180 and the VS) and the sTGC readout chain for the trigger path validation. In particular: Work on building the Trigger Slice Test Bench consisting of 12 sFEB, 12 pFEB, Repeaters, a Rim Crate (Pad Trigger, 4 Routers and the RimL1DDC) and performing data monitoring. This work will include the capability to operate the system as well as development of online software for signal monitoring. Work on testing and validating the system in collaboration with the sTGC Trigger group. Work on performing cross check of the Trigger output as compared with the regular data stream via the L1DDCs.

Thank you!


Back-up slides

Standard Model

- Even though it is a theory that predicted particles and interactions that were eventualy discovered, SM has some shortcomings:
  - Dark matter/energy
  - Matter anti-matter assymetry
  - Gravity
- Many theories BSM exist and need to be tested → building experiments to study/test SM or search for new physics
- Bosons
  - Gauge → the bosons arise from gauge invariance (symmetry principle where the L of the system is unchanged under local transformations)
  - Scalar → related to scalar fields (fields with the same value regardless of the direction in space)

SM Lagrangian

- $\mathcal{L} = \mathcal{L}_{EW} + \mathcal{L}_{QCD} + \mathcal{L}_{Higgs} + \mathcal{L}_{Yukawa}$
- $\mathcal{L}_{EW}$: The electroweak Lagrangian, which describes the electromagnetic and weak interactions, unifying them into a single theory.
- $\mathcal{L}_{QCD}$: The quantum chromodynamics Lagrangian, which describes the strong nuclear force and the interactions between quarks and gluons.
- $\mathcal{L}_{Higgs}$: The Higgs Lagrangian, which describes the Higgs field and its associated particle, the Higgs boson.
- $\mathcal{L}_{Yukawa}$:The Yukawa Lagrangian, which describes the interactions between fermions (quarks and leptons) and the Higgs field, leading to the generation of particle masses.

Standard Model - Particles

	Generation	Name	Symbol	Charge (e)	Mass
Quarks	1st	up	u	+2/3	2.16 MeV
		down	d	-1/3	4.67 MeV
	2nd	charm	c	+2/3	1.27 GeV
		strange	s	-1/3	93.4 MeV
	3rd	top	t	+2/3	172.69 GeV
		bottom	b	-1/3	4.18 GeV
Leptons	1st	electron	e	-1	0.511 MeV
		electron neutrino	ν_e	0	
	2nd	muon	μ	-1	105.658 MeV
		muon neutrino	ν_μ	0	
	3rd	tau	τ	-1	1776.86 MeV
		tau neutrino	ν_τ	0	
	Force	**Name**	**Symbol**	**Charge (e)**	**Mass**
Bosons	strong	gluon	g	0	0
	electromagnetic	photon	γ	0	0
	weak	W bosons	$W^\pm$	±1	80.377 GeV
	weak	Z boson	Z^0	0	91.1876 GeV
		Higgs boson	H	0	125.25 GeV

Table 1.1

Fermions (quarks and leptons) and bosons in the Standard Model. Fermions carry half-integer spin and bosons integer spin. Particle masses retrieved from PDG-2022 [28]. Neutrinos are considered massless in the SM but currents results, indicate that neutrino masses are non-zero. Note that the corresponding anti-particles carry the opposite electric charge.

BEH mechanism

The Brout-Englert-Higgs mechanism, introduced in the Standard Model, explains the process of spontaneous symmetry breaking in the Electroweak theory, offering insight into how particles acquire their masses. This mechanism introduces a new field, known as the Higgs field, that interacts with particles, thereby inducing spontaneous symmetry breaking.

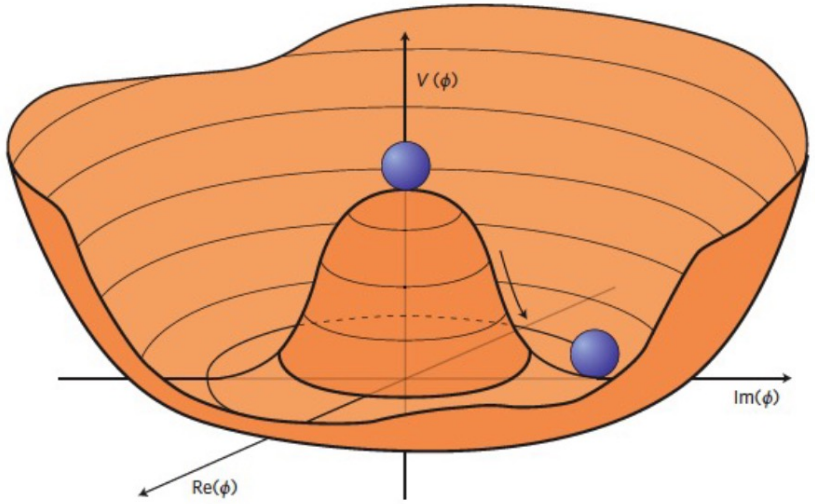

Figure 1.3: The shape of the Higgs potential $V(\phi)$ [9].

The Higgs field:

$$\varphi(x) = \begin{pmatrix} \varphi^{+}(x) \\ \varphi^{0}(x) \end{pmatrix}$$

$$V(\varphi) = \mu^2\varphi^{\dagger}\varphi + \lambda(\varphi^{\dagger}\varphi)^2 = \mu^2\varphi^2 + \lambda\varphi^4$$

The parameters μ^2 and λ determine the mass and self-interactions of the Higgs field, respectively

$$2\varphi(\mu^2 + 2\lambda\varphi^2) = 0$$

Assuming that, $\lambda > 0$ and $\mu^2 < 0$ the ground state of the Higgs potential becomes non-zero and $|\varphi| = \sqrt{-\mu^2/2\lambda}$ where $\upsilon^2 = -\mu^2/2\lambda$ is the non-zero vacuum expectation value.

$$m_H = \sqrt{2\lambda}\upsilon$$

$$m_W = \frac{1}{2} g\upsilon$$

$$m_Z = \frac{\upsilon^2}{2}\sqrt{g^2 + g'^2} = \frac{m_W}{\cos\theta_W}$$

Mesons and Z

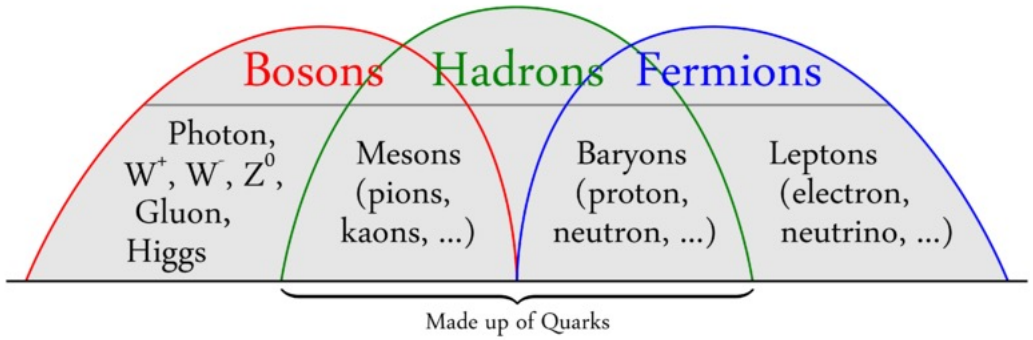

$$m_{J/\psi} = 3096.900 \pm 0.006\ MeV\ \ (c\bar{c})$$
$$m_{\Upsilon(1S)} = 9460.300 \pm 0.26\ MeV\ \ (b\bar{b})$$
$$m_Z = 91.1876\ \pm 0.0021\ GeV$$
$$m_W = 80.377 \pm 0.012\ GeV$$
$$m_H = 125.25 \pm 0.17 GeV$$

$J/\psi(1S)$ DECAY MODES

	Mode		Fraction (Γ_i/Γ)	Scale factor/ Confidence level
Γ_1	hadrons		(87.7 ±0.5) %	
Γ_2	virtual $\gamma \rightarrow$ hadrons		(13.50 ±0.30) %	
Γ_3	ggg		(64.1 ±1.0) %	
Γ_4	γgg		(8.8 ±1.1) %	
Γ_5	e^+e^-		(5.94 ±0.06) %	
Γ_6	$e^+e^-\gamma$	[a]	(8.8 ±1.4) $\times 10^{-3}$	
Γ_7	$\mu^+\mu^-$		(5.93 ±0.06) %	

Z DECAY MODES

	Mode		Fraction (Γ_i/Γ)	Scale factor/ Confidence level
Γ_1	e^+e^-	[a]	(3.3632±0.0042) %	
Γ_2	$\mu^+\mu^-$	[a]	(3.3662±0.0066) %	
Γ_3	$\tau^+\tau^-$	[a]	(3.3696±0.0083) %	
Γ_4	$\ell^+\ell^-$	[a,b]	(3.3658±0.0023) %	
Γ_5	$\ell^+\ell^-\ell^+\ell^-$	[c]	(3.5 ±0.4) $\times 10^{-6}$	S=1.7
Γ_6	invisible	[a]	(20.000 ±0.055) %	
Γ_7	hadrons	[a]	(69.911 ±0.056) %	
Γ_8	$(u\bar{u}+c\bar{c})/2$		(11.6 ±0.6) %	
Γ_9	$(d\bar{d}+s\bar{s}+b\bar{b})/3$		(15.6 ±0.4) %	
Γ_{10}	$c\bar{c}$		(12.03 ±0.21) %	
Γ_{11}	$b\bar{b}$		(15.12 ±0.05) %	
Γ_{12}	$b\bar{b}b\bar{b}$		(3.6 ±1.3) $\times 10^{-4}$	

W Boson

- $W^{\pm}$
- $m_W = 80.377 \pm 0.012\ GeV$
- EW mediator (CC)
- Presence of the ν adds complexity to the reco → Missing transverse energy E_T^{miss}.
- Measured Mass: The CDF collaboration measured the mass of the W boson to be 80,433.5 ± 9.4 MeV/c^2 → significantly higher than the value predicted by the SM and previous measurements. →Excellent accuracy. New Physics?

W^+ DECAY MODES

W^- modes are charge conjugates of the modes below.

	Mode		Fraction (Γ_i/Γ)		Confidence level
Γ_1	$\ell^+\nu$	[a]	(10.86 ± 0.09) %		
Γ_2	$e^+\nu$		(10.71 ± 0.16) %		
Γ_3	$\mu^+\nu$		(10.63 ± 0.15) %		
Γ_4	$\tau^+\nu$		(11.38 ± 0.21) %		
Γ_5	hadrons		(67.41 ± 0.27) %		
Γ_6	$\pi^+\gamma$		< 7	$\times 10^{-6}$	95%
Γ_7	$D_s^+\gamma$		< 1.3	$\times 10^{-3}$	95%
Γ_8	cX		(33.3 ± 2.6) %		
Γ_9	$c\bar{s}$		(31 $^{+13}_{-11}$) %		
Γ_{10}	invisible	[b]	(1.4 ± 2.9) %		

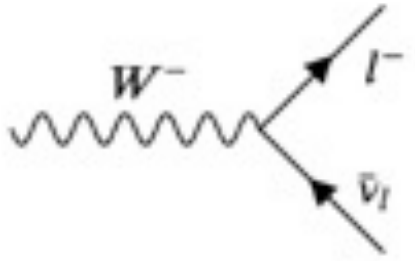

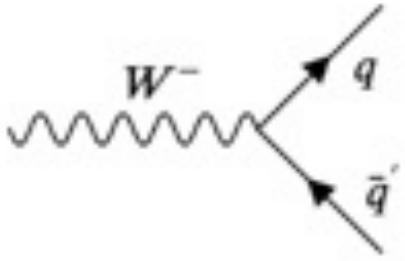

Miscelaneous

- Pseudorapidity $\eta = -\ln(\tan\frac{\theta}{2})$ (*the zero-mass limit of a relativistic particle's rapidity y*)
- Rapidity $\mathrm{y} = \frac{1}{2}\ln(\frac{E+p_z}{E-p_z})$
- Luminosity: numbers of particles through a given area
  - Instantaneous $L = \frac{N_b^2 f_\gamma F}{4\pi\sigma_x\sigma_y}$ ($cm^{-2}s^{-1}$)
  - Integrated $\mathcal{L} = \int L(t)dt$ (fb^{-1})
- 1 bunch (LHC) of protons = 1.15×10^{11} protons

The ATLAS detector

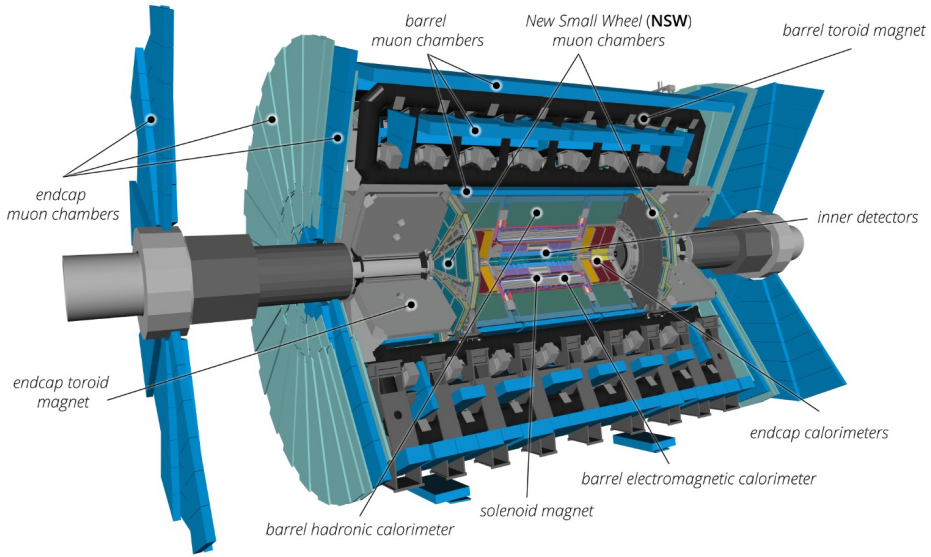

- **Inner Detector (ID)**: $|\eta| < 2.5$
- **Electromagnetic Calorimeter (EM Calorimeter)**: $|\eta| < 3.2$
  - **Barrel**: $|\eta| < 1.475$
  - **End-cap**: $1.375 < |\eta| < 3.2$
- **Hadronic Calorimeter (Had Calorimeter)**: $|\eta| < 4.9$
  - **Tile Calorimeter**: $|\eta| < 1.7$
  - **Hadronic end-cap calorimeter**: $1.5 < |\eta| < 3.2$
  - **Forward calorimeter**: $3.1 < |\eta| < 4.9$
- **Muon Spectrometer (MS)**: $|\eta| < 2.7$
  - **Barrel**: $|\eta| < 1.0$
  - **End-cap**: $1.0 < |\eta| < 2.7$

- Inner Tracker
  - Pixel (silicon pixel),
  - SCT (silicon microstrips)
  - TRT (drift tubes)
- Solenoid Magnet
- EM calorimeter (LAr acordeon shape tungsten/copper/lead)
- Hadronic Calorimeter
- Muon System with Toroid magnets (RPC, MDT)

Endcaps

- EM calorimeter
- Hadronic Calorimeter
- NSW (MMG/STG)
- Toroid Magnet
- BW (TGC/MDT)
- Outer Wheel (MDT)

IBERT/Eye Diagrams

Eye Diagrams

- An "eye diagram" is a tool used in signal processing, particularly in digital communication, to visually assess the quality of a signal being transmitted.
- It is superimposition of multiple digital signal waveform within one clock period onto a single graph.
- x-axis → time, y-axis → amplitude of the digital signal
- The diagram provides insights into the signal's performance, including its timing errors, amplitude noise, and the overall ability of the receiver to correctly interpret the incoming data.
- Factors like the "opening" of the eye in the diagram indicate the signal's robustness against potential noise and interference. Crucial tool for analysing and troubleshooting communication systems.
- 40-50% open UI the system has a reasonable margin for error in sampling the data correctly, indicating that the signal quality is good, jitter and noise are well-controlled but not entirely negligible → a well-performing system

IBERT Test

- The main goal of the IBERT test is to evaluate the performance of serial data communication channels and devices by determining the bit error ratio.
- This ratio is a critical metric that quantifies the number of errors in the bits received versus the total number of bits transmitted.
- The test involves sending a known PRBS data pattern from the transmitter to the receiver. The receiver then compares the incoming data with the original pattern to identify any discrepancies or errors.
- By analysing the frequency and type of these errors, the test provides insights into potential issues with the physical layer of the transmission, such as signal integrity, timing errors, and noise. It also helps in verifying the operational limits of the communication system.
- IBERT tests are commonly used in the development and quality assurance of network devices and systems, including fiber-optic transceivers, network routers, and switches that operate at high data rates. They are essential in environments where data corruption from transmission errors needs to be minimized, such as in telecommunications and data centers.
- The results from an iBERT test are crucial for diagnosing problems, optimizing system performance, and ensuring that the hardware meets the necessary standards and specifications for reliable operation.

NSW TDAQ elx

- FELIX: system that acts as interface between FE elx and DAQ. Routes data from FE to DAQ using high-speed opt links. Aggregates data from multiple channels. Serves and relays TTC info. Sends general purpose control data
- OPC: sw interface between user & SCA. Follows OPC-UA standard, compatible with SCADA.
- swROD: sw-based solution for handling data readout and processing tasks. Input data are being processed by using plug-ins for each subdetector.
- ALTI: VME bus module that replaced all legacy TTC modules. Controlled by SBC.
- L1DDC: Aggregator card. Collects data from mult FEBs. Initial data checks/processing, buffering and transmission to FELIX. Manages the data flow from detector --> FELIX and distributes TTC signals.

- VMM signal processing (amplification, shaping, digitization)
- TDS serializes trigger data, asigns BCID combines trigger info into a single datastream
- ROC controls the FE DAQ, formats the readout packets and sends them to FELIX

- GBTx hugh speed communication between FE/backend providing data transmission rates up to 4.8Gbps. Chipset
- GBTx (serializer deserializer multiplexer of serial data links rate 80, 160, 320 MBps),
- VTRx (optical link interface TT/TR).
- SCA distributes control/monitoring signals, communicates with FELIX through 80Mbps)

NSW Motivation

- $1.3 < |\eta| < 2.7$
- Precision tracking and triggering, able to work at high rates with excellent realtime spatial and time resolution
- They can provide the muon L1 trigger system with online track segments of good angular resolution to confirm that mu tracks originate from IP → reduce fake triggers
- The Level-1 low p_T single muon trigger rate will be kept at an acceptable level (Higgs production in pp collisions is mainly due to gluon fusion H→WW→lvlv (low p_T)
- Overall, ATLAS will be able to maintain its performance in the HL-LHC era

NSW Trigger

- NSW measures radial coordinate in 2 planes, φ, angle $\Delta\theta$ of track segments
- $\Delta\theta < \pm 7\ mrad$ (angle wrt the infinite mom track, line from IP
- Radial coordinate → high precision strips (averaging 4 centroids of strips signals)
- φ → triggering tower of the sTGC pads and for MM from the stereo strips
- $\Delta\theta$ is measured to an accuracy of $1\ mrad$ by calculating the track position in 2 virtual planes in NSW.
- NSW Trigger latency 1025 ns

NSW Trigger Grafana Dashboard

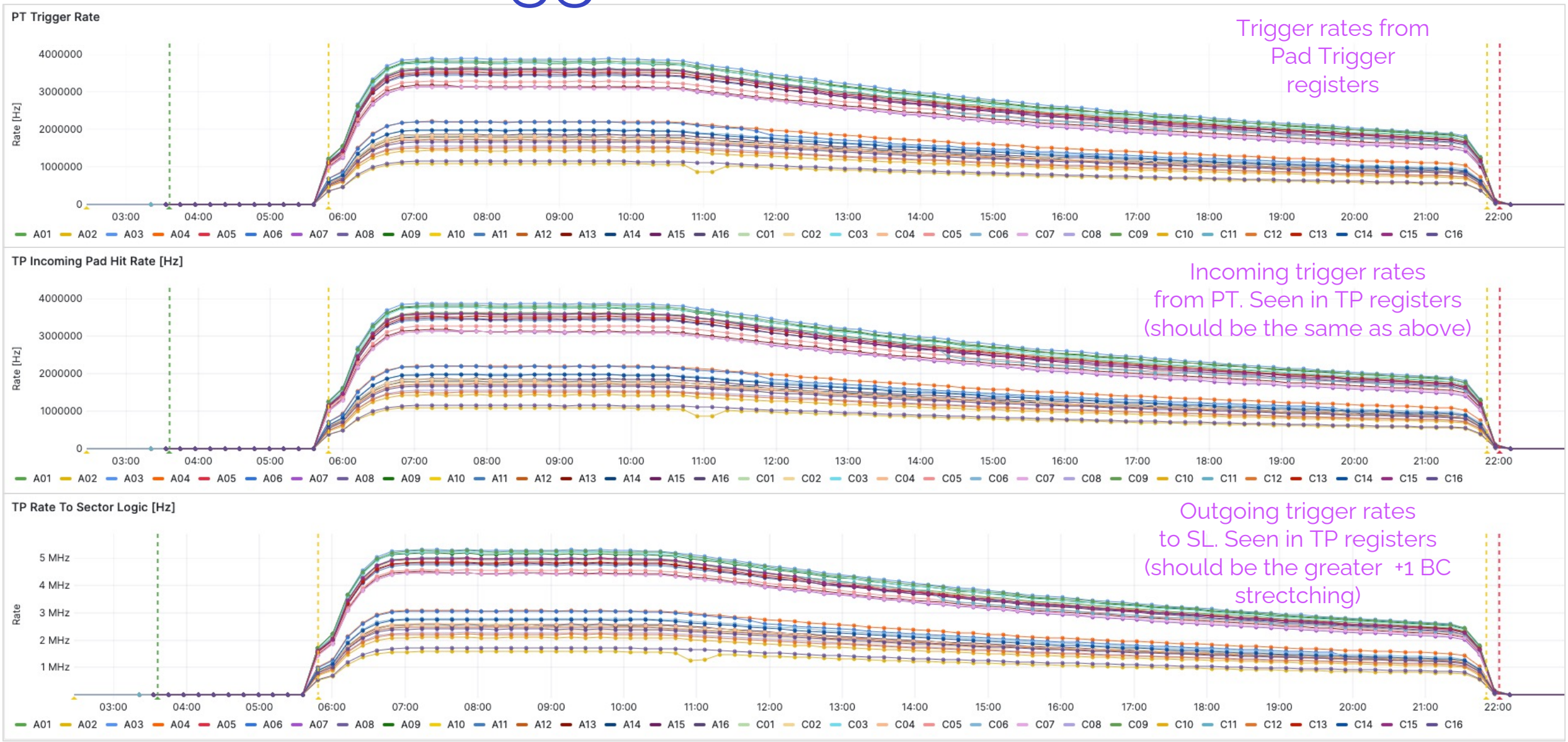

sTGC Trigger Electronics

pFEB

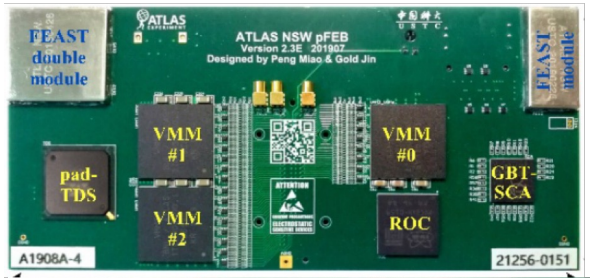

sFEB

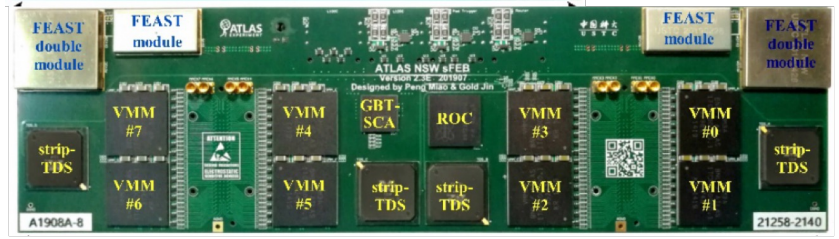

L1DDC

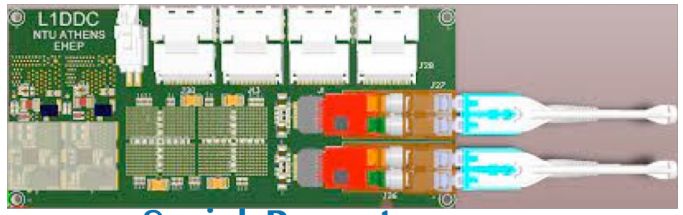

Serial Repeater

Photos taken from Espace of ATLAS NSW Electronics Group

LVD6R

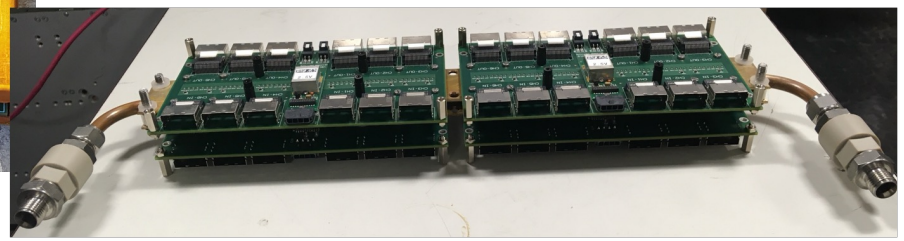

Twinax cable

Optical Fiber

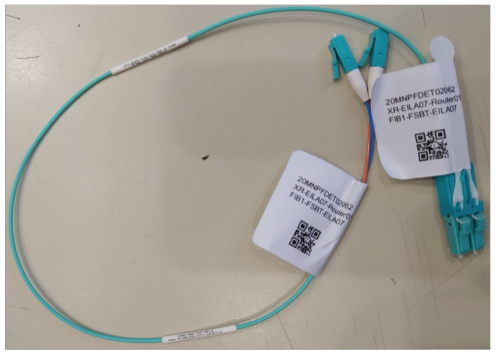

Router

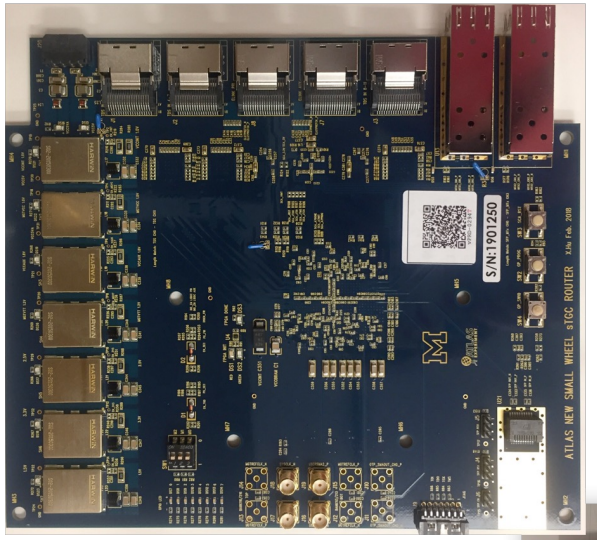

Trigger Processor

rimL1DDC

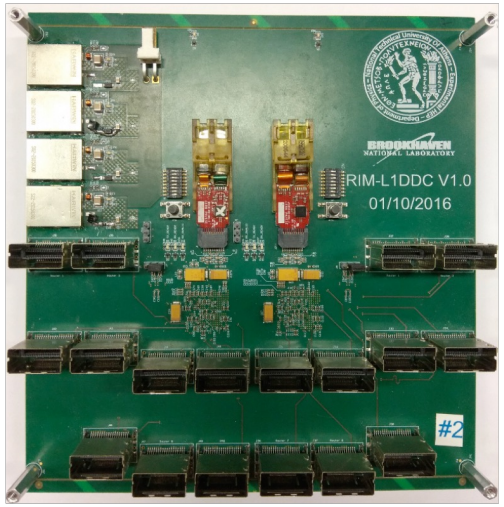

Pad Trigger

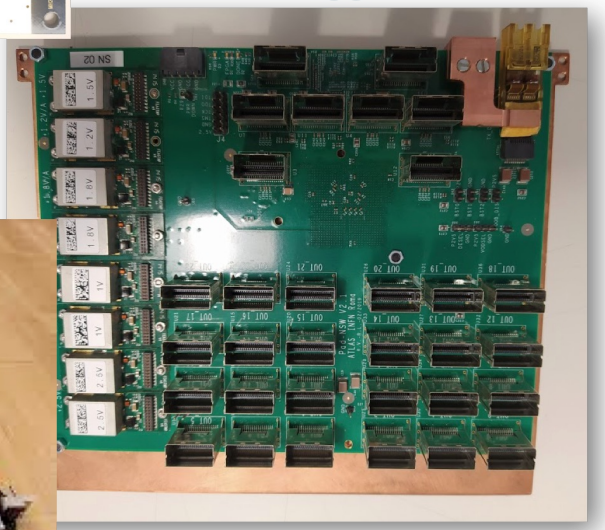

Trigger Slice Test Bench

1 wedge electronics
- 12 pFEBs
- 12 sFEBs
- 8 L1DDC
- 1/2 rim crate
  - 1 Pad Trigger
  - 1 rimL1DDC
  - 4 routers
- Trigger Processor inside soundproof air-cooled box
- FELIX
- swROD
- SBC/ALTI
- Water cooling system

Direct Clock at P1

- 1 direct clock board per wheel, installed at USA15
- Distribute low jitter clocks at 160 MHz to the rim electronics via rimL1DDC
- 32 clocks are needed for each wheel (2 per rimL1DDC, primary & auxiliary)
- 1 fiber from direct clock breaks-out in 32 fibers. Some of them were found to be broken but cannot be replaced

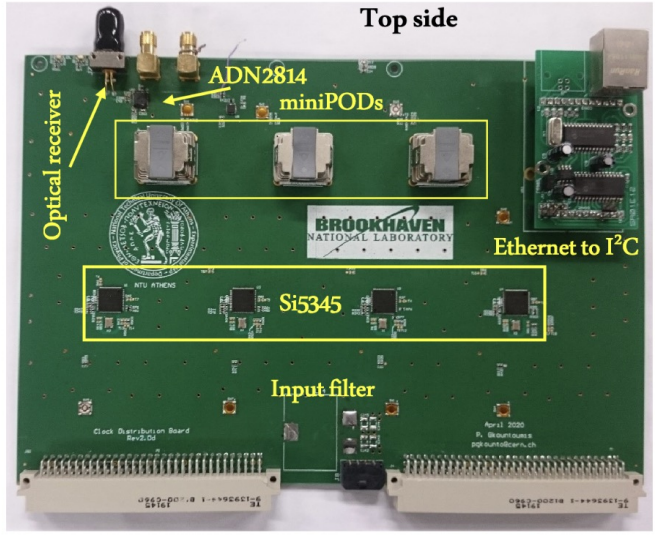

Primary side Auxiliary side

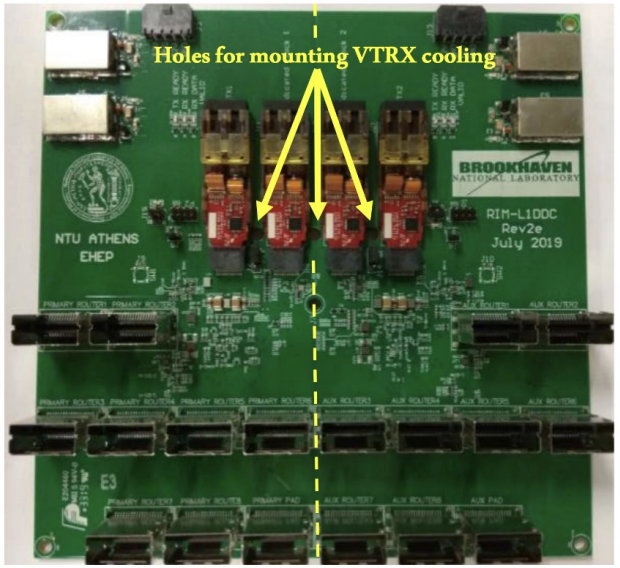

RSSI measurements – rimL1DDC

	REF1	REF2	Comments
A01	0,242	0,244	
A02	0,244	0,504	A02 REF1 is A01 REF2
A03	0,249	0,508	REF1 and REF2 swapped
A04	0,268	0,267	
A05	0,249	0,255	
A06	0,259	0,244	
A07	0,261	0,507	REF22 broken
A08	0,267	0,265	
A09	0,286	0,260	
A10	0,257	0,249	
A11	0,264	0,257	
A12	0,266	0,273	
A13	0,497	0,505	
A14	0,254	0,268	
A15	0,247	0,499	REF2 broken
A16	0,263	-	REF2 probably broken
C01	0,263	0,262	
C02	0,249	0,251	
C03	0,241	0,245	
C04	0,251	0,250	
C05	0,244	0,242	
C06	0,244	0,507	
C07	0,303	0,274	
C08	0,498	0,256	
C09	0,251	0,239	
C10	0,245	0,247	
C11	0,244	0,514	
C12	0,501	0,511	
C13	0,242	0,245	
C14	0,246	0,532	
C15	0,238	0,326	REF1 and REF2 swapped
C16	0,239	0,566	

- Some Direct Clock fibers were broken or in some cases the fiber were ok, but the RSSI value was not trustworthy.
- Tried to have REF1 is operational for all sectors:

  → swapped primary with auxiliary

  → swapped between sectors
- RSSI measurements will be repeated during YETS

Eye Diagrams using Direct Clock

Direct Clock was used for some data quality tests during P1 Commissioning. Improvement was observed

[–] Router_HO_L1

Felix clock

[–] Q1_SFEB

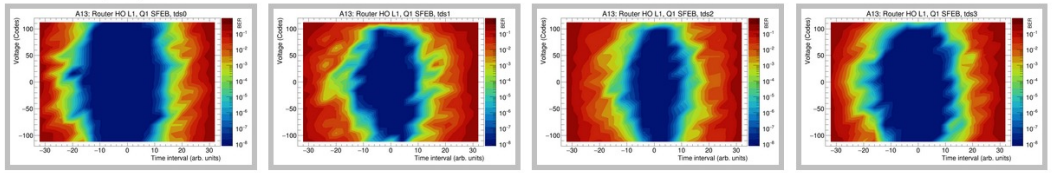

[–] Q2_SFEB

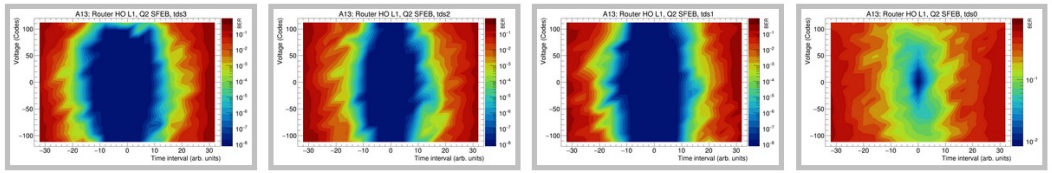

[–] Q3_SFEB

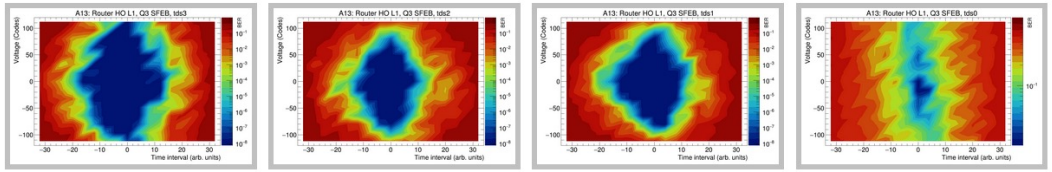

[–] Router_HO_L1

Direct clock

[–] Q1_SFEB

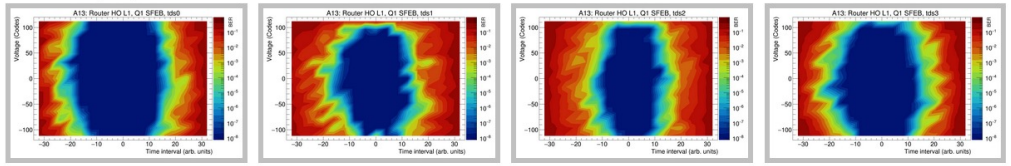

[–] Q2_SFEB

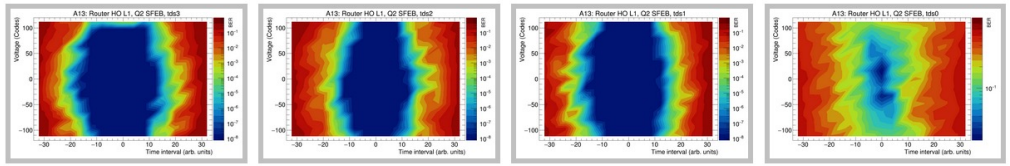

[–] Q3_SFEB

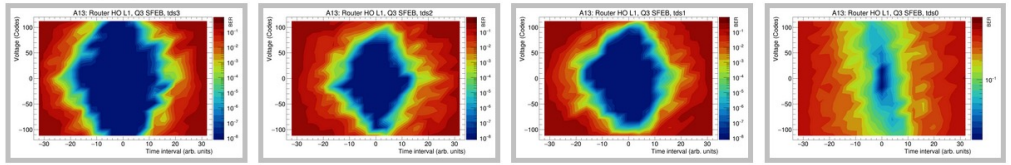

Direct clock as default config

- Direct Clock can be enabled using a NSWConfig command with these selection options:

```
configure_rim_l1ddc
--clock --sel 1 --sel0 1 --sel1 1
--sca_addr RimL1DDC_PRI
--opc_ip pc-tdq-flx-nsw-stgc-XX.cern.ch:4802X
```

	SEL	SEL1	SEL0
PRIMARY GBTX REFCLK2	0	X	X
PRIMARY GBTX REFCLK1	1	0	0
AUXILIARY GBTX REFCLK3	1	0	1
PRIMARY DEDICATED	1	1	1
AUXILIARY DEDICATED	1	1	0

- During `CONFIG` we can select direct clock.

  But if an SCA reset happens during a run,

  the selected clock will be automatically changed to default (primary GBTX REFCLK2).

  Similar problem if we select PT AUX side. *A solution needs to be found*

- Switching to the direct clock is a great idea but:
  - Check fiber status
  - Solve the SCA reset issue
  - New fw for PT/Router(?) + software

rimL1DDC block diagram

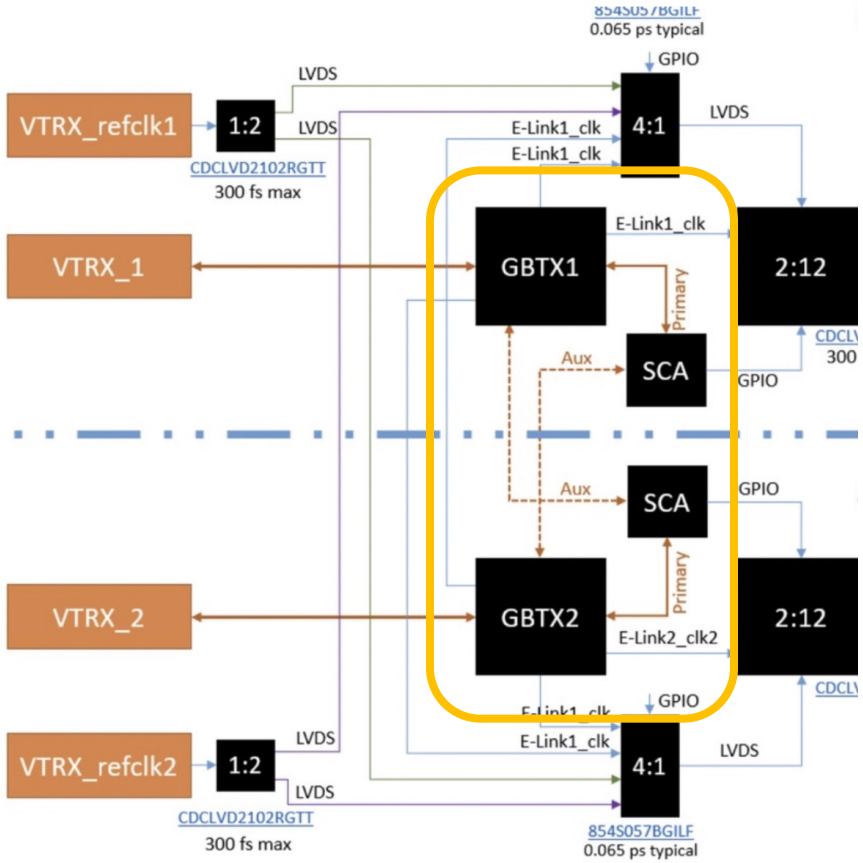

- PRI and AUX SCA can be reached by 2 paths
- `GBTX1 → PRI SCA (Pri)`
- `GBTX1 → AUX SCA (Aux)`
- `GBTX2 → AUX SCA (Pri)`
- `GBTX2 → PRI SCA (Aux)`

NSW Trigger Processor – block diagram

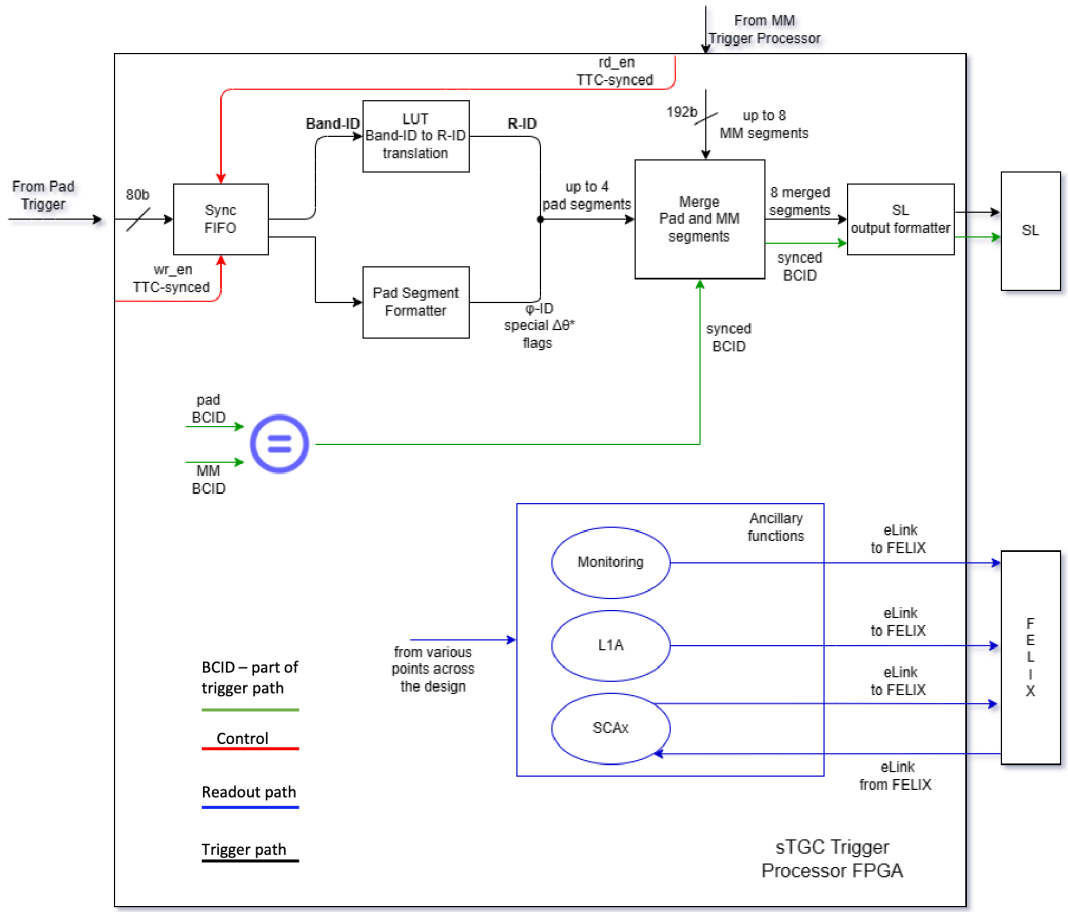

Router MTx issue

Luis Hervas (LAr) contacted us for an issue observed at the MTx/MTRx modules on their front-end boards.

Drop of light power in their data fibers related with luminosity ramp up.

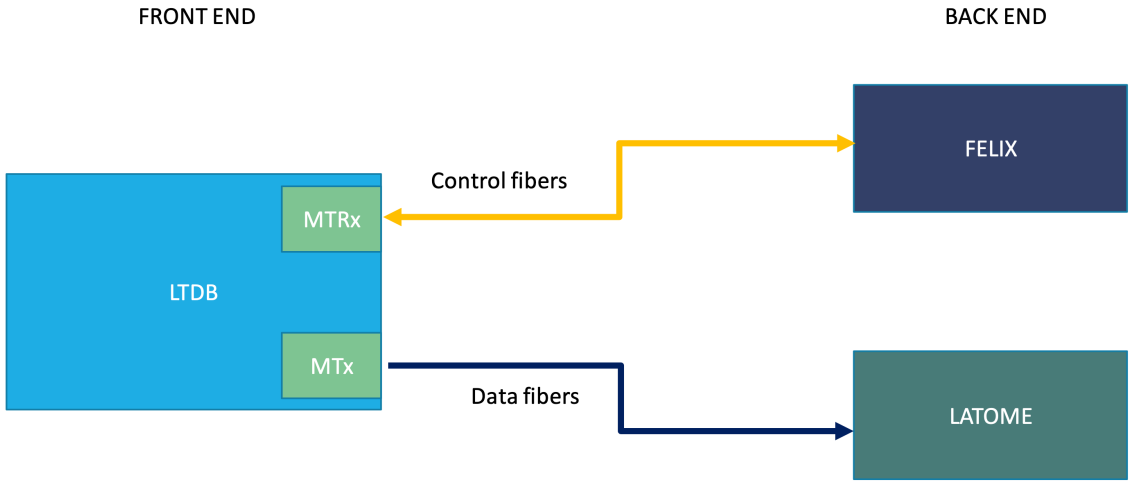

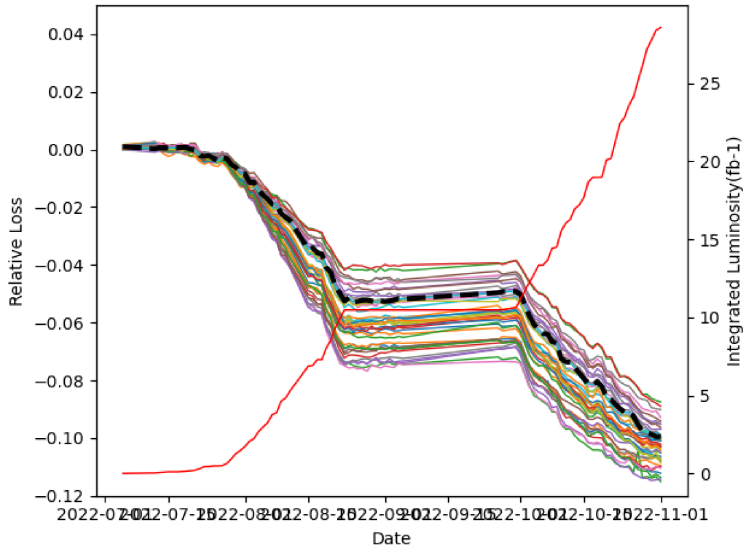

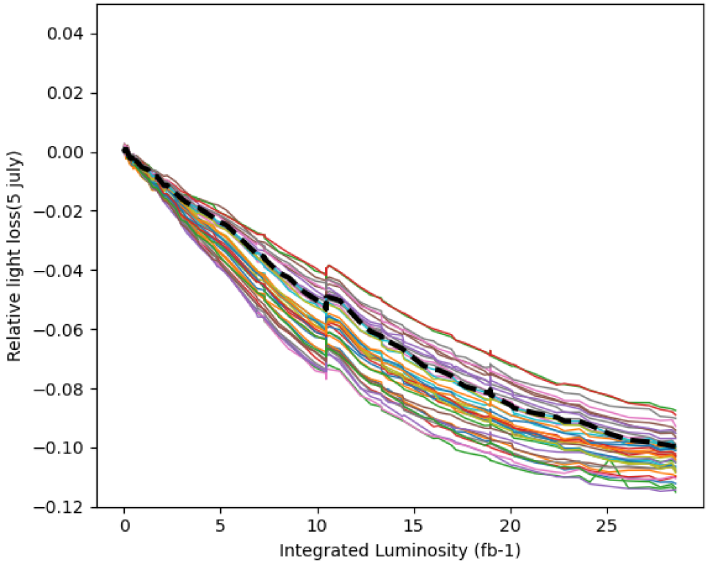

Router MTx issue

Interesting presentations by LAr people: here and here

LAr

Barrel fibers
- Mean light loss -7%
- For some max -20%

End-cap fibers
- Mean light loss -1%
- For some max -4%

NSW

MTx are used in the Routers
(4x8x32 = 1024 MTx)

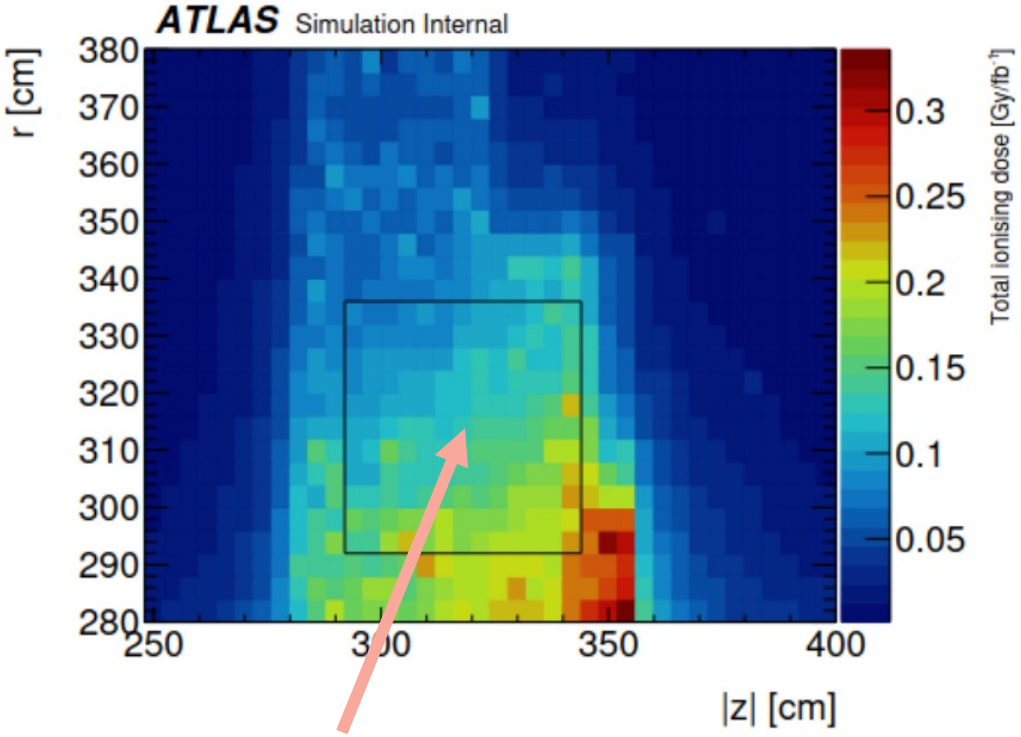

LAr boards are here

Router MTx issue

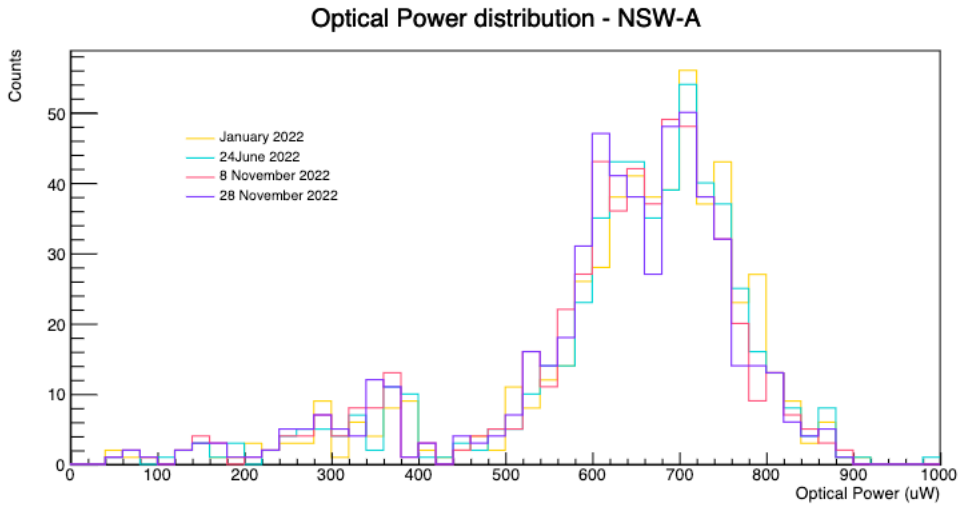

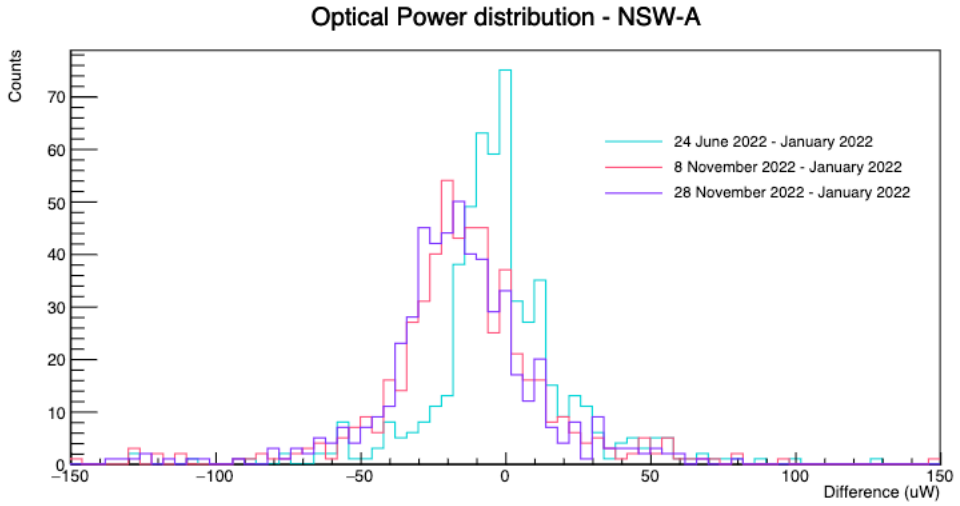

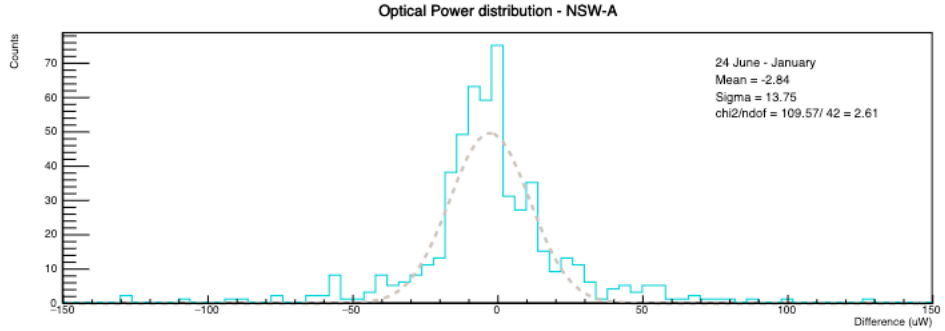

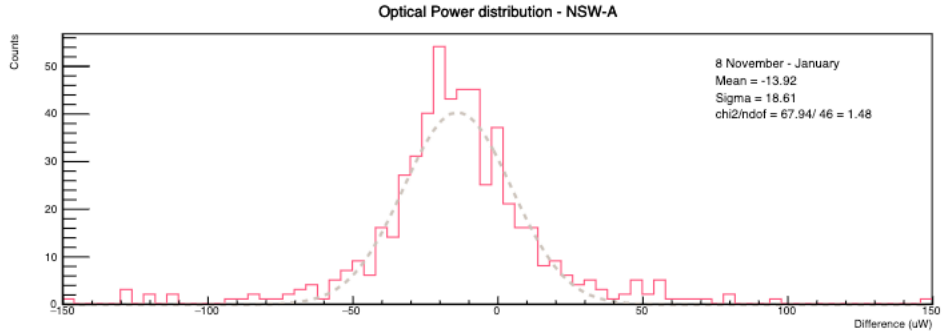

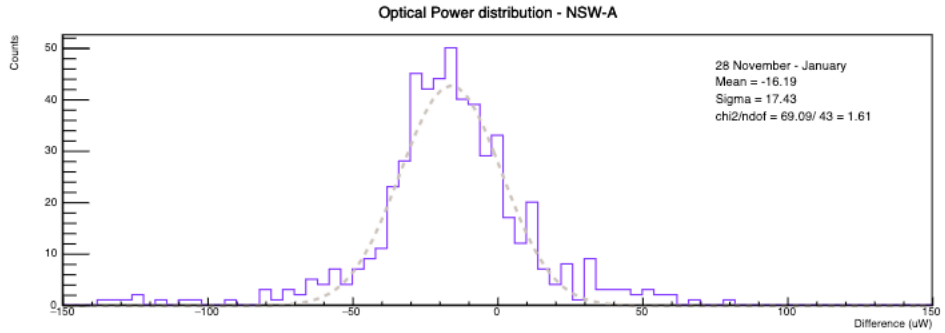

Router MTx issue

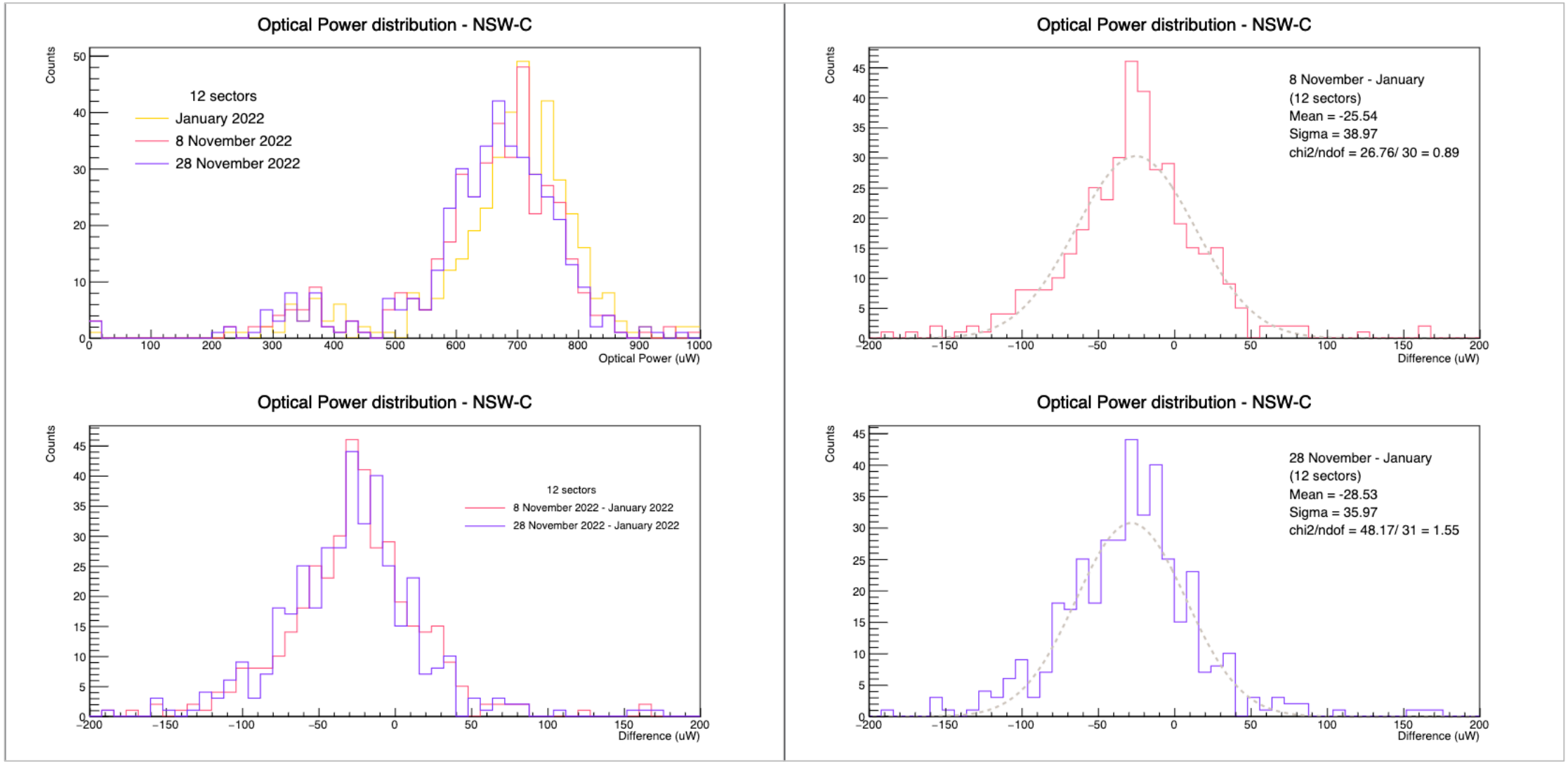

Router MTx issue

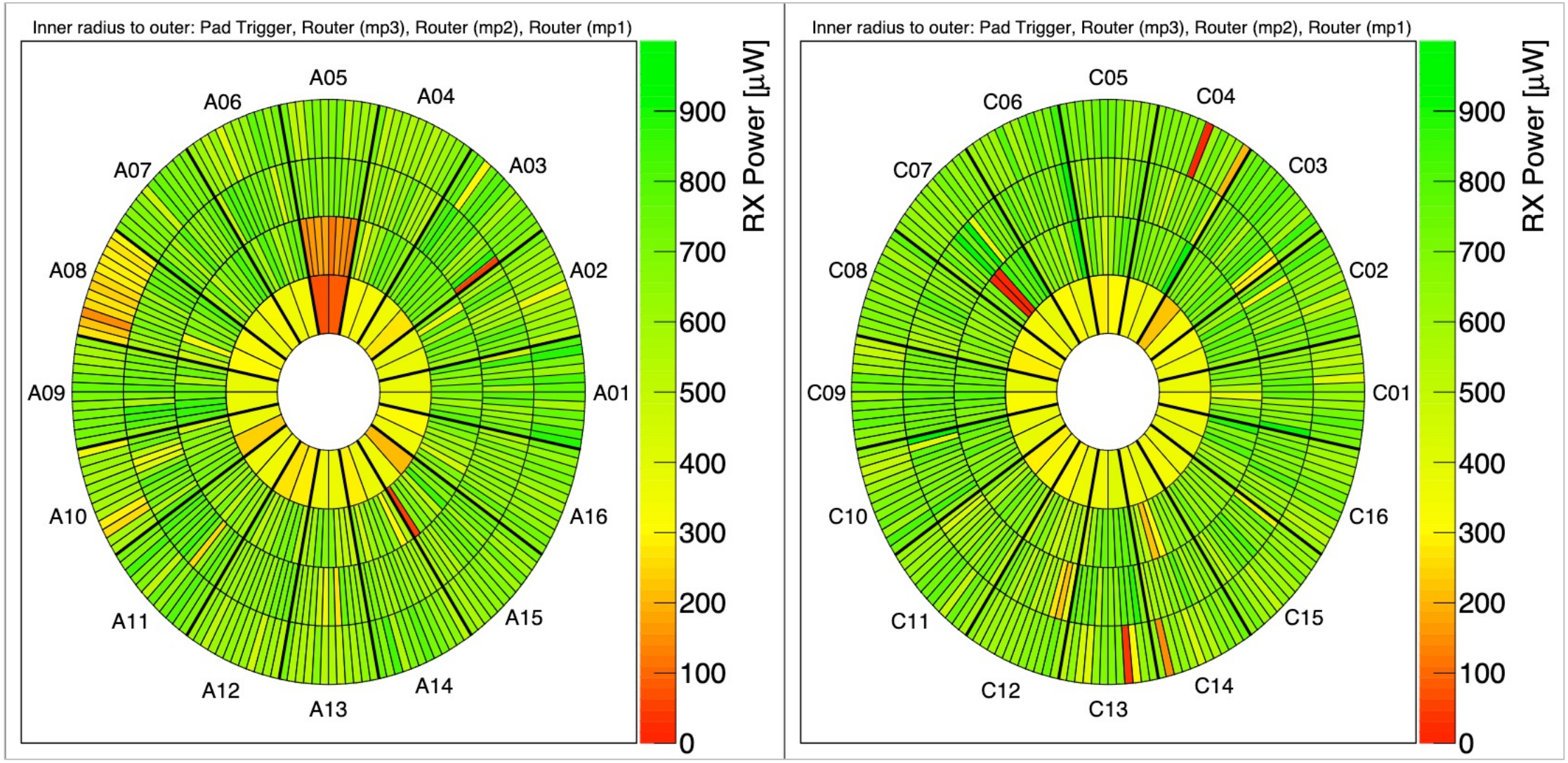

Full Chain Validation

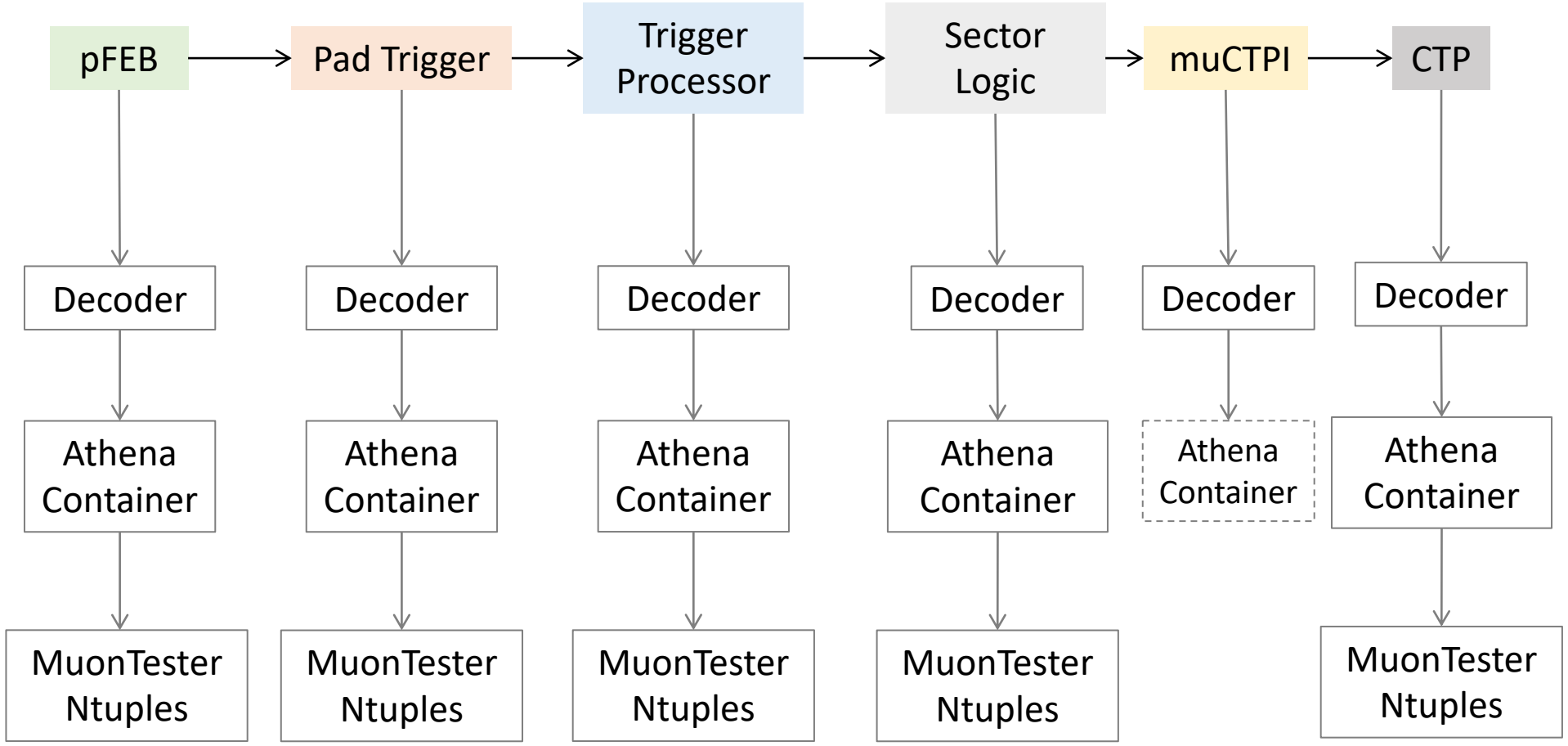

NSW TID

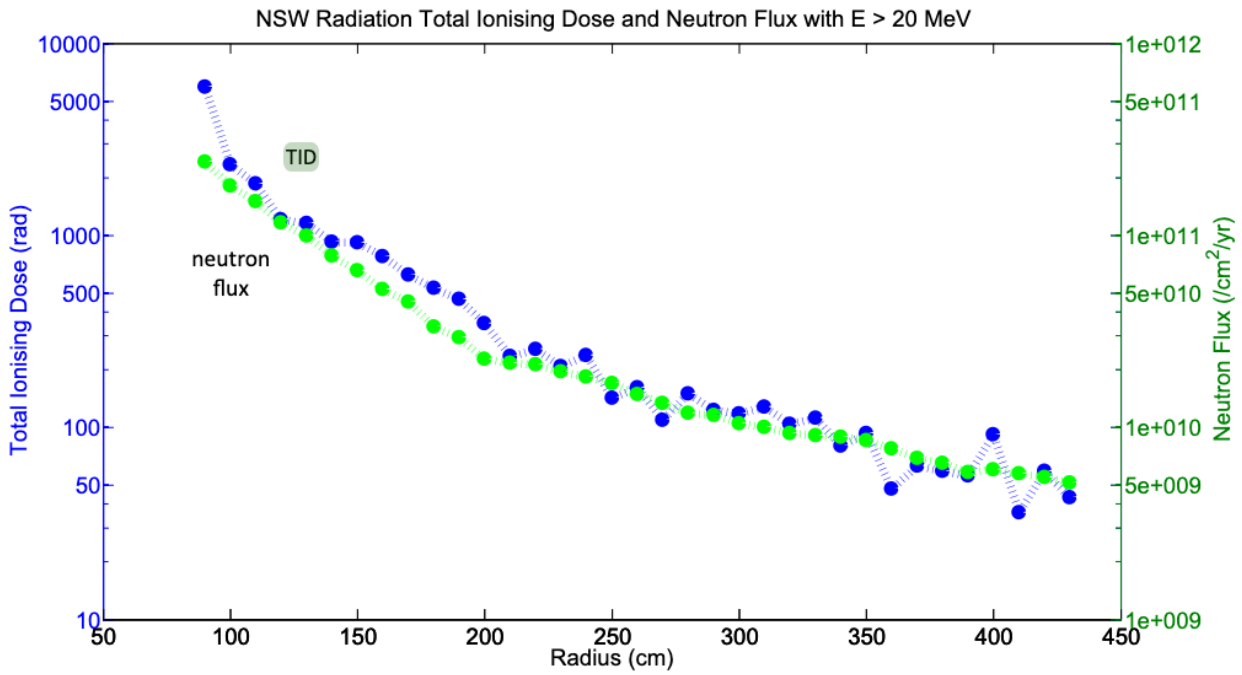

Figure 12.2: Total, per year, Ionizing Dose (TID) and neutron fluence (E > 20 MeV) vs. radius at the NSW for luminosity 10^{34} (from the 2005 Radiation Task Force Summary report)

Fig. 12.2 shows the Total Ionizing Dose (TID) and the fluence of neutrons with energy greater than 20 MeV for luminosity 1034 and for one year of LHC operation. Extrapolating to the expected luminosity of 5×10^{34} and for 10 years of operation, the TID at the highest pseudo-rapidity region of the NSW will be of the order of 0.5 Mrad (with some uncertainty factored in).

Rad Hits Distribution

Hit maps of Layer6
Various irradiations
Before/after selection

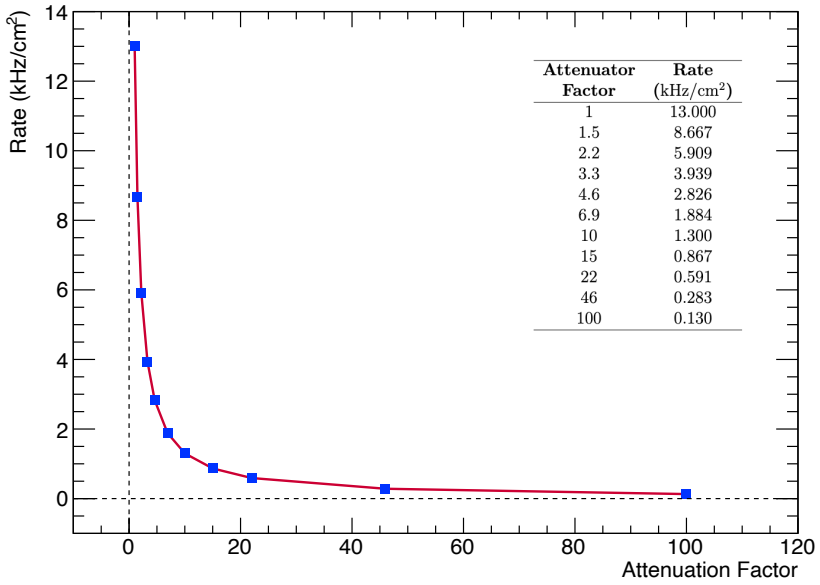

Attenuator Factor	Rate (kHz/cm²)
1	13.000
1.5	8.667
2.2	5.909
3.3	3.939
4.6	2.826
6.9	1.884
10	1.300
15	0.867
22	0.591
46	0.283
100	0.130

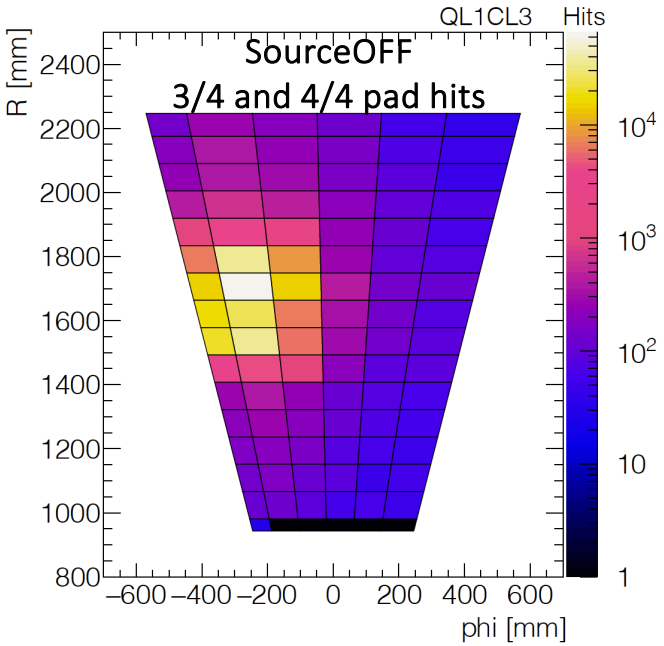

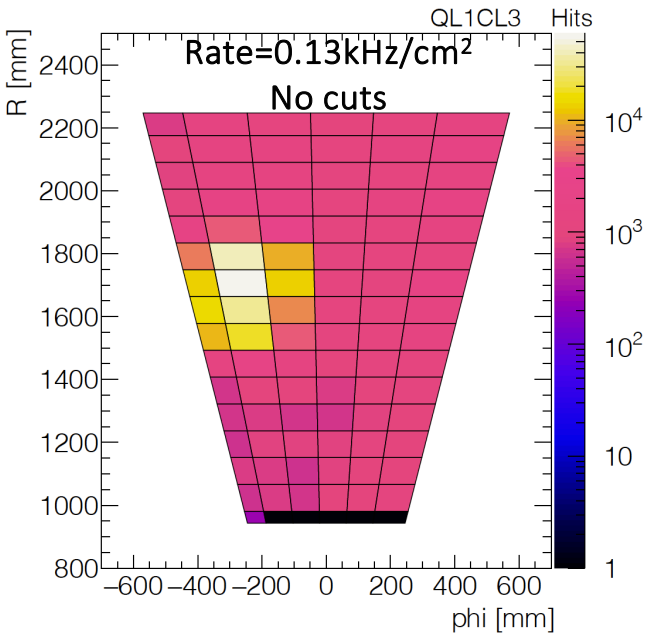

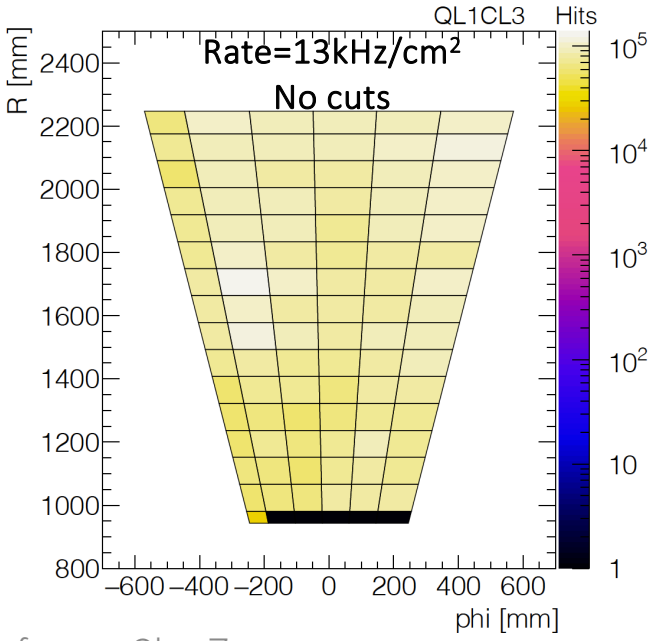

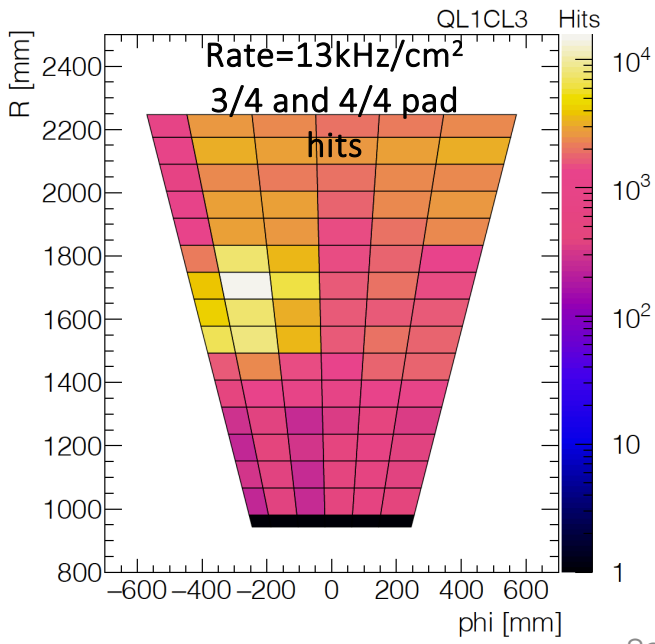

4 scintillator coincidence studies

- 4 scintillator coincidence data
- Pad efficiency per layer not trigger efficiency
- Pulse Peaking Time = 50ns
- Events with PDO > 1022 are removed

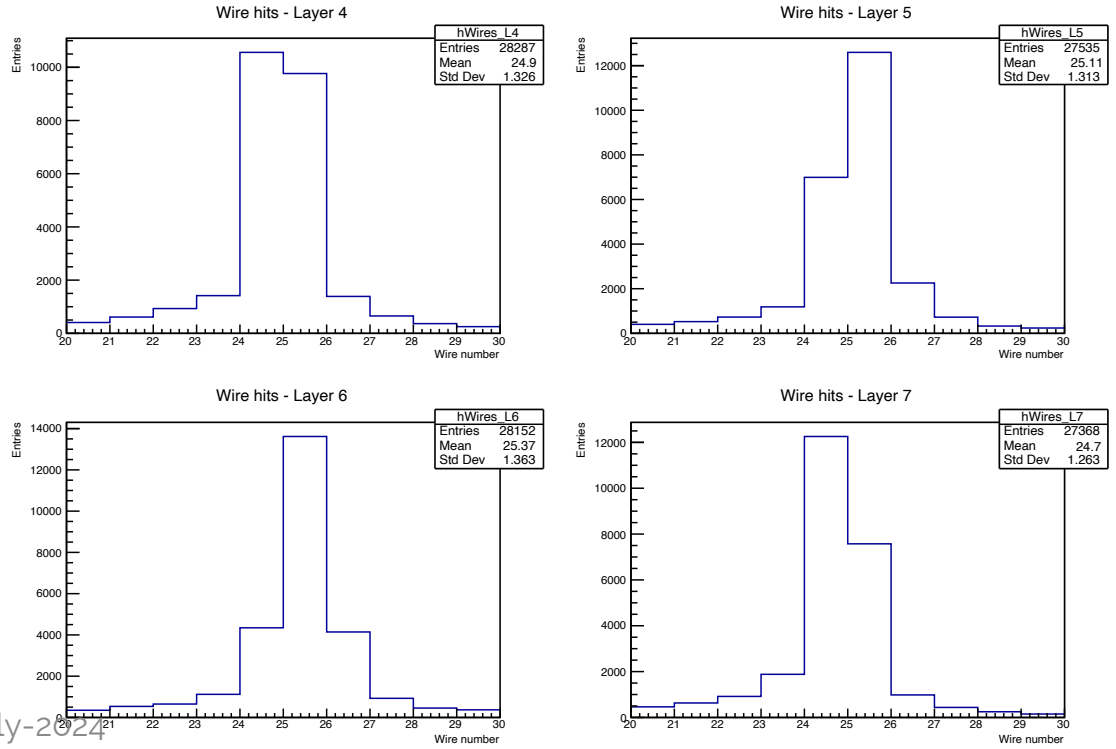

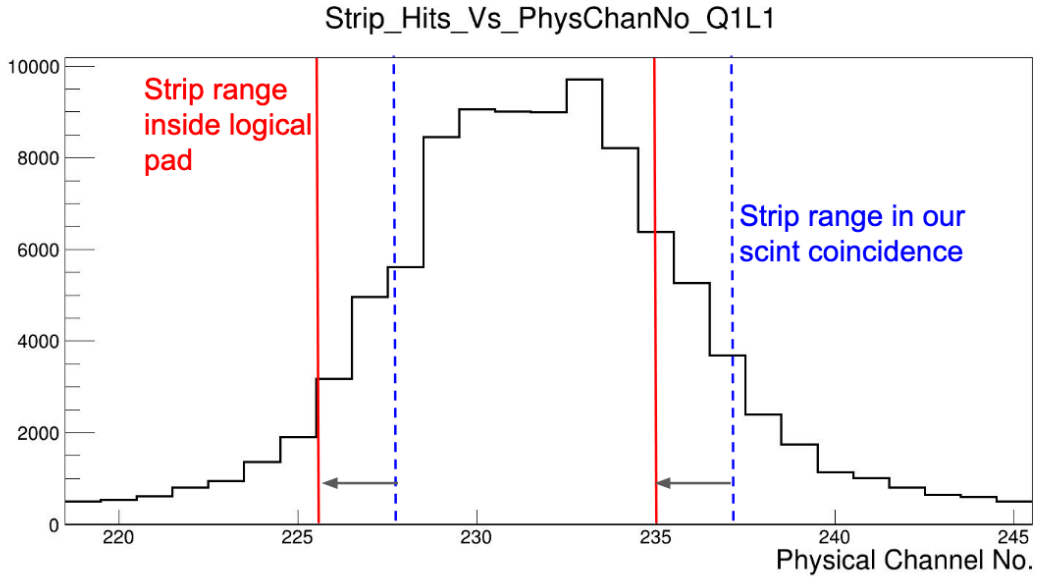

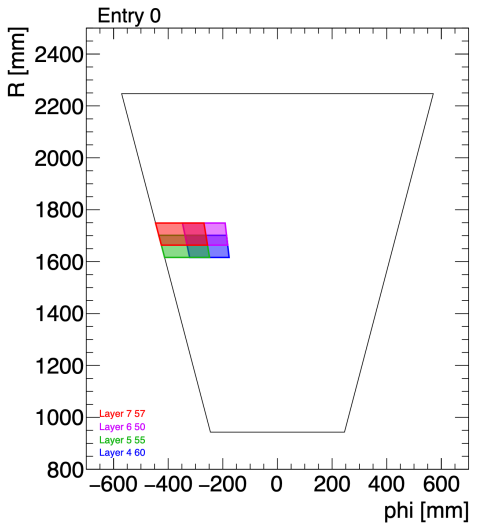

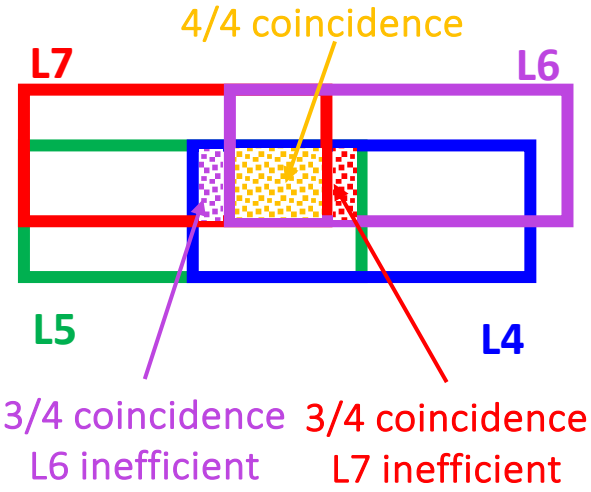

Z mass precision

Electroweak Fit

The global electroweak fit is a comprehensive analysis combining measurements of various electroweak observables to test the consistency of the SM and to determine the parameters of the electroweak sector with high precision. This includes the masses of the W and Z bosons, the weak mixing angle, and the top quark and Higgs boson masses. The fit also constrains the couplings and other properties of the particles involved in the electroweak interactions.

- Test the internal consistency of the SM and ccompare theoretical predictions with experimental data.
- Precisely determine the fundamental parameters of the SM, such as the Fermi constant G_F, the strong coupling constant α_s, the weak mixing angle $\sin^2\theta_W$, and the masses of the W boson, Z boson, top quark, and Higgs boson.
- Identify any deviations from the SM predictions that might suggest the presence of new physics BSM

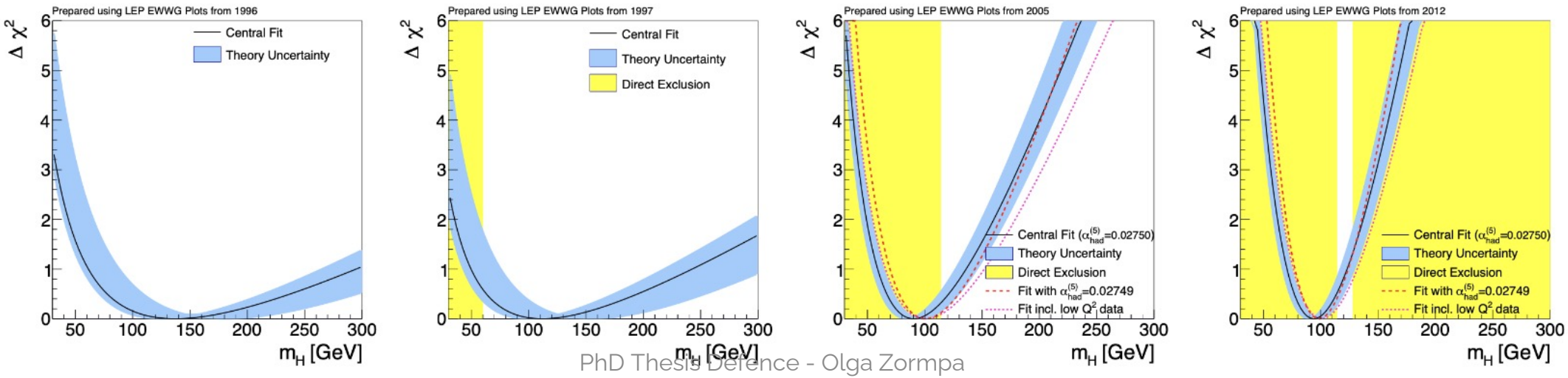

Z mass precision

Steps of the analysis

- Calibration
  - Sagitta bias correction (using the Z)
  - Momentum correction 1 (beta CURV, using Z)
  - Scale and momentum correction 2 (alpha and beta MULT, using J/psi), (background estimation), (scale), (resolution)
  - Material effect (syst)
  - Check with Upsilons
- Multijet estimation
- Physics modeling
- Statistical analysis

Z mass precision

Radial Distortion Analysis – Methodology

Model Fit

- Plot pseudo mass $m_{\mu\mu}$ wrt $\sin^2\theta_\rho$
- Slice $\sin^2\theta_\rho$ in bins and Project in Y
- Apply the model fit using PDFs
- Subtract background from the model
- Apply a Gaussian fit in the new distribution
- Retrieve mean and sigma from the Gaussian fit
- Plot mean wrt $\sin^2\theta_\rho$ and apply linear fit

Template Fit

- MC peak has a scale factor allowing the peak to open/close —> resolution
- Data peak has a scale factor allowing the peak to shift R/L —> scale
- Fit the MC to the data and produce a plot of mean wrt $\sin^2\theta_\rho$ and apply linear fit

$$intercept = m_{\mu\mu 0} \text{ and } slope = \epsilon\, m_{\mu\mu 0} \Rightarrow \epsilon = \frac{slope}{intercept}$$ (according to $m_{\mu\mu} = m_{\mu\mu 0}(1 + \epsilon \sin^2\theta_\rho)$)

Alignment Biases

Momentum biases resulting from correlated detector misalignments can be categorized into two distinct types:

- Sagitta biases manifest as detector geometry distortions occurring within the bending plane. These deformations affect the curvature of reconstructed tracks differently for positively and negatively charged particles. Specifically, they introduce discrepancies in the bending of particle trajectories, leading to deviations in the calculated momentum.
- Length scale biases are characterized by detector geometry distortions along the trajectory of the track. Unlike sagitta deformations, these biases impact the reconstructed curvature uniformly for both positively and negatively charged particles. Such distortions alter the spatial measurements along the track trajectory, resulting in systematic errors in momentum determination.

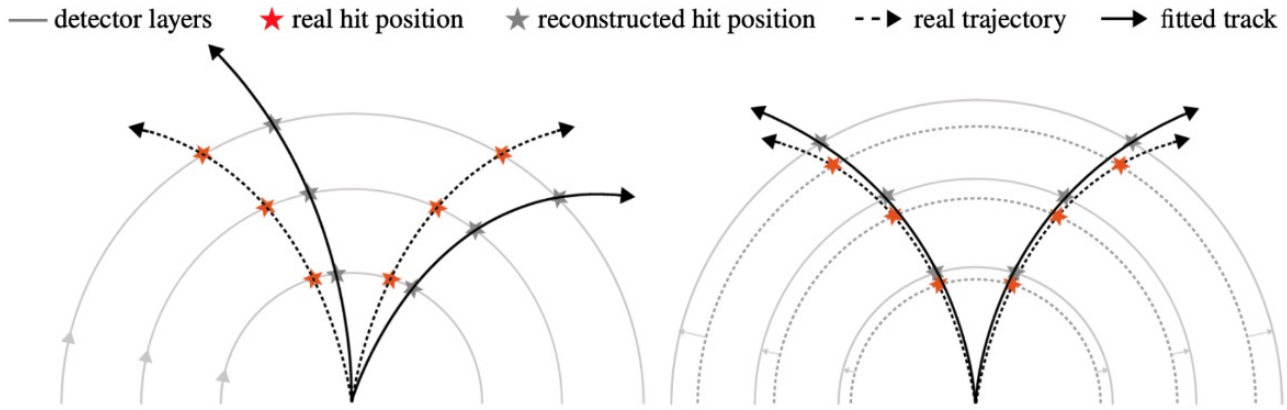

Figure 8.5: Visual representation of the weak modes; the sagitta bias (left) appears due to a deformation in the bending plane of the track with linear dependence on radius and the length scale bias (right) a deformation along the track trajectory, such as a radial expansion of the detector layers depending linearly on the radius. The legend above the graphs indicate that the dashed black line shows the real particle trajectories from the real hit positions represented by red stars, while the solid black line shows the fitted particle trajectories from the biased reconstructed hit positions represented by grey stars. The detector layers are represented by grey full/dashed lines [6]

Z mass precision

Radial Distortion Analysis - Results

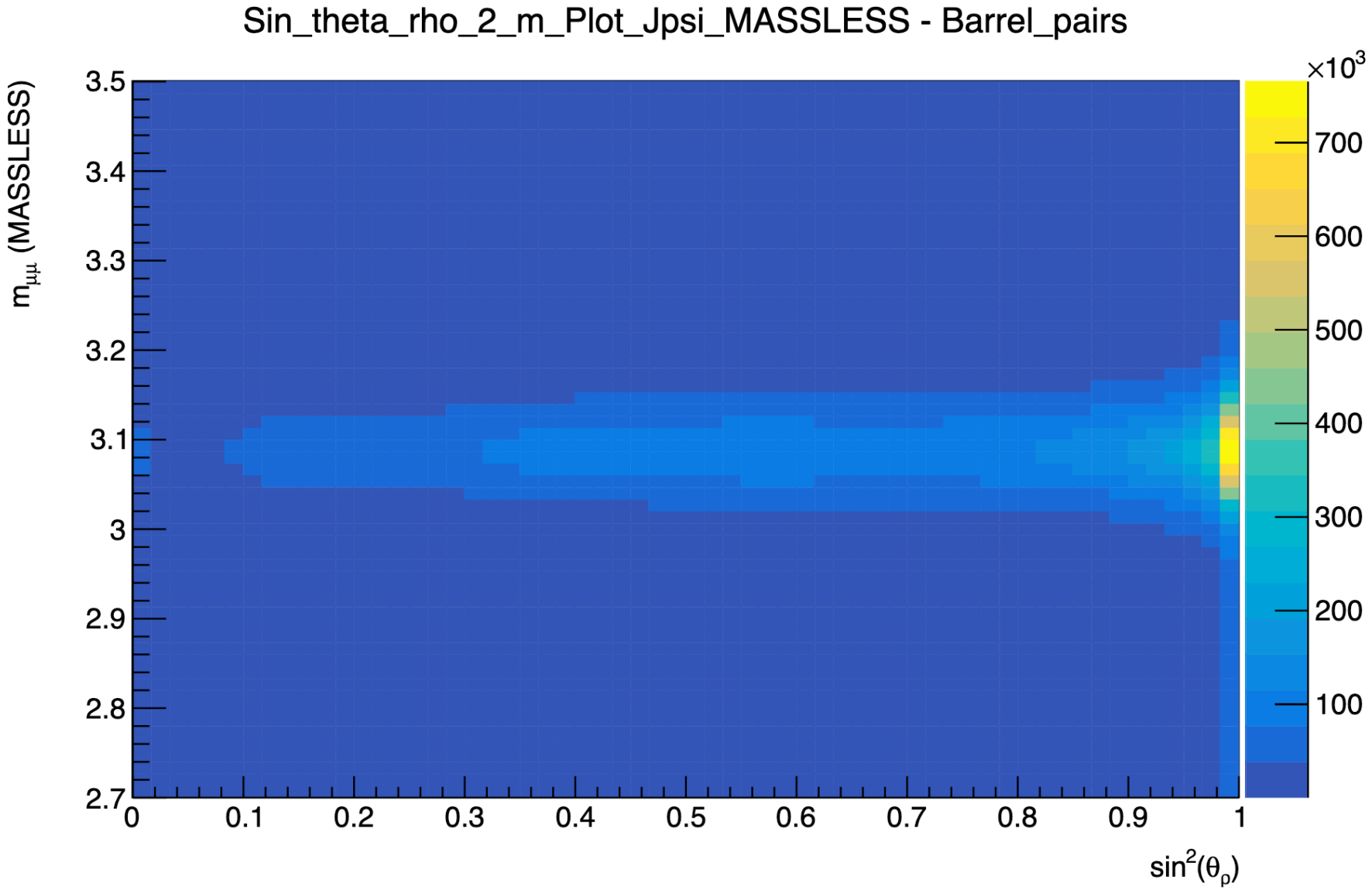

Radial Distortion Analysis - Results

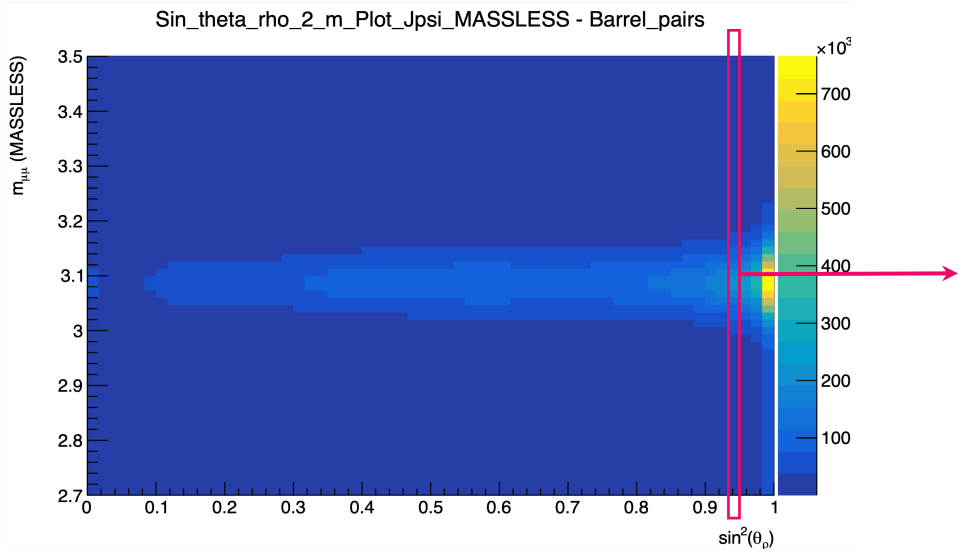

2D histo of $m_{\mu\mu}$ wrt $\sin^2\theta_\rho$

Selecting a random bin as an example.

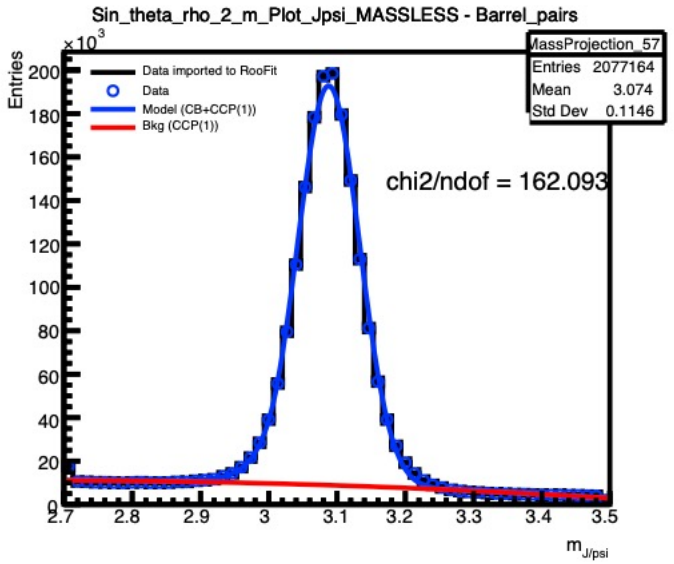

Fitting the data (black line) using the Model created by 1 Crystal Ball and 1 Chebyshev pol 1st degree PDFs.

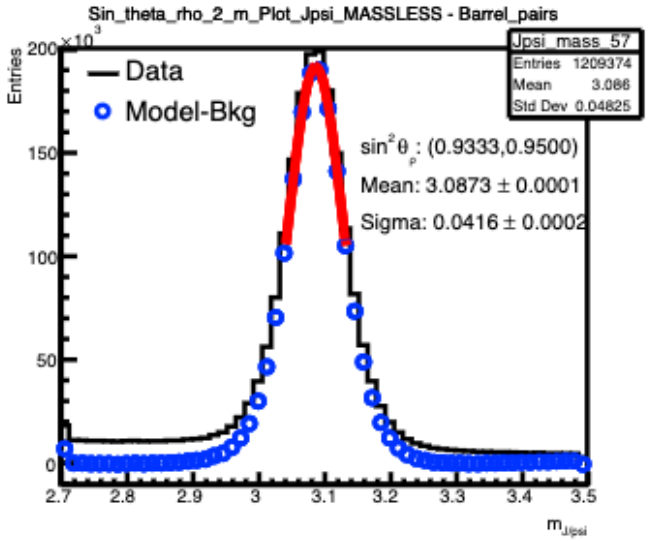

Black line indicates the data and blue points indicate the result after subtracting bkg from model.

Gaussian fit is applied, with the results shown in the legend. Fit range ± 1σ.

Z mass precision

Radial Bias Analysis - Results

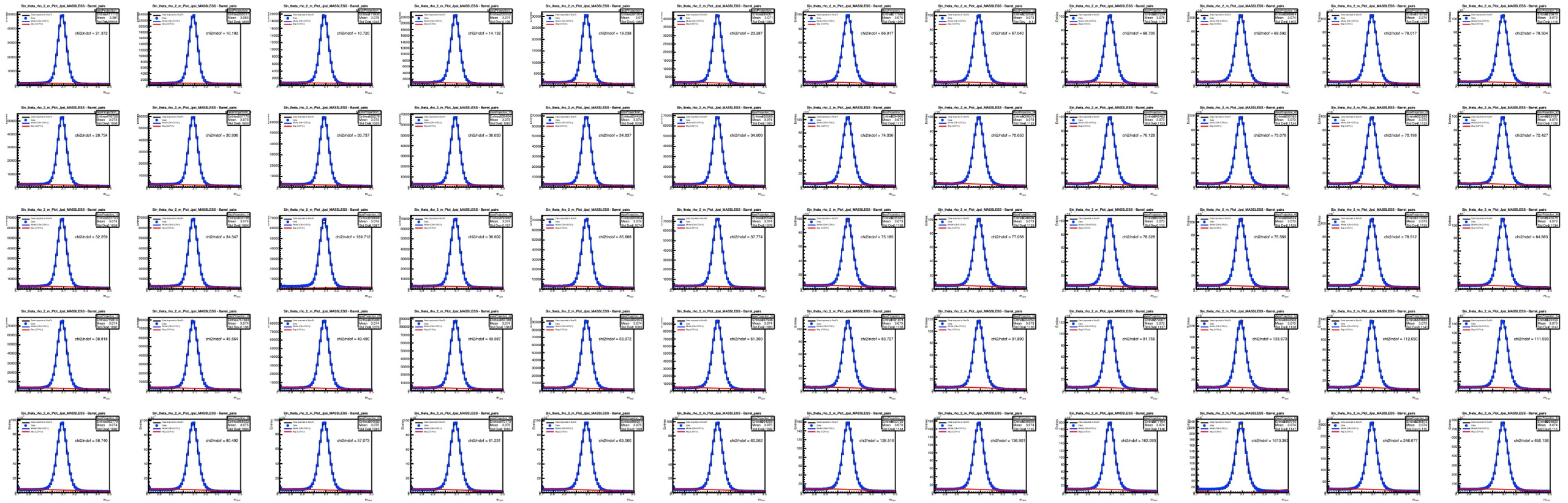

Z mass precision

Radial Bias Analysis - Results

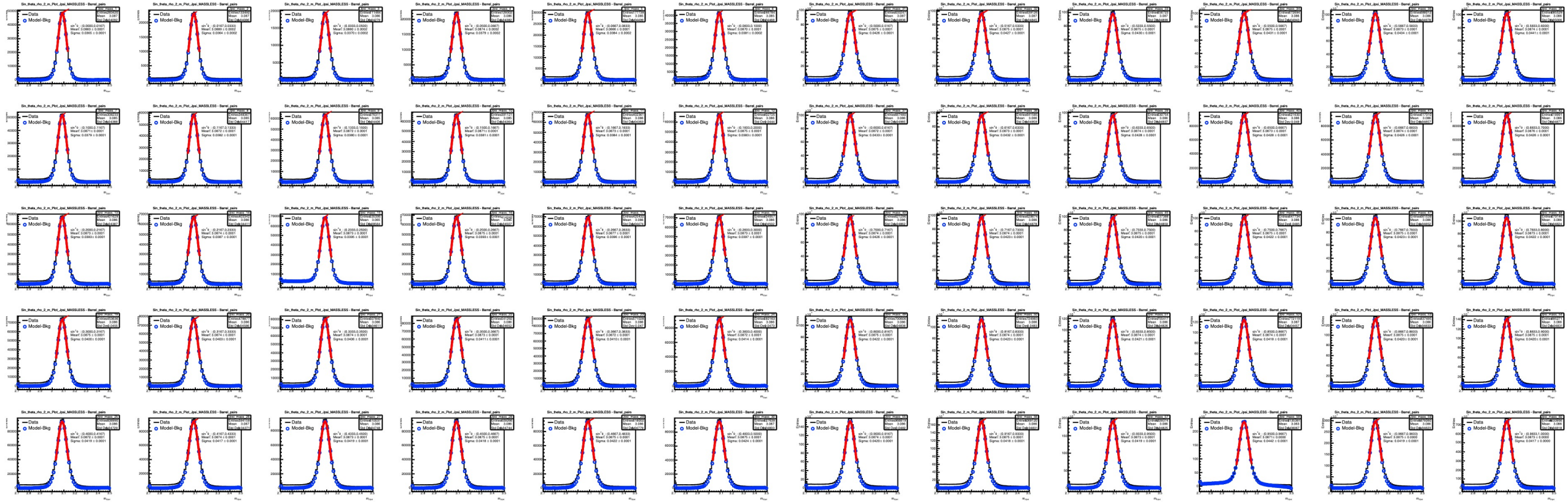

Radial Bias Analysis - Results

- Template Fit
- Tails and Peak
- 5 bins out of 60 in this screenshot

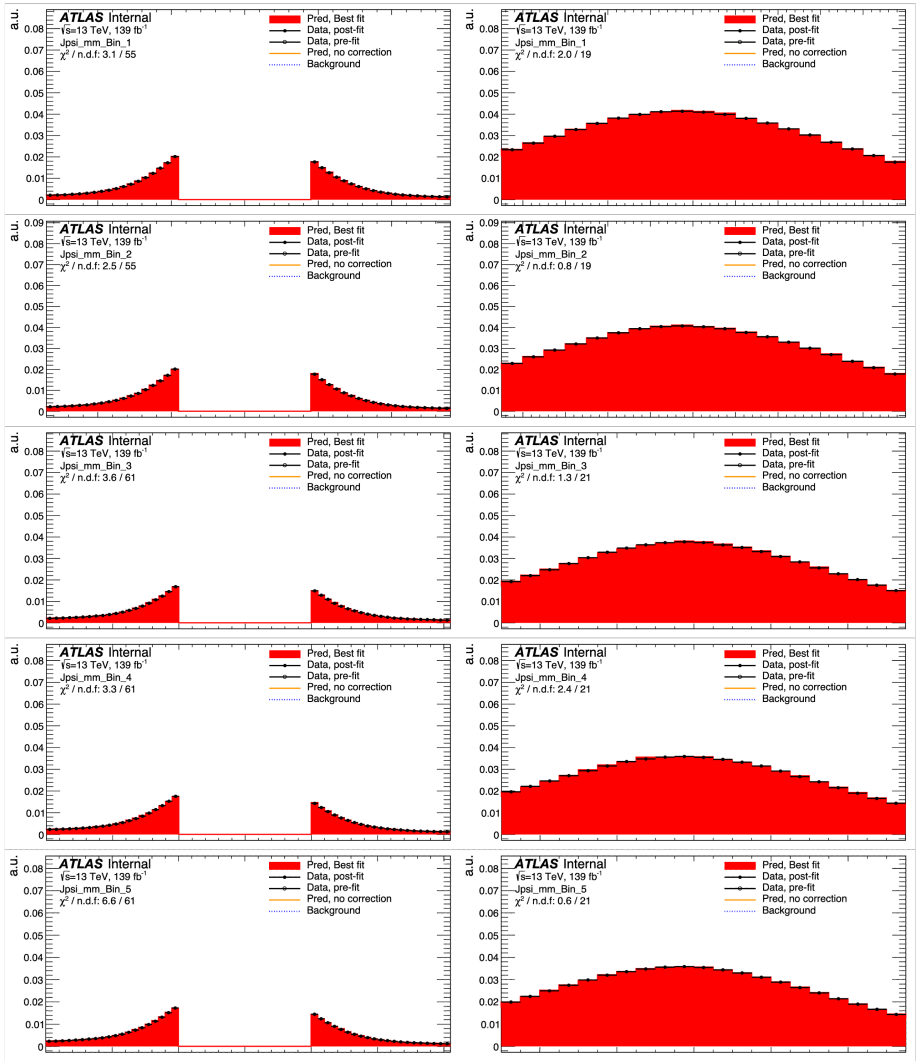

Selections on eta regions - Results

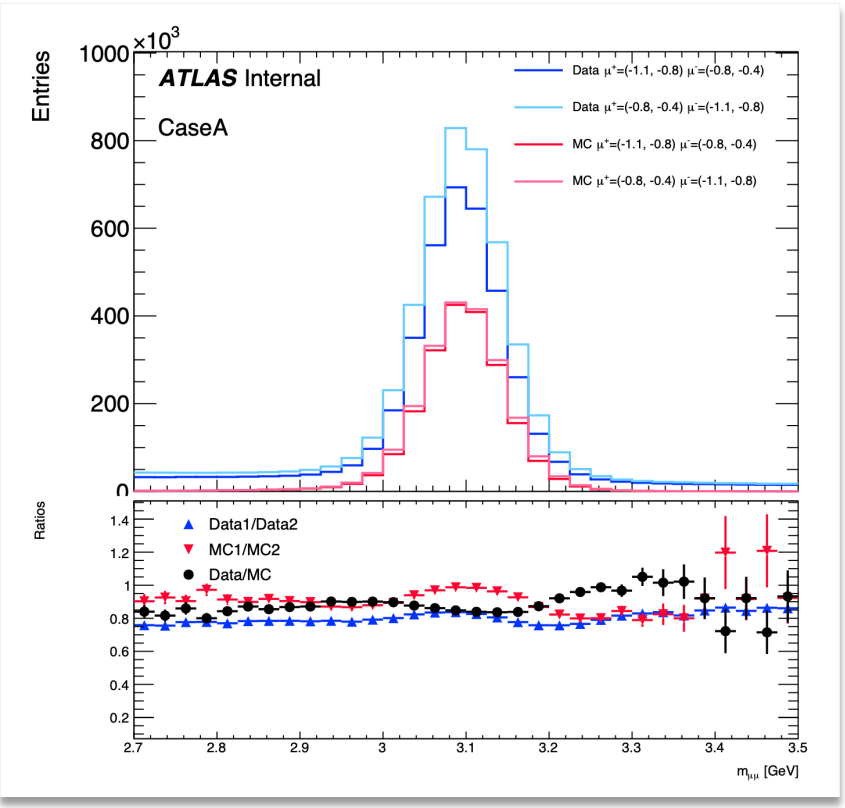

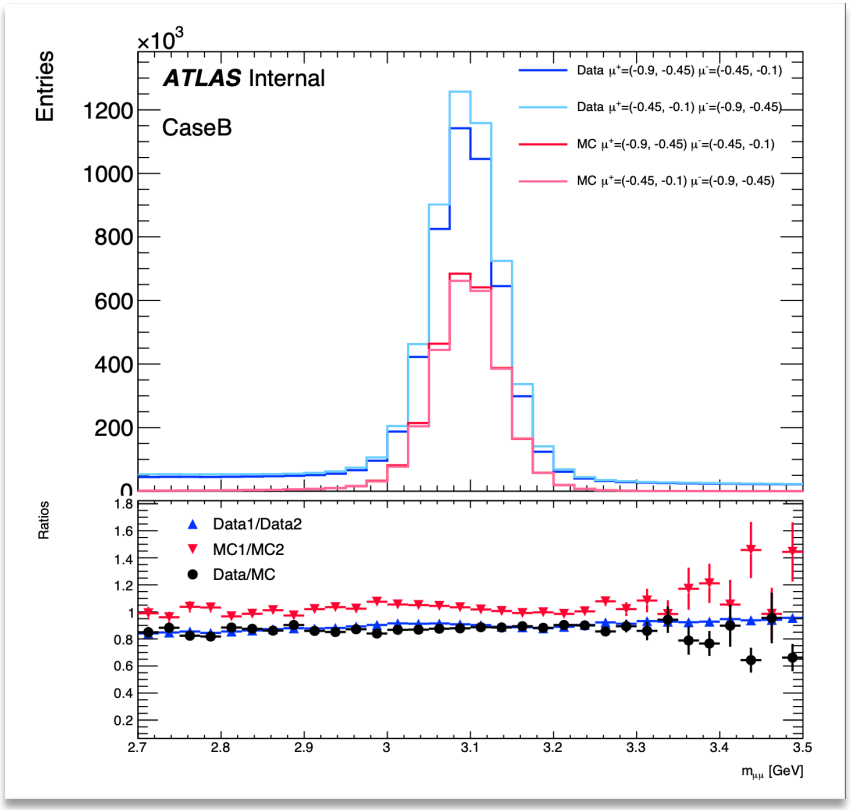

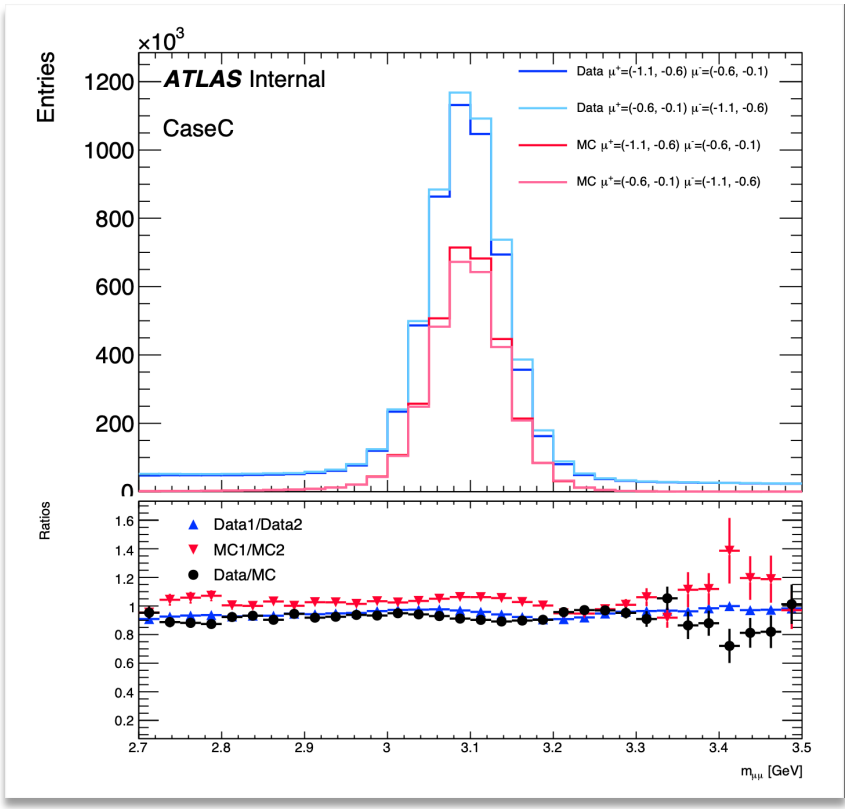

J/psi analysis for the absolute scale

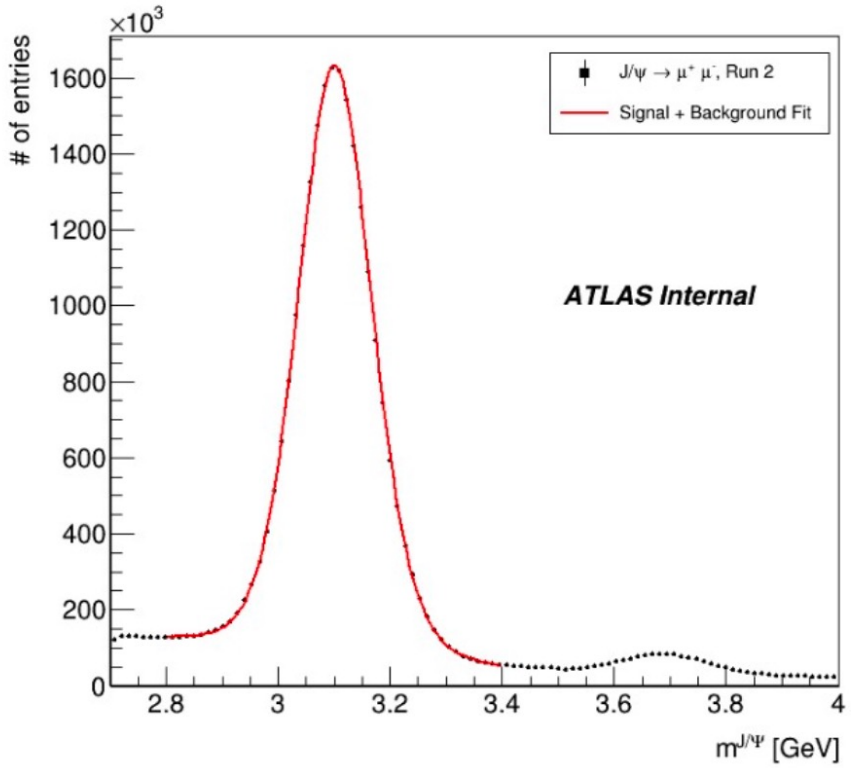

Muon momentum scale determined from the J/psi resonance is expected to be the dominant uncertainty
Order of 300×10^6 J/psi events, expect a few 10^{-6} of statistical uncertainty
J/y mass known at 2×10^{-6}
Dominant systematics from: alignment, material, propagation from J/psi to m_Z
Target for the uncertainty on m_Z:

- Conservative: 10 MeV
- Reasonable: 5 MeV
- Optimistic: 2 MeV

Z mass precision

CDF Run II result

$$m_W = 80\,433.5 \pm 6.4_{stat} \pm 6.9_{syst}\, MeV$$

• Also includes Z mass measurements in μμ and ee:

$$m_Z^{\mu\mu} = 91\,192.0 \pm 6.4_{stat} \pm 4.0_{syst}\, MeV$$

$$m_Z^{ee} = 91\,194.3 \pm 13.8_{stat} \pm 7.6_{syst}\, MeV$$

• Systematic uncertainties on MZ result from uncertainties on the longitudinal coordinate measurements in the COT (1.0 MeV), the momentum calibration (2.3 MeV), and the QED radiative corrections (3.1 MeV).

• "The systematic uncertainties stemming from the magnetic field nonuniformity dominate the total uncertainty of 25 ppm in the combined momentum calibration."

Run 1 vs Run 2

- Run 1: Significant p_T dependence of the muon momentum scale → m_Z measurement not possible
  - dependence of the muon momentum scale on the transverse momentum → the momentum scale was not uniform across the p_T spectrum → unreliable measurement of the Z boson mass
- Run 2: Uniform scale across pT range
  - ATLAS detector upgrades → better resolution and efficiency
  - Improved alignment
  - Higher collision energy $13\ TeV$ (Run 2) vs $7-8\ TeV$ (Run 1)
  - Higher LHC luminosity $150\ fb^{-1}$ (Run 2) vs $30\ fb^{-1}$ (Run 1)

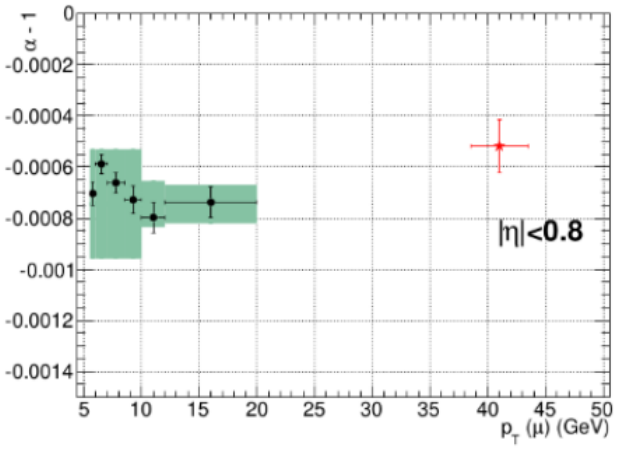

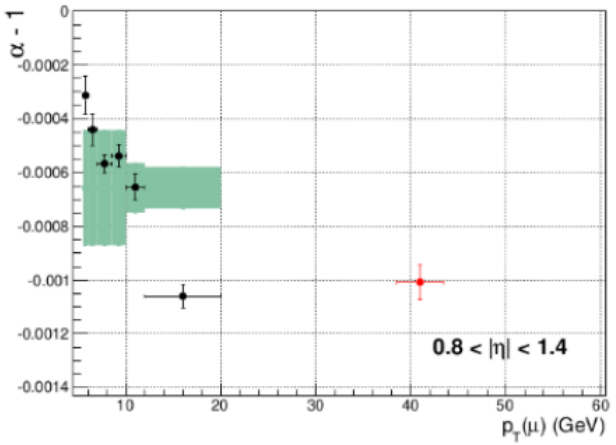

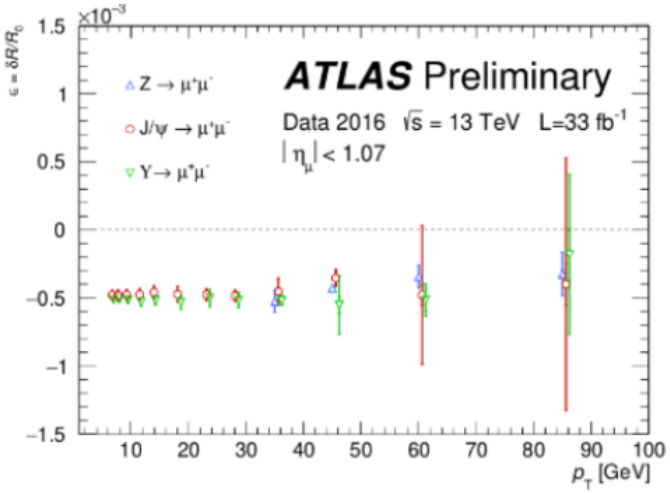

Event Selection - Samples

- Only muon channel
- $p_T > 35$ GeV
- Focus on Central region (defined by SCT **barrel**): $|\eta| < 1.17$
- Medium ID
- No additional (if possible) cut on track quality; d_0, z_0, or vertex probability

- Release 22
- Full Run-2
- Z MC sample: Powheg-Pythia8EvtGen_AZNLOCTEQ6L1_Zmumu(361107)
- J/ψ MC sample: P8B_A14_CTEQ6L1_Jpsi1S_mu6mu4(801115)
  - Extension added: 250M prompt + 250M non-prompt.
  - Jira Ticket: ATLMCPROD-101132

4

Systematic Uncertainties

Systematics	MeV
Longitudinal Scale ID	1.0
QED radiative corrections (FSR)	?
Stat.	0.1?
Stat. Uncertainty of the momentum calibration	?
Background	0.1?
β_{CURV}	few MeV
Material budget	<2?
QCD scales and PDFs	sub. MeV

Preliminary uncertainties

Systematics	MeV
Longitudinal Scale COT	1.0
QED radiative corrections (FSR)	3.1
Stat	6.4
Momentum calibration	2.3

Uncertainties obtained from mZ in mW measurement CDF-II

15

Z mass precision

Miscellaneous

Drell-Yan

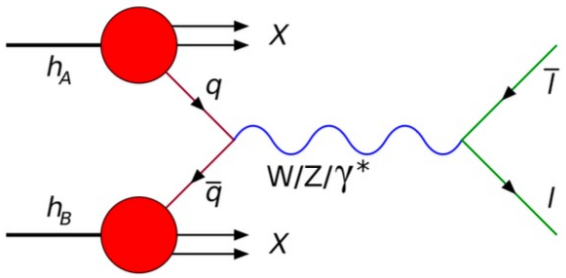

$m_{J/\psi} = 3096.900 \pm 0.006 MeV \ \ (c\bar{c})$

$m_Z = 91.1876 \ \pm 0.0021 \ GeV$

$m_W = 80.377 \pm 0.012 \ GeV$

$m_H = 125.25 \pm 0.17 GeV$

Calibration Strategy

ID track momentum calibration using **three sets** of corrections:

$$p_T^{\text{Measured}} = p_T^{\text{Reco}} \times \frac{1}{1 + q\,\delta s\,(\eta)\,p_T^{\text{Reco}}} \times (1 + \alpha(\eta,\phi)) \times \left(1 + \beta_{\text{Mult}}(\eta)\,\mathcal{G}(0,1) + \beta_{\text{curv}}\,\mathcal{G}(0,1)\,p_T^{\text{Reco}}\right)$$

Sagitta Bias → Scale and scattering Resolution → Intrinsic Resolution

Sagitta Bias from Z→μμ

- Standard approach: (Slightly) sensitive to m_Z
- Using alternative method

Scale and scattering term from J/ψ

- Simultaneous determination
- Scale Extrapolation to Z scale

Intrinsic resolution from Z

- Default ATLAS calibration uses m_Z
- Using Φ_{CS} instead

- Avoid iterative procedures where possible – prefer **simultaneous** measurements
  - Convergence, control over correlations

24.05.2023 Z boson mass measurement 1

ESSnuSB/ ESSnuSB+

- A H2020 EU Design Study has been submitted March 2017 (Call INFRADEV-01-2017)
  - Title of Proposal: **Discovery and measurement of leptonic CP violation using an intensive neutrino Super Beam generated with the exceptionally powerful ESS linear accelerator.**
  - Total cost: 4.7 M€
  - EU funding received: 3 M€
  - Timeline: 01/01/2018 - 31/12/2021 → 31/03/2022
- A Conceptual Design Report was published in 2022
  - Title of Design Report: **The European Spallation Source neutrino Super Beam Conceptual Design Report**
  - Approved → ESSnuSB+ ongoing

#	Institutions / organisations name	Accronym	Country
1	Centre National de la Recherche Scientifique	CNRS	France
2	University of Uppsala	UU	Sweden
3	Kungliga Tekniska Hoegskolan	KTH	Sweden
4	European Spallation Source Eric	ESS	Sweden
5	University of Cukurova	CU	Turkey
6	Universidad Autonoma de Madrid	UAD	Spain
7	National Center for Scientific Research "Demokritos"	DEMOKRITOS	Greece
8	Instituto Nationale di Fisica Nucleare	INFN	Italy
9	Ruder Boskovi Instgitute	RBI	Croatia
10	Sofiiski Universitet Sveti Kliment Ohridski	UniSofia	Bulgaria
11	Lunds Universitet	ULUND	Sweden
12	Akademia Gorniczo-Hutnicza Im. Stanislawa Staszica w Krakowie	AGH / AGH-UST	Poland
13	European Organization for Nuclear Resarch	CERN	Switzerland
14	University of Geneva	UNIGE	Switzerland
15	University of Durham	UDUR	United Kingdom

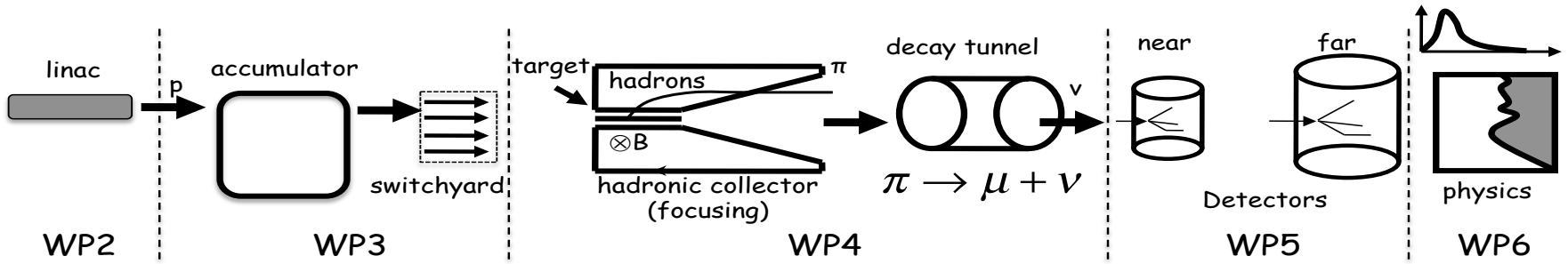

ESSnuSB – The Beam

- The process involves creating a pion beam that decays in-flight into muons and neutrinos via $\pi^+ \rightarrow \mu^+ + \nu_\mu$ (and its charge conjugate).
- Pions are produced by directing a proton beam onto a thin target, resulting in hadrons that decay, leaving weak-stable particles called secondaries, primarily pions and heavier hadrons.
- An electromagnetic horn focuses particles of a selected charge and de-focuses the opposite, enabling the selection of neutrino or antineutrino beam

Results

$$\nu_e + n \rightarrow e^- + p$$
$$\nu_\mu + n \rightarrow \mu^- + p$$
$$\bar{\nu}_e + p \rightarrow e^+ + n$$
$$\bar{\nu}_\mu + p \rightarrow \mu^+ + n$$

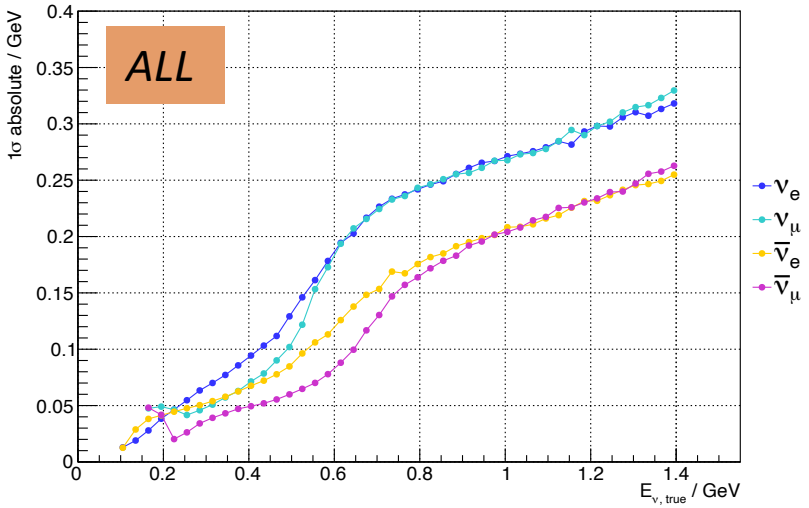

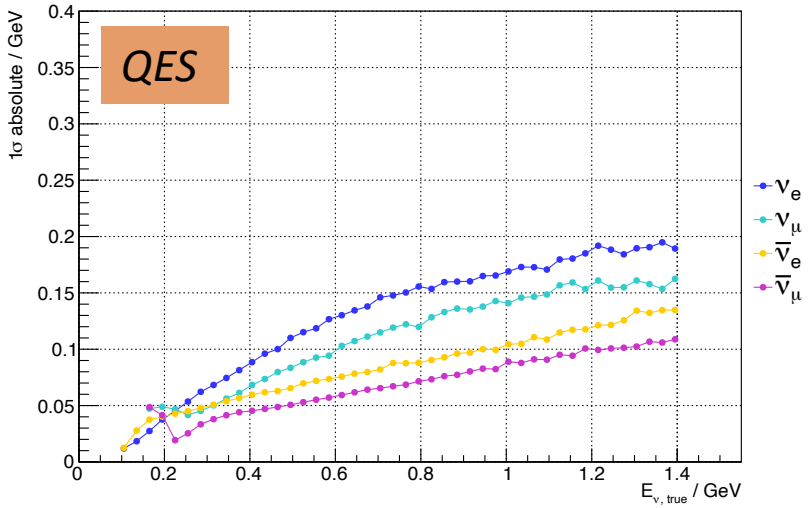

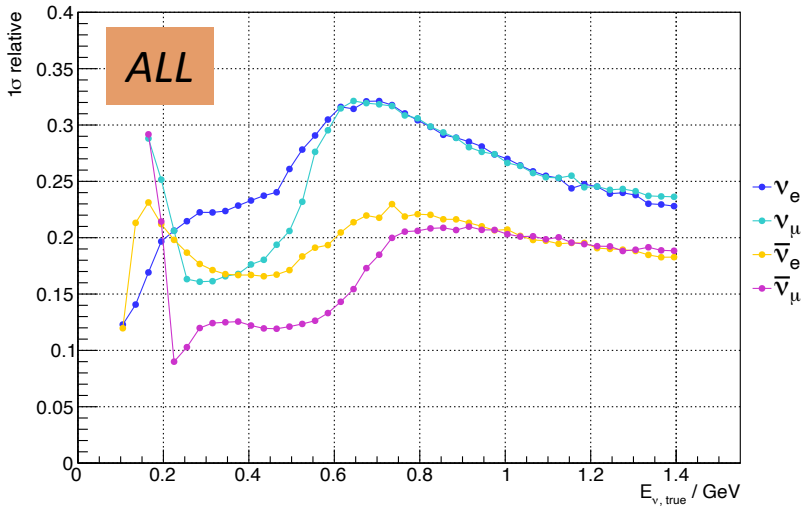

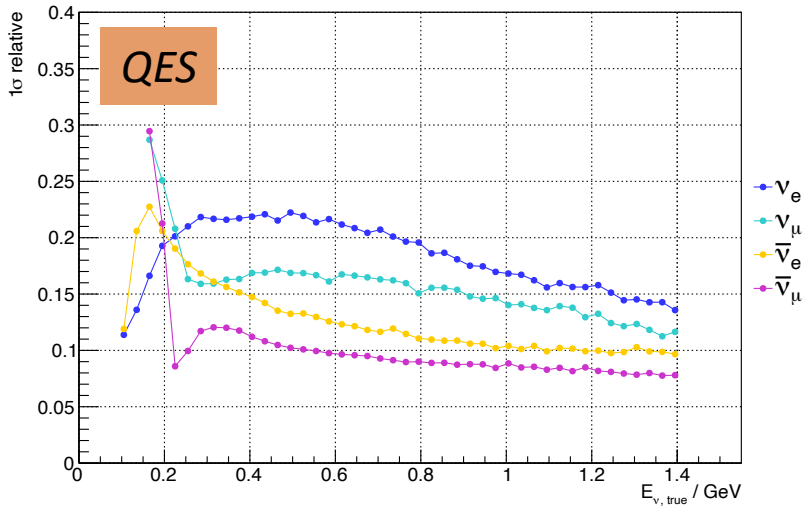

ESSnuSB Comments

1st step

- e, μ reconstruction is successful and well-calibrated
- It can be seen that the reconstruction of muons is better than the one of electrons; electrons scatter more, and the Cherenkov ring is fuzzier than the one for muons.
- Note that the first events for electron start at approximately 0.5 GeV while for muons at approximately 1.5 GeV, in agreement with the Cherenkov threshold $E_{th} = \frac{m_p c^2}{\sqrt{1-\left(\frac{1}{n}\right)^2}}$
- The relative resolution of the (anti)electron momentum is below 10 % for momenta larger than 100 MeV and dropping below 8% for momenta greater than 800 MeV. For (anti)muon momenta, relative resolution is best at lower momenta, beginning below 4% for momenta up to 400 MeV and reaching 6% for energies above 1 GeV.

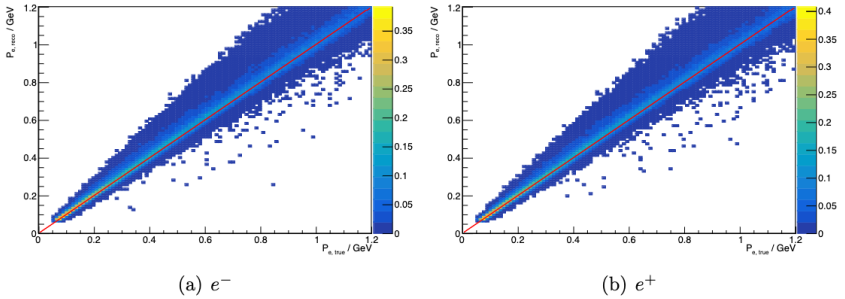

(a) e^- (b) e^+

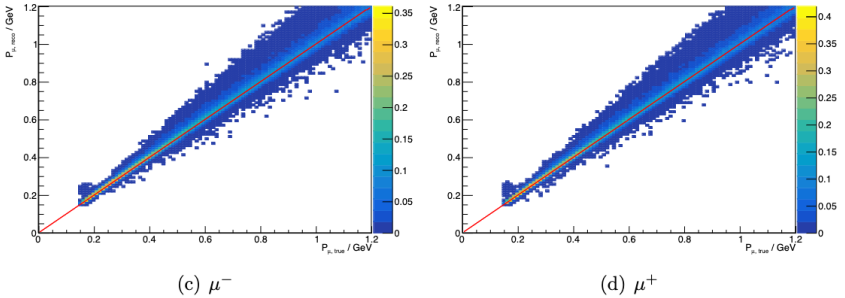

(c) μ^- (d) μ^+

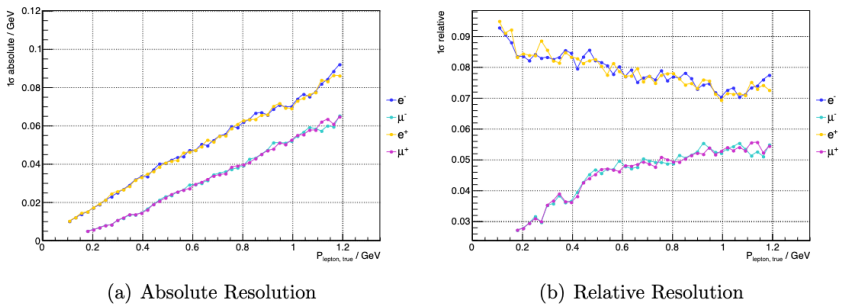

(a) Absolute Resolution (b) Relative Resolution

ESSnuSB Comments

2nd step

Neutrino energy resolution is consistently worse than that for antineutrinos. This is because, at ESSnuSB energies, antineutrinos tend to scatter forward, whereas neutrinos scatter isotropically, influenced by the nature of weak forces. The forward scattering results in less momentum transfer, reducing dependence on the initial target momentum and thus lowering the uncertainty on neutrino energy from the Fermi momentum of nucleons.

Above 250 MeV, the resolution is better for muon (anti)neutrinos than for electron (anti)neutrinos. Muons do not produce electromagnetic showers making their Cherenkov rings sharper and easier to reconstruct compared to electrons. However, in the lower energy region, muon (anti)neutrino reconstruction is worse because the resulting muons are close to or below the Cherenkov threshold, making them harder to observe. In contrast, electrons are well above the Cherenkov threshold at all ESSνSB neutrino energies

$$E_\nu = \frac{m_F^2 - m_{IB}^2 - m_l^2 + 2m_{IB}E_l}{2(m_{IB} - E_l + p_l cos\theta)}$$

Neutrino interactions in WatCher detector

- Charged Current (CC) Interactions - exchange of a W boson and result in the production of a charged lepton
  - $\nu_x + n \rightarrow x^- + p$
- Neutral Current (NC) Interactions - exchange of a Z boson and do not change the type of neutrino
  - Elastic Scattering - neutrino scatters off an electron, transferring some energy to the electron, which emits Cherenkov radiation
    - $\nu_x + e^- \rightarrow \nu_x + e^-$
  - Inelastic Scattering - neutrino scatters off a nucleon, producing other particles (X) that may emit Cherenkov radiation
    - $\nu_x + N \rightarrow \nu_x + X$
- Quasi-Elastic Scattering (QES) - neutrino interacts with a nucleon, producing a lepton and changing the nucleon's state.
- Resonant Scattering (RES) - neutrino interacts with a nucleon, producing a baryon resonance that subsequently decays into a nucleon and a meson.
  - $\nu_\mu + p \rightarrow \mu^- + \Delta^{++}$
- Deep Inelastic Scattering (DIS) - neutrino interacts with a nucleon, breaking it apart and producing multiple particles.
  - $\nu_\mu + N \rightarrow \mu^- + hadrons$
- Coherent Scattering - neutrino interacts with the entire nucleus coherently, producing a single meson without breaking the nucleus.
  - $\nu_\mu + (A, Z) \rightarrow \mu^- + (A, Z) + \pi^+$